Chem Soc Rev

Multifarious Facets of Sugar-derived Molecular Gels: Molecular Features, Mechanism of Self-assembly and Emerging Applications

Journal:	*Chemical Society Reviews*
Manuscript ID:	CS-REV-01-2015-000093.R1
Article Type:	Review Article
Date Submitted by the Author:	07-Apr-2015
Complete List of Authors:	Datta, Sougata; indian institute of science, department of organic chemistry Bhattacharya, Santanu; Indian Institute of Science, Organic Chemistry

Chem Soc Rev

INVITED REVIEW

Multifarious Facets of Sugar-derived Molecular Gels: Molecular Features, Mechanism of Self-assembly and Emerging Applications

Sougata Datta,[a] and Santanu Bhattacharya*[a,b]

Remarkable capability of nature in designing and creation of excellent self-assembled nano-structures especially in the biological world motivated chemists to mimic such systems with synthetic molecular and supramolecular systems. Hierarchically organized self-assembly of low molecular weight gelators (LMWGs) based on non-covalent interactions has been proven to be a useful tool in the development of well-defined nanostructures. Among them, self-assembly of sugar-derived LMWGs has received immense attention because of their propensity to furnish biocompatible, hierarchical, supramolecular architectures that are macroscopically expressed in gel formation. This review sheds light on various aspects of sugar-derived LMWGs uncovering the mechanism of gelation, structural analysis, tailorable properties and their diverse applications in stimuli-responsiveness, sensing, self-healing, environmental problems, nano and biomaterials synthesis etc.

1. Introduction

Albert Einstein once said, "*Look deep into nature, and then you will understand everything better*". There is no doubt that the Mother Nature has ingeniously developed each entity of this living world using fundamental principles of chemistry. Several natural phenomena exemplify these. For instance, various life forms such as plants, algae and photosynthetic bacteria thrive via photosynthesis using pigments like chlorophylls and carotenoids. Similarly existence of complex superstructures like the double-stranded DNA, three-dimensionally folded proteins, and biologically active cell membranes *etc.* spurs the scientific community to mimic such processes by rational design and syntheses of numerous molecules as artificial systems and investigating the mechanism of their self-assembly processes. Extensive research efforts towards the evolution of novel properties utilizing the underlying principles of self-assembly

(*i.e.*, hydrogen bonding, π-π stacking, solvophobic effects, van der Waals forces, charge-transfer interactions and metal-ligand coordination *etc.*) as a key route led to the generation of a vast area of research known as supramolecular chemistry'.[1,2]

In this context, low molecular-weight gelators (LMWGs) have gained remarkable interest because of spontaneous formation of various self-assembled three-dimensional nano-structures (helical, and bundles of fibers of high aspect ratio, ribbons, sheets, particles, rods, tapes, strands, rings, tubules, globules, micelles and vesicles *etc.*). In the course of sol-to-gel transitions, the transcription of intrinsic molecular features from molecular level to complex supramolecular structures occurs.[3-8] Non-covalent 'cross-links' and physical entanglements among such self-assemblies result in the formation of a 3D-network, where the solvent molecules are entrapped and immobilized by interfacial forces to furnish viscoelastic materials.[9] LMWGs often exhibit properties that are different compared to their polymeric counterparts or biopolymers.[10-12] Generally, the gels derived from LMWGs are rheologically weaker than the polymeric gels.[13] Hence, the polymeric gelators are often superior to the LMWGs in the preparation self-sustaining materials. Both of them show reversible gel-to-sol transition upon heating above the respective melting temperatures ($T_{gel-sol}$). However, relatively smaller size of the LMWGs often assists in the 'intelligent' design and in understanding complex mechanistic pathways encountered in various self-assembly

[a] *Department of Organic Chemistry, Indian Institute of Science, Bangalore, India. Fax: +91-80-23600529; Tel: +91-80-22932664; E-mail: sb@orgchem.iisc.ernet.in*

[b] *Jawaharlal Nehru Centre for Advanced Scientific Research, Bangalore, India. Fax: +91-80-23600529; Tel: +91-80-22932664; E-mail: sb@orgchem.iisc.ernet.in*

processes. Furthermore, it is easier to synthesize and purify small molecules to furnish materials with a single molecular weight, in contrast to polymers, which have a distribution of molecular weights. The structural features of the LMWGs can also be readily modulated in order to get desired physical properties. Hence, they have both advantages and disadvantages as gels depending on the context of their applications. The resulting soft materials are termed as organogels or hydrogels depending on the entrapped solvent being either organic or water, respectively.[14] However, there are a few exceptions such as, xerogels (*e.g.,* vulcanized rubber and dried gelatin) and aerogels which are dispersions of a gas within a solid.[15] It may be important to note that gelation always leads to the formation of a certain self-assembled structure, however, all self-assemblies do not result in gelation. Such gels are attractive candidates for a diverse range of applications in a number of diverse fields, including the design and synthesis of biomaterials,[16-21] nano-materials,[22-31] stimuli-responsive materials,[32] sensors,[33-36] templating components for inorganic or organic nanostructures,[37] and in molecular electronics[38-41] and catalysis[42] *etc*.

Although a library of large number LMWGs has appeared in literature because of over two decades of research work, still there is no certain rule or structural parameter for a molecule to exhibit gelation. Thus, discovery of many of the LMWGs is serendipitous. However, putative design of LMWGs and an understanding of the molecular level arrangements and mode of aggregation may convey valuable information towards the production of new gels.[43] Diverse molecular building blocks derived from long chain hydrocarbons or steroid derivatives,[44-48] amino acid derivatives,[49-54] ureas,[55] carbohydrate-derived systems,[56] metal complexes,[57-61] charge-transfer complexes,[62,63] macrocycles[64,65] and organic salts[66,67] *etc*. have been used to synthesize low molecular-weight organogelators (LMOGs) as well as hydrogelators (LMHGs).

Thus, investigation of a series of simple and structurally related compounds often provides key insights into the self-assembly mechanism. There are several review articles in contemporary literature on various aspects of gels.[8-21,23,24,30,32,35,36,37,42,43,45-52,55-58,60-66,68-75] However, there is no review that addresses the interesting topic related to the sugar-derived gels. In the present review, we critically discuss the origin, evolution and future perspectives of the sugar-derived LMWGs (Fig. 1).
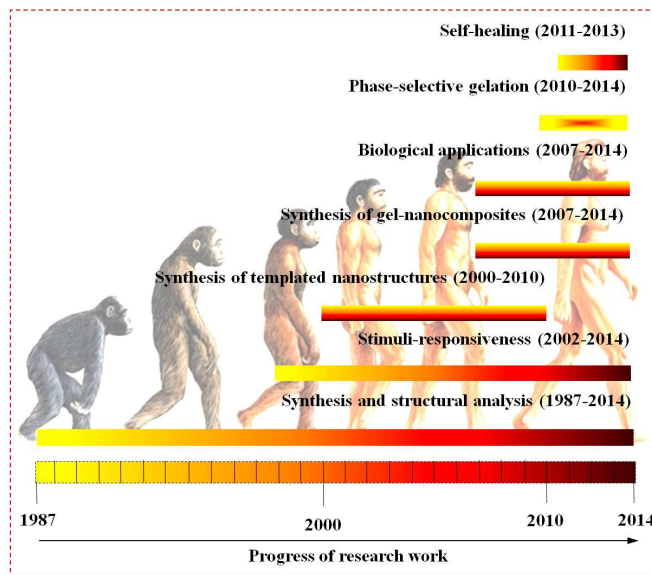

Fig. 1 Progress of research themes in the area of sugar-derived LMWGs discussed in the present review.

1.1. Importance of sugar and the corresponding gels

Sugars serve organisms as energy sources. Therefore as a substrate for the generation of cellular energy, glucose is of

Sougata Datta was born in West Bengal, India, in 1987. He earned his B.Sc. degree (with honours in chemistry) from the Ramakrishna Mission Vidyamandira, Belur Math of the University of Calcutta in 2007. He obtained his Master's degree (MS) from the Division of Chemical Sciences, Indian Institute of Science, Bangalore in 2009. He obtained his PhD degree under the supervision of Prof. Santanu Bhattacharya and currently he is working as a research associate

Sougata Datta

there. He is interested in molecular gels including surfactants, stimuli-responsive self-assemblies, nano-materials and their relevant applications.

Santanu Bhattacharya obtained his PhD from Rutgers University, New Brunswick, NJ working with Robert A. Moss. This was followed by a three-year stint as a NIH postdoctoral research associate at Massachusetts Institute of Technology, Cambridge, MA under the tutelage of Hargobind Khorana. He is currently a Professor of the Department of Organic Chemistry at the Indian Institute of Science, Bangalore. He received numerous awards including the TWAS prize in

Santanu Bhattacharya

Chemistry and an elected fellow of the INSA, New Delhi and the IASc, Bangalore. His research interests include supramolecular chemistry, nanoscience and chemical biology. He has published >220 refereed research papers.

fundamental importance in the metabolism of various life forms. It is one of the main products of photosynthesis, using which plants and algae convert energy from sunlight into chemical energy to be used by their cells. Other sugars also occur in nature. These include deoxyribose in DNA (living information storage system), ribose in RNA, starch in plants, cellulose in the cell walls of plant and algae, glycogen in animals *etc*. In our daily life, the dessert 'jelly' or 'jell-o' (combination of water, denatured collagen or agar sugar, flavourings and artificial colouring) represents a classic example of a gel, where water is immobilized by gelatin, a biopolymer made by the hydrolysis of collagen. In 1897, Pearle B. Wait a carpenter in LeRoy, NY, put up a cough remedy and laxative tea in his home. He experimented with gelatin and came up with a fruit flavoured dessert which his wife, May, named Jell-O.[76]

Supramolecular chemists try to follow the same pathway traversed by the Mother Nature in the construction of biological architectures and functional bio-systems essential for the occurrence of life. The non-covalent interactions involved in such self-assembly processes should be directional to enforce anisotropic one-dimensional assembly of nanofibres.[74] Based on the nature of the self-complementary driving force for the molecular aggregation, the gelator molecules defined by certain functionality may be classified into the following categories. Firstly the amides (R1CONHR2) and ureas (R1NHCONHR2) are capable of forming self-complementary hydrogen bonding interactions (C=O···H–N). Secondly the carbohydrates contain multiple O-H groups and exhibit extensive hydrogen bonding interactions. Thirdly the nucleobases utilize hydrogen bonding and π-π stacking interactions. Fourthly the steroids and bile salts, having hydrophobic surfaces and finally the aliphatic hydrocarbons use significant extent of van der Waals forces and solvophobic interactions. Among the various non-covalent interactions, inter- and intra-molecular hydrogen bonding interactions have been extensively utilized in the production of complex organized systems due to the reversibility, specificity, directionality and cooperativity of such interactions. Hydrogen bond forming gelators generally include amides (amino acids)/ ureas, nucleobases and carbohydrates. It is clearly evident that carbohydrates are far superior to amides/ ureas/ nucleobases in the hydrogen bonding mediated self-assembly processes because of their significantly greater number of hydrogen bonding sites (-OH groups).

Initially, the investigation of hydrogen bond forming gelators was limited to few amino acids (*e.g.*, L-Lysine,[52] L-serine[77] and L-cystine[78,79] *etc*.)-based amphiphiles and urea derivatives[80-82]. In recent advances, the use of bioactive small molecules (*e.g.*, vancomycin[83,84]) is more profound owing to their biomedical application in three-dimensional cell cultures,[85] biomolecular screening,[75] wound healing[86,87] and drug delivery.[75,88] These developments have prompted the exploitation of fundamental biological building blocks (*i.e.*, saccharides, peptides and nucleic acids) as supramolecular gelators because they offer excellent opportunity for mimicking

the structures and mechanism of unexpected functions of various bio-macromolecules.

Self-assembly of sugar-derived LMWGs has received particular attention because of various reasons (Fig. 2). They are often biodegradable, non-toxic and eco-friendly, which make them ideal building blocks for the regeneration of tissues and organs.[18] They offer diverse functionality and cell signalling capacity with rapid and facile synthesis of complex molecules.[18] Carbohydrate-protein interactions are extremely important in numerous biological phenomena, such as blood coagulation, immune response, viral infection, inflammation, embryogenesis and inter-cellular signal transfer *etc*.[89-91] Furthermore, the design and synthesis of carbohydrate-derived artificial systems that imitate the polyvalent carbohydrate organization at the cell surface and molecular recognition in bio-systems is also a fertile approach to investigate and intervene in various carbohydrate-mediated interactions. Yamanaka *et al*. reported a pale-yellow transparent hydrogel derived from a carbohydrate amphiphile.[92] Since the surface of the resultant fibers was enriched with dense packing of glucosides, this hydrogel exhibited selective responsiveness to lectin (carbohydrate binding proteins) such as, concanavalin A (ConA).
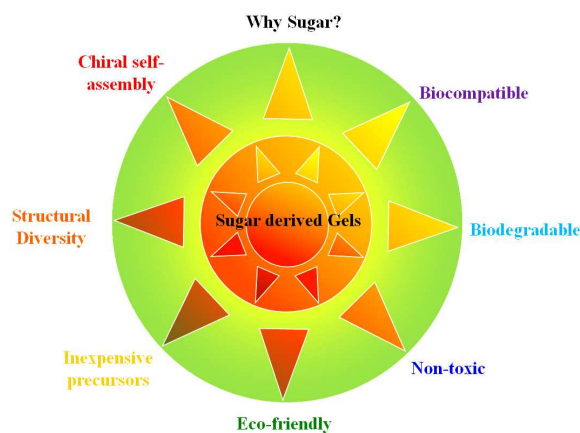

Fig. 2 Various advantages of sugar-derived LMWGs.

The precursors of sugar-derived LMWGs are generally inexpensive and commercially available. They may be derived from abundant renewable resources (Fig. 3). John and co-workers attempted various approaches for making hydrogelators from the renewable resources.[19,30,56] For example, these authors synthesized fatty acid derivatives of amygdalin which is a by-product of the fruit industry, and a naturally occurring glycoside found in many food plants such as the kernels of apricots, almonds and apples *etc*.[93] These authors demonstrated enzyme triggered release of curcumin, a known chemotherapeutic and anti-inflammatory agent, as a model drug *via* the degradation of the hydrogel of fatty acid esters of amygdalin.[94] Similarly, these authors reported *in situ* synthesis of gold nanoparticles using ascorbic acid (vitamin C)-based amphiphiles, which is a sugar-based building block abundantly found in citrus fruits and plants.[95]

There are several established synthetic strategies in literature to construct various building blocks made up of monosaccharides, disaccharides or polysaccharides towards gelation. Thus, the carbohydrates are amenable to preparing broad classes of LMWGs. Gelation properties of saccharides can be easily modulated by simple protection or deprotection of their multiple hydroxyl groups. Hence, the structural diversity, the variability of sugar-units, their sequence and linkage points, the anomeric configuration, the chemical modification and/or substitution at different positions, the inter-conversion of conformers are uniquely suited for the creation of a wide range of organo- and hydro-gelators as well as ambidextrous gelators.

For example, it was observed that methyl 4, 6-O-benzylidene derivatives of monosaccharides are perfect scaffolds for the study of the minimal structural requisites for the gelation ability.[96-102] These are capable of forming rigid, strong, and highly directional hydrogen bonds in their corresponding gels.[96] The unique yet well-defined molecular architecture could be derived from the choice of a wide variety of isomers. Each of these isomers allows systematic investigations in order to make correlation between the monomer structure and the gelation ability. There is no other report of any gelator discovered so far which exhibits such a diversity in its homologues.
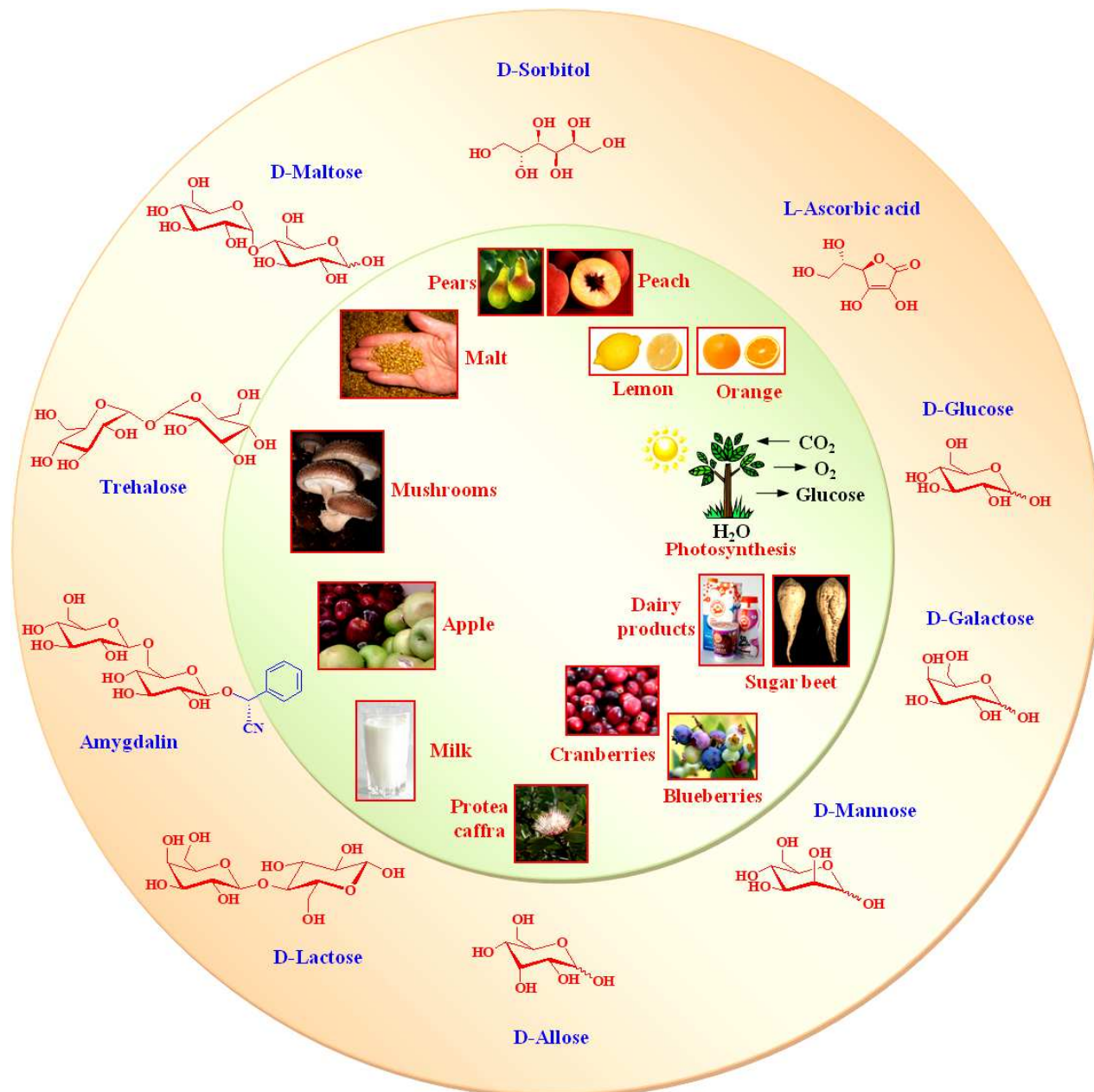

Fig. 3 Chemical structures and natural sources of basic sugar motifs discussed in the current review article.[103]

Unquestionably, this is one of the merits of the carbohydrate-derived LMWGs. Wang *et al*. explored several strategies to offer a diverse range of methyl 4, 6-*O*-benzylidene-α-D-glucopyranose-derived LMWGs *via* simple synthetic steps.[104-109]

In addition, careful search for sugars as well as for appropriate hydrophobic groups may lead to discovery of excellent amphiphilic gelators.[110] Cyclic sugars are conformationally more restricted and also have multiple as well as directional -OH groups in contrast to their acyclic analogues. Consequently, amphiphilic molecules containing cyclic sugar residues have tendency to form strong cooperative hydrogen-bonded networks. Furthermore, cyclic nature of the sugar moiety imparts significant rigid character to the headgroup of the amphiphile. Bhattacharya *et al*.[111] and Shimizu *et al*.[112] independently worked on various amphiphilic and bolaamphiphilic LMWGs having carbohydrate headgroups, which has been discussed later in detail.

Carbohydrates are useful not only as a hydrogen-bond forming segment in the gelators, but also helpful to introduce easily a variety of stereogenic centers into gelators by selection from a saccharide library. The inherent chiral information programmed in such molecular entities derived from a sugar moiety may often manifest in the form of supramolecular chirality in the gel phase *via* spatiotemporal self-assembly process which helps in the fabrication of chiral superstructures. The presence of chiral sugar moiety further offers an opportunity to investigate the mechanism of growth of such chiral aggregates by various physical methods including circular dichroism (CD) spectroscopy.[113,114] Their intrinsic chirality may help in evolving important tools in ferroelectric liquid crystals or separation of biologically important agents such as proteins and DNA. Furthermore, the chirality in supramolecular structures may be useful in molecular recognition with other chiral compounds. Though, amino acids are also chiral, carbohydrates are superior to the former in the construction of complex chiral superstructures attributed to the existence of multiple chiral centers. In one of the earlier reports, Fuhrhop *et al*. reported quadruple helical structure formation from a simple carbohydrate-based amphiphile, *N*-octyl-D-gluconamide.[115] While, Stupp and co-workers demonstrated generation of similar type of quadruple helical fibers in the self-assembly of an amphiphile[116] containing a palmitoyl tail, the 2-nitrobenzyl group, and an oligopeptide segment $GV_3A_3E_3$ which is structurally and synthetically more complicated compared to that of *N*-octyl-D-gluconamide.

1.2. Mechanism and pathway of gelation

Since, various non-covalent interactions that hold these superstructures are weak and reversible; self-assemblies of the LMWGs are inherently responsive toward thermal stimuli. Accordingly they often show reversible sol-to-gel transitions when their heated solutions are cooled below the respective gelation temperatures ($T_{gel-sol}$).[117] There are some parallel pathways (*e.g.,* crystallization and precipitation) which may also occur during the sol-to-gel transition (Fig. 4).[118] Extent of molecular ordering is higher in a crystal compared to that in the aggregates of the corresponding gel. Furthermore, crystallization or precipitation may also occur after gel formation. In that case, the kinetically stable gel may slowly transform to thermodynamically stable crystals (Fig. 4).[118]
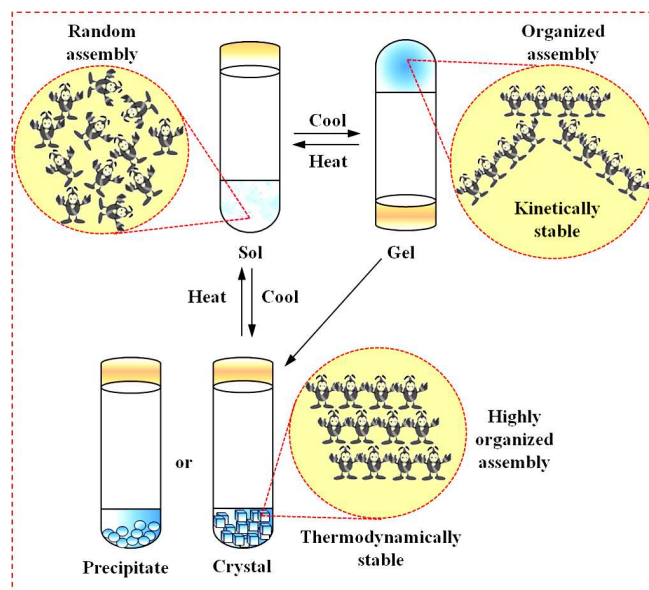

Fig. 4 Schematic illustration of the supramolecular sol-to-gel transition process.

Intelligent molecular design is essential to maintain the subtle balance between the extent of crystallization and solubilization of LMWGs. Single-crystal X-ray crystallography is the most powerful method to understand the molecular packing in the solid state.[119] In this respect two types of problems frequently occur. First, obtaining crystals of a gelator suitable for single crystal X-ray diffraction is very difficult. Second, gels and crystals are generally formed from different experimental conditions (*ca.* solvent). Hence, it is also difficult to confirm the difference in molecular packing between single crystals and gels. Cui *et al.* demonstrated formation of the hierarchical structures and the transitions of sugar-based gelator 4-(4'-ethoxyphenyl)phenyl-β-*O*-D-glucoside (**1**), in a mixture of water and 1,4-dioxane (Fig. 5).[118] In a mixture of water/1,4-dioxane (8/2, v/v), first a gel formed and then subsequently transformed into a needle-like crystal. Moreover, the gel-crystal transition could be modulated by tuning the solvent composition. However, a perfect crystal of **1** was obtained from an acetonitrile solution. Interestingly, the XRD pattern of the perfect single crystal obtained from acetonitrile matched with that of the collapsed gel of water/1, 4-dioxane (8/2, v/v). On the other hand, Weiss found significant difference in the molecular packing in the gel fibers of cholesteryl anthraquinone-2-carboxylate compared to that of the single crystal.[120]

Gelation is a hierarchical self-assembly process which takes place through multiple steps.[15] Multiple non-covalent interactions among the supramolecular building blocks allow

them to self-assemble into supramolecular polymers of ~1-5 nm width called fibrils (Scheme 1). These fibrils further collate with one another to result in nanoscale bundles having ~20-50 nm width referred to as fibers.[68] Finally, fibers entangle to form a 3D 'solid-like' network where the gelating solvent molecules are entrapped and immobilized by interfacial forces (Scheme 1).[74] One-dimensional fibrous growth is achieved by the involvement of strong self-complementary and unidirectional non-covalent interactions among the building blocks.[121] However, some favourable factors that induce the non-covalent cross-linking of primary aggregates such as fibrils and microcrystals to form networks are also required.
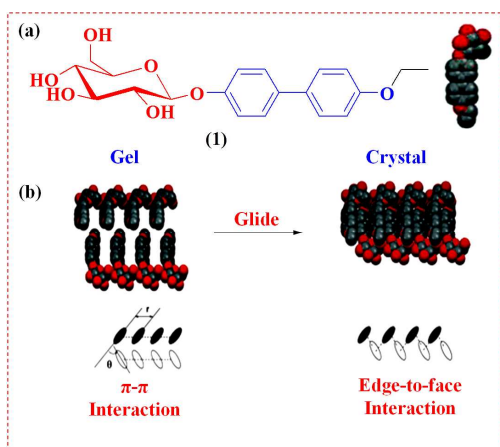
Fig. 5 (a) Chemical structure and (b) a molecular packing model illustrating gel-to-crystal transition of **1**. Reprinted with permission from ref. 118. Copyright 2009, American Chemical Society.

2. Structurally diverse platforms of sugar-based LMWGs

How do sugar derivatives self-assemble in solution, and eventually give rise to a physical gel strong enough to immobilize a significant amount of solvent? What are the major driving forces involved in such gelation process? Generally, strong and highly directional inter-molecular hydrogen bonding among the -OH linkages and solvent molecules (*ca.* H$_2$O for hydrogelation) is one of the major interactions that governs the self-assembly process of sugar derivatives. However, attachment of a chromophoric π-aromatic platform or a hydrophobic segment invokes π-π stacking or van der Waals interaction respectively in the supramolecular aggregates (Fig. 6). It is also important to note that a delicate balance of gelator-gelator and gelator-solvent interactions is always crucial to drive the equilibrium to gel formation instead of precipitation or crystallization or homogeneous sol formation.[122]

2.1. D-sorbitol and associated derivatives

D-sorbitol (**2**) which is also known as glucitol is one of the simplest examples of the LMWGs investigated by Grassi *et al* (Fig. 7).[123] Cooling of an ethanol sol of D-sorbitol leads to the formation of huge, jellybean shaped gel. However, a proper gel is produced only upon cooling the ethanolic sol followed by

sonication. The hydrogen bonding interaction is primarily responsible for the gelation induced by this molecule.
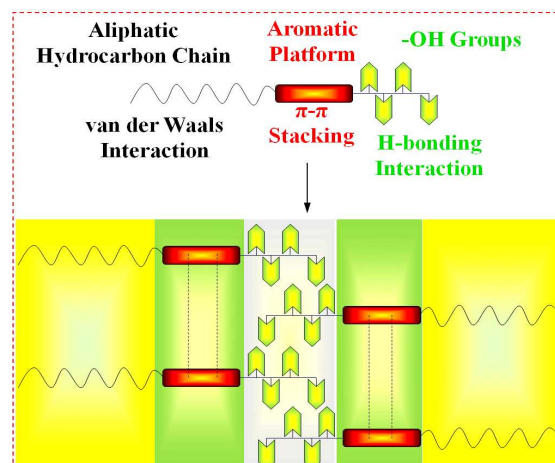

Fig. 6 A generalized schematic illustration of the non-covalent interaction mediated self-assembly by sugar-derived LMWGs.

1,3:2, 4-di-*O*-benzylidene sorbitol (DBS), a butterfly-shaped amphiphilic low molecular-weight organogelator (LMOG) is derived from the sugar alcohol D-glucitol (Fig. 7).[124] Meunier first reported 1, 3:2, 4-di-*O*-benzylidene-D-sorbitol (**3**) as a LMOG in 1891. After more than 50 years, Yamamoto reported the gelation characteristics of **3** in about 70 different liquids.[125,126] Spontak and co-workers explored the microstructural features and stability of organogels of **3** in poly (propylene glycol) (PPG) at various concentrations using polarized light microscopy, transmission electron microscopy (TEM), X-ray diffraction and spectrophotometry.[127] Spontak also provided valuable information concerning the fundamental factors, which govern the gelation process of **3**.[128] By systematic modulation the chemical nature of the end groups of PEG from polar (hydroxy-end-capped) to nonpolar (methoxy-end-capped), it was demonstrated that matrix polarity had a detrimental effect on **3**/PEG gelation.
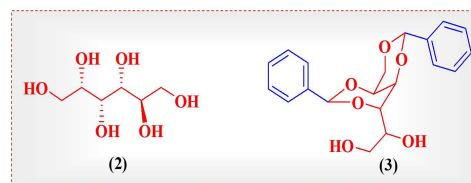

Fig. 7 Molecular structures of D-sorbitol (**2**) and 1, 3:2, 4-di-*O*-benzylidene sorbitol (**3**).

Craythorne *et al*. analysed the single crystal structure of 2,5-di-*O*-methanesulfonyl-1, 4:3, 6-dianhydro-D-sorbitol (**4**), which exhibited versatile gelation in a diverse range of solvents such as, aromatics, alcohols and water (Fig. 8a).[129] Surprisingly, analysis of the packing of the molecules in the crystal of **4** obtained from ethanol-propan-2-one revealed no strong hydrogen bonds. However, two possible C-H⋯O bonds as short contacts with angles of 162° could be confirmed (Fig. 8b).
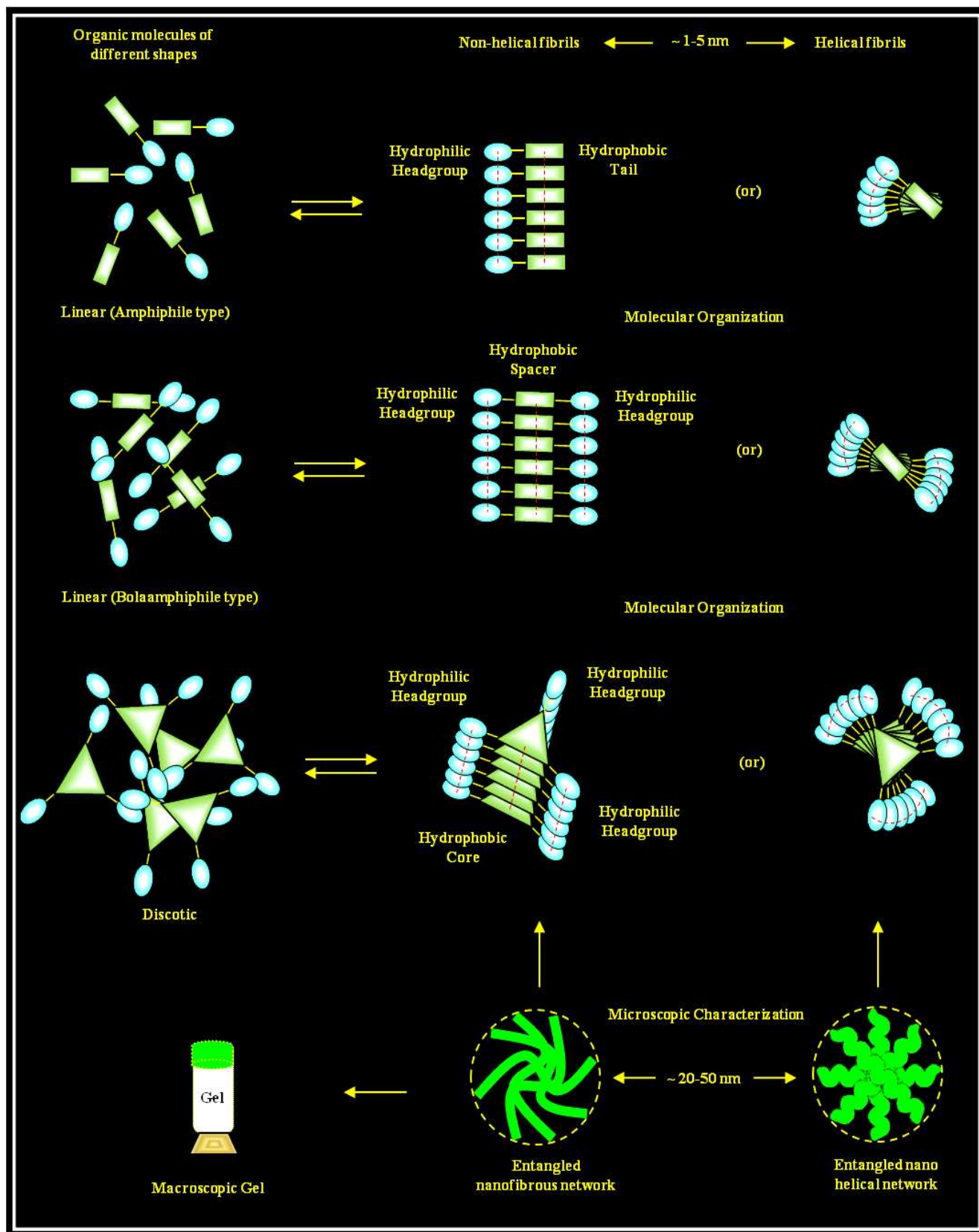
Scheme 1 A generalized schematic illustration of nanofibrous gel network formation by LMWGs.
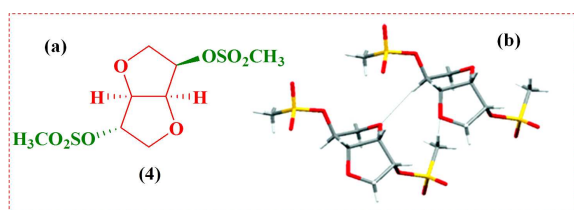
Fig. 8 (a) Molecular structure and (b) short contacts in the crystal of 2,5-di-*O*-methanesulfonyl-1, 4:3, 6-dianhydro-D-sorbitol (**4**), C(6)-H(6A)···O(8) 3.381(3) Å, 162°; C(16)-H(16C)···O(11) 3.444(3) Å, 162°. Reprinted with permission from ref. 129. Copyright 2009, The Royal Society of Chemistry and the Centre National de la Recherche Scientifique.

2.2. β-Cyclodextrin

Cyclodextrins (CDs) are cyclic oligosaccharides of α-1, 4 linked glucosidic units. They consist of six, seven, or eight glucose entities are called α- (**5a**), β- (**5b**), or γ- (**5c**) CDs, respectively (Fig. 9a). They adopt a toroidal (or cone) shape where the primary hydroxyl groups reside at the narrower side and the secondary hydroxyl groups occupy the wider side (Fig. 9b).[130] In one of the earlier reports, Rango *et al*. reported isotropic physical gel formation from solutions of rigorously anhydrous β-CD in dry pyridine or in liquids like toluene or chloroform in the presence of small amount of water as a co-solvent.[131] β-CD offers interesting opportunities in the design of fascinating gels since it can act as a host in various types of host-guest complexes (see below).
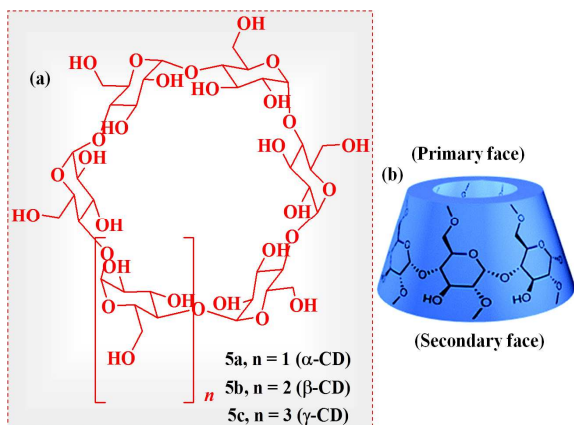

Fig. 9 (a) Chemical structures and (b) 3D-representation of cyclodextrins (CDs). Reprinted with permission from ref. 130. Copyright 2010, The Royal Society of Chemistry.

2.3. Methyl 4, 6-*O*-benzylidene derivatives of monosaccharides

Methyl 4, 6-*O*-benzylidene derivatives of monosaccharides were well investigated to study the structural rudiments for gelation ability. Their structural characteristics are (i) un-modified 2-OH and 3-OH group; (ii) protected 1-OH group by a methyl group; and (iii) protected 4-OH and 6-OH group with

a benzylidene group, whereas their different abilities to gelate solvents are solely due to configurational isomerism.

2.3.1. Structure-property correlation

Shinkai and co-workers investigated gelation properties of this type of gelators (**6-10**) extensively (Fig. 10).[96-99] Among the α-monosaccharides, only the *manno*-**6a**, *gluco*-**7a** and *galacto*-**10a** isomers act as gelators in organic solvents. According to the T_{gel} values and the variety of liquids gelated, the trend in the gelation ability is **6b** > **6a** > **7a**. In contrast, among the β-isomers only the *manno*-**6b** and *galacto*-**10b** isomers act as gelators. The gelation efficiency and T_{gel} of the β-anomer of galactose derivative **10b** are better than that of the α-anomer (**10a**). However, the α-allo-**8a** and α-altro-**9a** were insoluble or resulted in precipitation. The inability of these gelators to gelate a variety of organic liquids could be explained by their inability to form 1-D aggregates in which both hydroxyl groups participate.[100] Gelators often form fibrous structures. However, the β-gluco, allo and altropyranosides (**7b**, **8b** and **9b**) did not satisfy the requirements to gelate organic liquids concerning the direction of OH groups though they exhibited fibers under scanning electron microscope (SEM).[101]
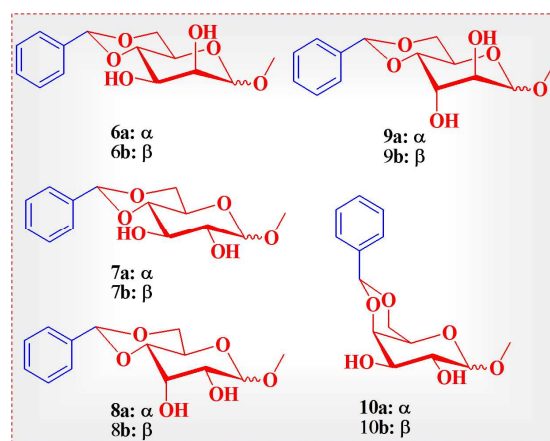

Fig. 10 Chemical structures of methyl 4, 6-*O*-benzylidene derivatives of various monosaccharides, **6-10**.

2.3.2. Structural analysis

Crystals of **7a** were grown from ethyl acetate in order to understand the molecular packing by a single-crystal X-ray diffraction analysis (Fig. 11).[96] Interestingly, the crystals grown from the gelating liquid also revealed similar packing arrangements. However, their diffracting quality was worse. Molecules of **7a** were connected by two hydrogen bonds using the 2-OH and 3-OH groups to generate 1-D zigzag chains.

Small-angle X-ray scattering (SAXS), is a useful technique to acquire information regarding the supramolecular structures present in the gels. Fig. 12 shows a typical temperature-dependent SAXS profile of methyl 4, 6-*O*-benzylidene-α-D-mannopyranoside (**6b**) (1.5 wt-% in *p*-xylene).[96]
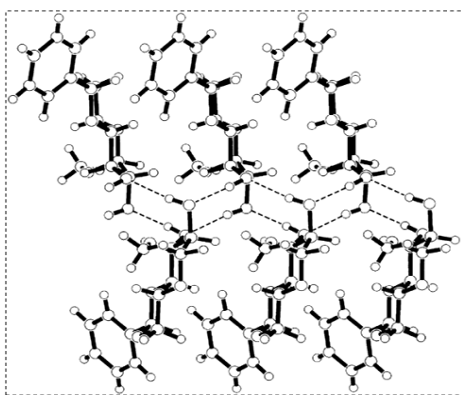
Fig. 11 Single crystal structure of methyl 4, 6-*O*-benzylidene-α-D-glucopyranoside (**7a**). Reprinted with permission from ref. 96. Copyright 2001, Wiley-VCH Verlag GmbH.

It exhibited two broad peaks at q = 0.018 and 0.11 Å^{-1}. With increasing temperature (60 °C) the position of these peaks remains unaffected, however, the intensity of the peak at q = 0.018 Å^{-1} diminished about 50% and vanished completely at 70 °C due to gel-to-sol transition.
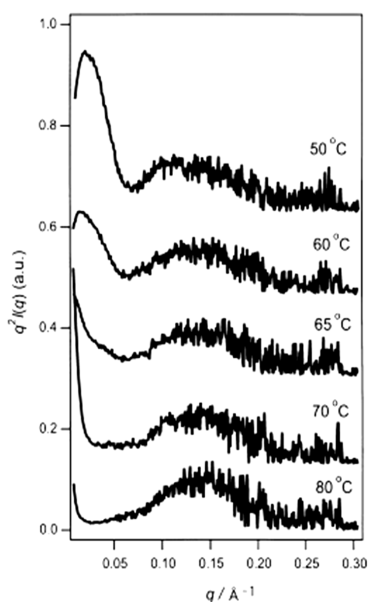

Fig. 12 Temperature-dependent SAXS profiles of **6b** (1.5 wt-% in *p*-xylene). Reprinted with permission from ref 96. Copyright 2001, Wiley-VCH Verlag GmbH.

Later, the same group performed a SAXS study of an organogel system derived from **6b** and *p*-xylene.[102] Detailed analysis of the SAXS data revealed existence of hexagonal organization of fibrils in the gel state and the inter-fibrillar spacing was evaluated to be ~60 Å. Temperature-dependent changes in the time-resolved SAXS experiment of 1.0 wt-% gel were collected in the temperature range of 20-100 °C. The lower panel of Fig. 13 refers to the scattering at the low *q* regime, which appeared within 400 s possibly because of the phase separation for the gelator rich phase and the solvent-rich phase. The peaks associated with the hexagonal structure did

not show up until 1540 s and they grew gradually after 1540 s (upper panel of Fig. 13). Thus, development of hexagonal structure occurred after the phase separation, and the gelation took place just before the development of the hexagonal structure.
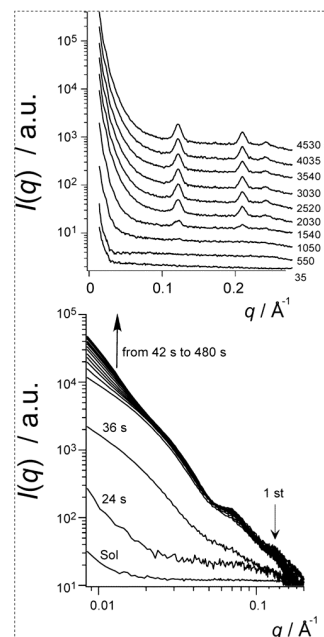

Fig. 13 Changes in the scattering profiles of **6b** with time after temperature was changed from 100 (sol) to 20 (gel) °C for 1.0 wt-% gel in *p*-xylene. The initial change is shown in the lower panel, and the later stage is the upper panel. Reprinted with permission from ref. 102. Copyright 2003, American Chemical Society respectively.
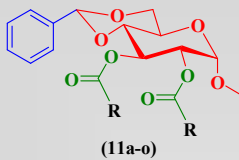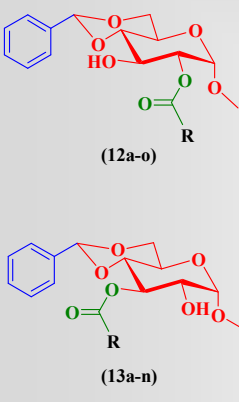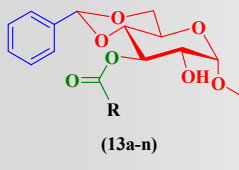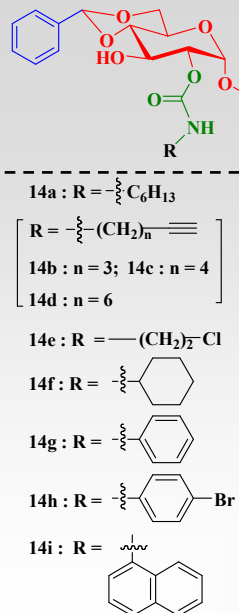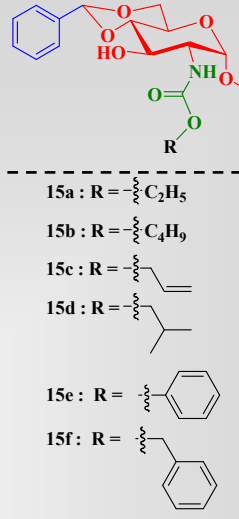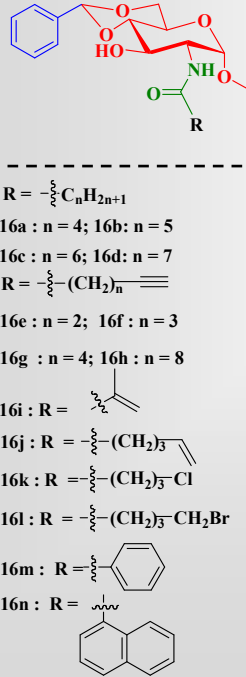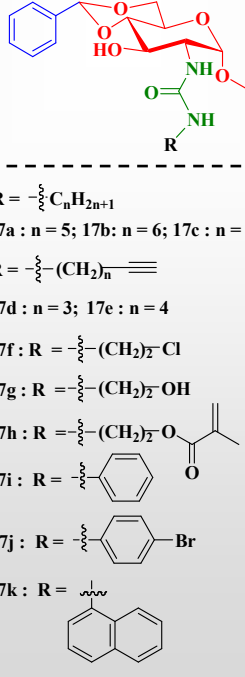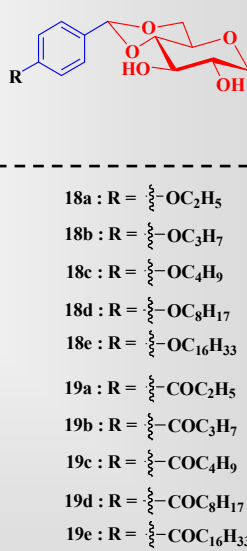
2.3.3. Structural modification

Wang and co-workers investigated gelation properties of a large number of methyl 4, 6-*O*-benzylidene-α-D-glucopyranose derived LMWGs.[104-109] Modification of the 2- and 3-hydroxyl groups of methyl 4, 6-*O*-benzylidene-α-D-glucopyranose *via* ester,[104,105] carbamate,[106] amide[107] and urea[107,108] linkages offers a wide range of opportunities to study the influence of these functionalities on their self-assembly processes. Among the ester derivatives containing terminal alkynyl group (**11a-f**, **12a-e** and **13a-f**), the diesters (**11a-f**) appeared as insoluble in water because of the lack of free –OH groups (Table 1).[104] However, the diester derivative having shorter chain (**11a**) could form gel in *n*-hexane and ethanol. Interestingly, shorter chain monoesters (**12a-c** and **13a-c**) with one free –OH group exhibited versatile gelation in *n*-hexane and in water but they led to sol formation in ethanol. This observation indicates that the participation of the free –OH group in the self-assembly process is necessary for hydrogelation. However, attachment of two aliphatic acyl chains (**11g** and **11i-m**) disfavoured gelation process in any of these solvents presumably due to the compact packing of the saturated hydrocarbon chains in contrast to alkynyl chains (Table 1).[105] Grafting of aromatic platforms (**11n** and **11o**)

could modulate the aggregation behaviour to result in gelation in 1:1 EtOH/water mixtures. In case of 2-monoesters (**12g-o**) and 3-monoesters (**13g-n**), compounds with terminal C=C (**12h** and **12m** in water, **13m** in 1:1 ethanol/water) or naphthyl moiety (**12o** in water) showed promising results. However, the benzoate monoesters (**12n** and **13n**) did not induce gelation in any of the solvents tested. Hydrogen bonding is the major driving force for the methyl 4, 6-*O*-benzylidene-methyl-α-D-glucopyranose analogues to induce hydrogelation. Hence, using carbamate[106] or amide[107] or urea[107,108] groups instead of ester as linkages improves gelation efficiency because they offer additional accessible hydrogen bonding donor (-N-H) and acceptor (-C=O) sites. Since carbamate linkage has strong influence in the gelation process over ester, presence of a terminal acetylene group is no more a necessary requirement to exhibit efficient gelation in case of O-linked carbamates (**14a-i**).[106] The saturated alkyl (**14a**) and cyclohexyl (**14f**) derivatives exhibited efficient hydrogelation in the presence of 33% co-solvent (DMSO or EtOH).

Table 1. Molecular structures of methyl 4, 6-*O*-benzylidene-α-D-glucopyranose derivatives **11-19**.

For **11a-o**:
R = –(CH$_2$)$_n$–C≡CH
a : n = 2;   d : n = 6
b : n = 3;   e : n = 8
c : n = 4;   f : n = 10
g : R = –(CH$_2$)$_3$–Cl
h : R = –(CH$_2$)$_2$–CH=CH$_2$
i : R = –(CH$_2$)$_3$–CH$_3$
j : R = CHMe$_2$
k : R = C$_6$H$_{13}$
l : R = C$_8$H$_{17}$
m : R = CH$_2$=C(CH$_3$)–
n : R = phenyl
o : R = naphthyl

14a : R = C$_6$H$_{13}$
R = –(CH$_2$)$_n$–C≡CH
14b : n = 3; **14c** : n = 4
14d : n = 6
14e : R = –(CH$_2$)$_2$–Cl
14f : R = cyclohexyl
14g : R = phenyl
14h : R = –C$_6$H$_4$–Br
14i : R = naphthyl

15a : R = C$_2$H$_5$
15b : R = C$_4$H$_9$
15c : R = CH=CH$_2$ alkenyl
15d : R = isobutyl
15e : R = phenyl
15f : R = benzyl

For **16**:
R = C$_n$H$_{2n+1}$
16a : n = 4; **16b** : n = 5
16c : n = 6; **16d** : n = 7
R = –(CH$_2$)$_n$–C≡CH
16e : n = 2; **16f** : n = 3
16g : n = 4; **16h** : n = 8
16i : R = isopropenyl
16j : R = –(CH$_2$)$_3$–CH=CH$_2$
16k : R = –(CH$_2$)$_3$–Cl
16l : R = –(CH$_2$)$_3$–CH$_2$Br
16m : R = phenyl
16n : R = naphthyl

For **17**:
R = C$_n$H$_{2n+1}$
17a : n = 5; **17b** : n = 6; **17c** : n = 7
R = –(CH$_2$)$_n$–C≡CH
17d : n = 3; **17e** : n = 4
17f : R = –(CH$_2$)$_2$–Cl
17g : R = –(CH$_2$)$_2$–OH
17h : R = –(CH$_2$)$_2$–O–C(=O)–C(CH$_3$)=CH$_2$
17i : R = phenyl
17j : R = –C$_6$H$_4$–Br
17k : R = naphthyl

18a : R = OC$_2$H$_5$
18b : R = OC$_3$H$_7$
18c : R = OC$_4$H$_9$
18d : R = OC$_8$H$_{17}$
18e : R = OC$_{16}$H$_{33}$
19a : R = COC$_2$H$_5$
19b : R = COC$_3$H$_7$
19c : R = COC$_4$H$_9$
19d : R = COC$_8$H$_{17}$
19e : R = COC$_{16}$H$_{33}$

Interchanging the positions of the nitrogen and the oxygen atoms of the carbamates (N-linked carbamates) afforded another series of efficient gelators (**15a-f**) capable of immobilizing water/DMSO mixture (2:1).[106] Most of the synthesized amide derivatives (**16a-h**, **16j-m**) formed stable hydrogels at significantly low concentrations (< 5%) in presence of 33% co-solvents such as, DMSO or ethanol (Table 1).[107] Compounds **16i** and **16n** could immobilize only water/ethanol (2:1) mixture at a significantly higher concentration (10 mg/mL). Similar to the amides, urea derivatives (**17a-k**) also exhibited excellent gelation ability in the same solvent mixtures.

Decoration of the para-position of the phenyl ring of methyl 4, 6-O-benzylidene-α-D-glucopyranoside by n-alkoxy (**18a-e**) or n-alkoxycarbonyl (**19a-e**) substituents of various lengths afforded a new series of sugar-derived LMWGs (Table 1).[132] Among these sugar derivatives, **18b-e** and **19b-e** were capable of forming gels in a diverse range of organic solvents such as, alcohols (methanol, 1-propanol, 1-butanol), aliphatic (n-heptane and n-dodecane), aromatic (benzene and toluene) and halogenated (CCl$_4$ and C$_2$Cl$_4$) solvents depending upon the gelator chain length. Versatility of gelation enhanced upon increasing the length of the hydrocarbon chain. Compounds **18e** and **19e** behaved as most efficient gelators among this series of compounds. Importantly, gelation process became sluggish in methanol indicating presence of hydrogen bonding interactions between the gelator and solvent molecules. Compound **18a** formed gel only in n-dodecane whereas, compound **19a** failed to immobilize any of these solvents tested.

2.3.4. Charge-transfer

Charge-transfer (CT) gelators comprise certain class of gelators, which are capable of forming gel in a desired solvent in the presence of electron-rich or electron-deficient guests often accompanied by significant visual changes in colour. CT-interaction is comparable to hydrogen bonding because of its complementary nature, which allows alternate stacking of aromatic donor (D) and acceptor (A) chromophores.[63] Gel formation mediated by CT-interaction has been extensively applied to promote the self-assembly process in aqueous and organic medium. Maitra *et al.* reported the first example of a donor-acceptor based organogelation of pyrene derivatives in presence of 2, 4, 7-trinitroflurenone (TNF) as an acceptor.[133]

Shinkai and co-workers introduced the first example of donor-acceptor type interactions in sugar-based two-component system, where both the donor and the acceptor moieties are gelators independently.[134] These authors investigated charge-transfer (CT) mediated two-component gelation in a variety of organic liquids and water at different compositions of two sugar-based molecules, one containing an electron-donor group and the other an electron-acceptor functionality. The p-nitrophenyl derivative **20a** was capable of gelling both aromatic solvents, as well as non-aromatic polar solvents. It was also an efficient gelator for water, while it showed poor performance in non-aromatic nonpolar solvents because of its high tendency to

form precipitates (Fig. 14a). In contrast, the p-amino phenyl derivative **20b**, induced gelation in limited solvents (Fig. 14a).

When a mixture of **20a** and **20b** in a 1:1 molar ratio, in n-octanol or diphenyl ether, was heated, the white powders were rendered soluble to result in a colourless solution, which subsequently transformed into a yellow gel upon cooling to room temperature. Furthermore, investigation of thermal stability by T$_{gel}$ measurements revealed that presence of acceptor (**20a**) and donor (**20b**) in equal proportion (1:1) enhanced the thermal stability of the resulting gel. The donor-acceptor interaction associated with the gelation was monitored by UV-Vis spectroscopy (Fig. 14b). Initially, the intensity of the shoulder at 335 nm diminished followed by a simultaneous increase in the intensity at higher wavelengths (380-800 nm) during sol-to-gel transition (from t = 0 to t = 10 min). During this time, a light yellow colour appeared. Subsequently, intensity of the shoulder at 335 nm monotonically decreased and the signal around 420 nm enhanced due to the intensification of the yellow colour of the gel (Fig. 14b). Such behaviour of UV-Vis absorption spectra in the 350-600 nm range indicates the formation of a charge-transfer complex. Fibrous networks were found under TEM for single-component gels in diphenyl ether while the dual-component gel exhibited helical fibers attributed to the charge-transfer interaction.
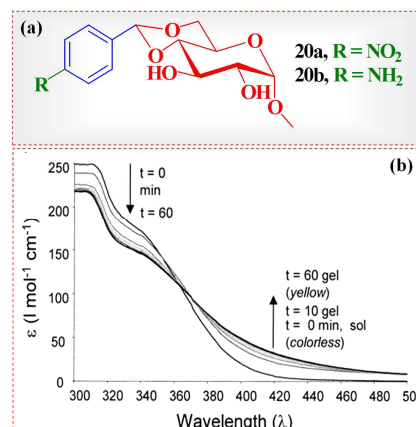

Fig. 14 (a) Chemical structures of **20a** and **20b**. (b) Time-dependent changes in the UV-Vis spectra of a 2 wt-% sample in n-octanol containing 1:1 molar ratio of **20a** and **20b**. At t = 0 min, the sample completely dissolves, at t = 10 min gelation occurs, and between t = 10 and t = 60 min the yellow colour of the gel intensifies significantly. Reprinted with permission from ref. 134. Copyright 2002, American Chemical Society.

2.4. Sugar-derived amphiphilic LMWGs

2.4.1. Monosaccharide-based amphiphiles

Aliphatic hydrocarbon chain linked sugar-based amphiphiles self-assemble *via* hydrogen bonding and van der Waals interactions in water. This type of molecules are similar to the lipids or surfactants due to the presence of hydrocarbon segments and the hydrogen bond forming sugar moiety based hydrophilic headgroups. However, strong hydrogen bonding interaction among the headgroups induces unidirectional

propagation of molecular self-assembly which finally leads to formation of fibers or ribbons, as illustrated in Fig. 6.

In one of the early reports, Bhattacharya *et al.* demonstrated facile hydrogelation from D-maltose and D-lactose based *N*-alkyl disaccharide amphiphiles (Fig. 15).[111] Among six disaccharides (**21a-c** and **22a-c**), compounds **21a** and **22a** exhibited efficient immobilization of water (>6000 molecules of water per gelator molecule). In contrast, **21b** and **22b** did not result in gel formation at all even after 24 h. The low mgc values of the *N*-alkyl disaccharide amphiphiles (**21a** and **22a**) were attributed to the presence of large inter-lamellar spaces where the water molecules are immobilized by capillary forces. However, compound **21c** or **22c** exhibited low gelation efficiency and only ~800 molecules of water per gelator molecule were gelated.
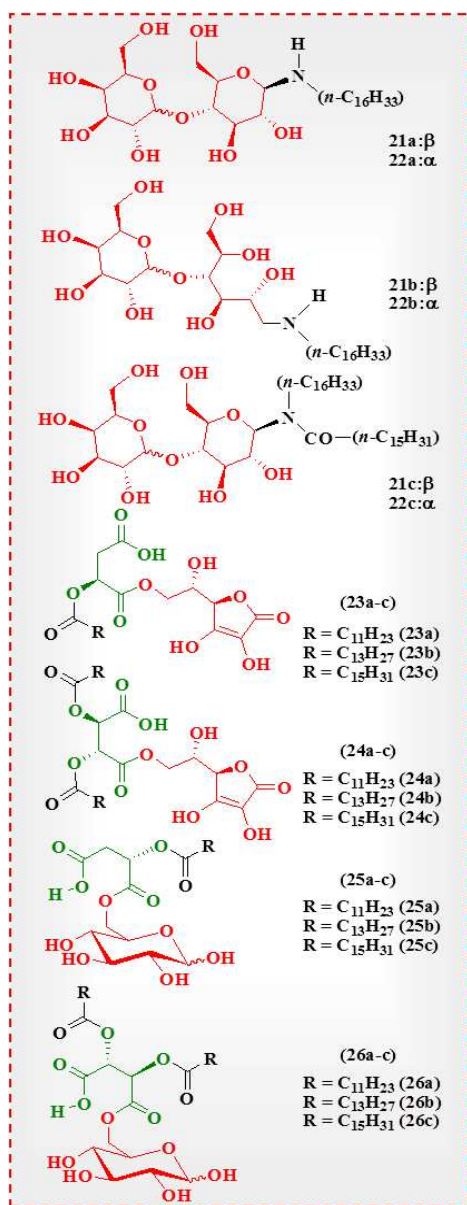

Fig. 15 Chemical structures of some sugar-derived amphiphiles **21-26**.

Nandi and co-workers synthesized a series of novel lipid-modified vitamin C derivatives (**23a-c** and **24a-c**), which are combination products of fatty acids and hydroxy carboxylic acids (tartaric acid and malic acid) linked to the primary hydroxy group of ascorbic acid *via* ester bonds (Fig. 15).[135] These authors investigated the influence of variation of hydrocarbon chain length toward gelation. These compounds exhibited interesting properties as surfactants, emulsifiers, oil-soluble antioxidants, and highly effective gelators in both organic solvents and in water. It was found that the gelation ability and gel stability in water were highly influenced by the length of the hydrocarbon chains. Amphiphile **23c**, **24b**, and **24c** formed significantly stable hydrogels at room temperature. In contrast, tartaric and malic acid based amphiphiles with shorter chains (C_{12}) produced stable hydrogels only at low temperatures. Thus, increase in the chain lengths for both tartaric and malic acid amphiphiles promoted higher extent of association among the fibers through van der Waals forces and drove these amphiphiles to organize in lamellar arrangements.

In another report, these authors also explored a series of similar type of amphiphilic molecules (Fig. 15) by systematic variation of the alkyl chains (C_{12} to C_{16}) of the *O*-acylated hydroxycarboxylic acid anhydrides (tartaric and malic acid anhydride) linked to the D-glucose moiety *via* an ester bond (**25a-c** and **26a-c**).[136] Among these amphiphiles, **26a** could gelate both non-polar solvents and water. However, **25a-c**, **26b** and **26c** were capable of gelling only a few solvents other than water. This implied presence of a subtle balance between hydrogen bonding and van der Waals interactions is essential to induce gelation in water or in an organic medium.

Aldopyranoside-derived gelators **27a** and **27b** represent good examples of amphiphilic gelators containing a sugar moiety, an aminophenyl, and a long alkyl chain reported by Jung *et al.* (Fig. 16a).[110,112] These compounds formed opaque gels in a series of organic solvents and in water in presence of small amount of alcoholic solvents. Interestingly, their bolaamphiphilic analogues (**28a** and **28b**) could immobilize both organic solvents and water without addition of any co-solvent indicating higher solubility owing to the presence of two sugar headgroups. Bolaamphiphilic aldopyranosides are superior to simple monomeric amphiphiles concerning mgc and stability. A combination of hydrogen bonding, π-π stacking and hydrophobic forces led to the formation of a bilayer arrangement in supramolecular assemblies of these amphiphiles as confirmed by ^{1}H-NMR and WAXD studies (Fig. 16b-e).

Kameta *et al.* showed nanotape and nanotube formation from self-assemblies of two glycolipids depending upon the nature of the headgroup differed by the bonding position of the boron atom in the naphthalene ring (Fig. 17a).[137] Compound **29b** furnished an organogel (mgc = 0.1 wt-%) upon cooling a hot solution of the gelator to room temperature (Inset, Fig. 17b), whereas compound **29a** led to precipitation. Morphological investigation of the precipitates and the xerogel obtained from **29a** and **29b** respectively by electron microscopy revealed the existence of nanotapes (20-100 nm) and nanotubular structures with uniform nanochannel of 15 nm

inner diameters (Fig. 17b and c). These results clearly ascribe strong morphological dependence on the bonding position of the boron atom in the naphthalene ring.
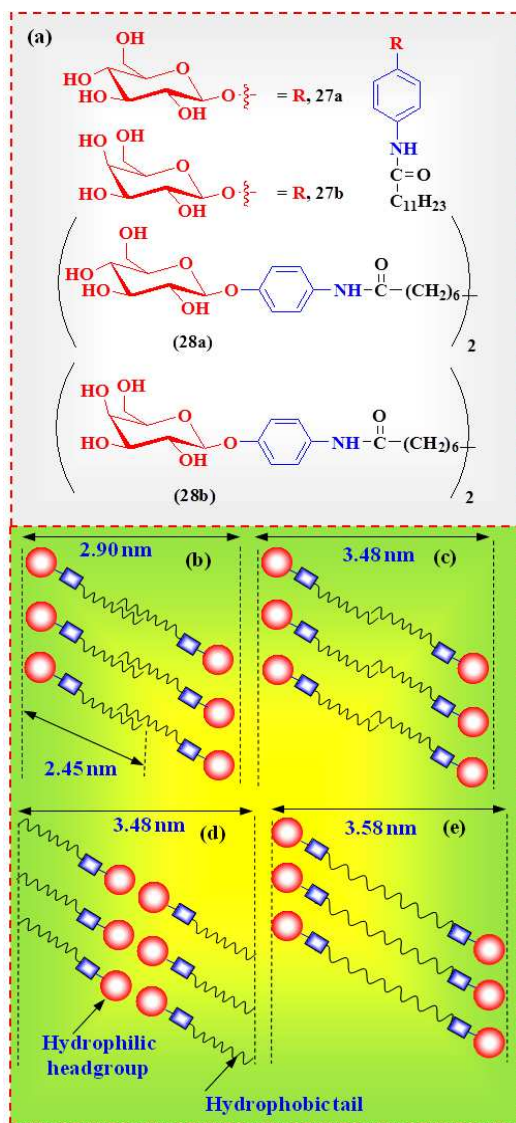
Fig. 16 (a) Chemical structures of some sugar-based amphiphiles and bolaamphiphiles having aromatic spacer **27** and **28**. Proposed molecular arrangement in the supramolecular aggregates of (b) the hydrogels **27a** and **27b**, (c) and (d) the organogels **27a** and **27b**, and (e) the hydrogel **28b**.

The nanotube from **29b** exhibited an intense narrow fluorescence band at 350 nm associated with the monomeric species of the naphthalene group. However, a weak and broad fluorescence band in the region of 405 nm was observed in case of the nanotape from **29a** attributed to the excimer species of the naphthalene unit. This result suggests tighter packing of the molecules in the bilayer membranes of nanotubes compared to that in nanotapes. Furthermore, anthracene as a guest fluorescent acceptor could be encapsulated in the nanochannel of the nanotubes of **29b** in order to induce efficient energy-transfer (Fig. 17d-f). This is owing to the characteristic

absorption band of anthracene, which overlaps, well with the emission band associated with the naphthalene moieties in the nanotube. It was further observed that light energy adsorbed by the densely packed naphthalene moieties in the bilayer membrane could be transferred into the encapsulated acceptor (anthracene), with high quantum efficiency.
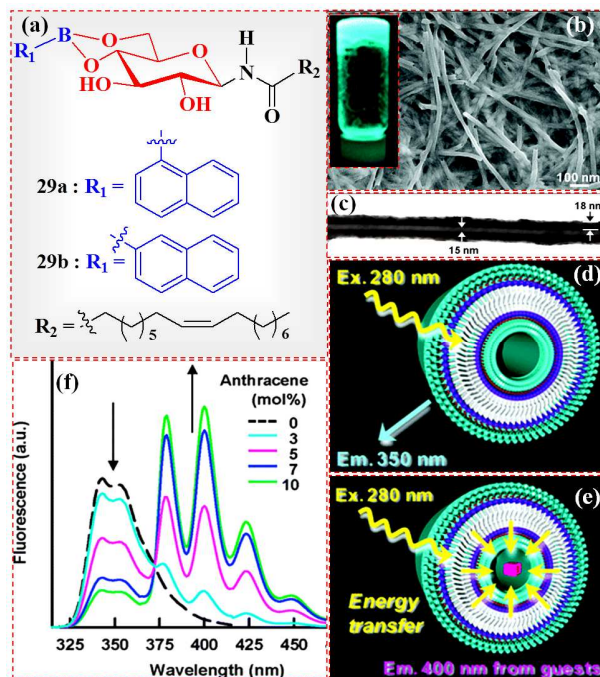
Fig. 17 (a) Chemical structures of glycolipids **29a** and **29b**. (b) SEM and (c) TEM images of nanotubular structures formed from **29b**; Inset shows photograph of the associated toluene gel of **29b**. (d) and (e) Schematic representations of the energy transfer from the naphthalene moieties (the host) within the bilayer membranes of the nanotube wall to the encapsulated anthracenes (the guest) in the nanochannel. (f) Fluorescence spectra of the nanotube encapsulating anthracenes in the nanochannel (solid lines) and the only nanotube (dotted line) in CHCl₃. Reprinted with permission from ref. 137. Copyright 2011, American Chemical Society respectively.

2.4.1.1. Effect of unsaturation of the hydrocarbon chains

Presence double or triple bond in the hydrocarbon chain of amphiphilic sugar-based gelator may have strong influence towards the gelation properties. Shimizu *et al.* showed that gelation and aggregation behaviour of a series of cardanyl (glucoside)s (**30a-d**) could be modulated by the unsaturation of the alkyl chain (Fig. 18).[138] Saturated member **30a** and the monoene **30b** both were capable of forming gel in 1:1 water/EtOH mixture (v/v). DSC studies revealed that the T_{gel} of **30a** in water/ethanol (1:1, v/v) gel was 69 °C, which decreased to 30 °C upon insertion of a single cis double bond in the case of monoene **30b**. Interestingly, the diene **30c** and triene **30d** hardly exhibited gelation in any solvent system undertaken, even upon cooling to -6 °C. This result clearly shows the strong influence of the number of double bonds located on the lipophilic part of the gelator on the stability of the gel.

In an another instance, Jung *et al.* introduced a sugar-based gelator **31a** (Fig. 18) bearing a lipophilic diacetylene group which showed efficient hydrogelation in the absence of organic solvent even at significantly low concentration (0.05 wt-%).[139] In contrast, the gelator **31b** failed to form hydrogel indicating the crucial role of a triple bond in the hydrogelation process. This result is attributed to the comparatively stronger inter-molecular hydrogen bonding interactions between the sugar moieties of **31a** by disordered molecular packing between the diacetylene moieties, compared to that of the gelator **31b**.
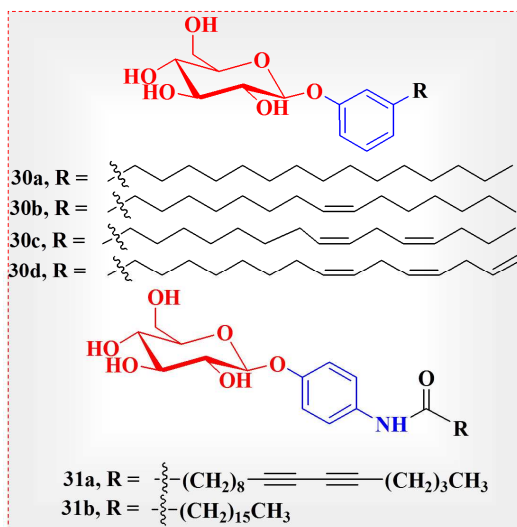

Fig. 18 Chemical structures of **30** and **31**.

2.4.2. Liquid-crystalline disaccharide-based LMWGs

Fig. 19 shows three amphiphilic glycolipids (**32a-c**) containing a maltose[140] (**32a**) or a cellobiose[141] (**32b**) or a lactose[141] (**32c**) as polar headgroup and a hydrocarbon chain reported by Oriol and co-workers. Each of these glycolipids gave rise to thermoreversible and stable gels in water. Maltose and lactose derivatives both formed gels at mgc of ~1 wt-%, while the cellobiose based lipid exhibited comparatively higher gelation efficiency (mgc ~0.5 wt-%). Morphological studies of cellobiose or lactose lipid aggregates by transmission electron microscopy (TEM) showed right and left-handed helical ribons respectively whereas the maltose derivative showed simple fibers.

Interestingly, these glycolipids showed characteristic birefringent textures under POM associated with thermotropic liquid-crystalline properties. The maltose derivative exhibited a thermotropic transition peak around 50 °C, above which it remained as a viscous liquid, and became a mobile fluid above ~90 °C. Similar behaviour was observed for the cellobiose and lactose compounds as well, although the mesophases appeared at relatively higher temperatures, around 160 and 150 °C, respectively. Textures observed under POM in these cases were similar to that of the maltose derivative.
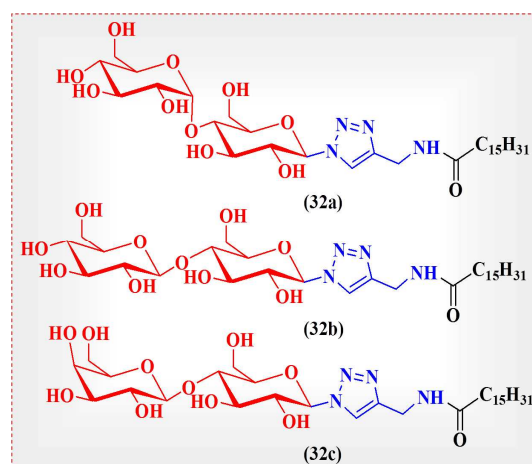

Fig. 19 Molecular structures of amphiphilic glycolipids **32a-c**.

2.5. Advantages of attaching porphyrin

Suitable modification of sugar derivatives by integration of planar π-conjugated molecules has allowed the formation of self-assembled structures in organic solvents or in water (Fig. 6). Porphyrins are well known to form one-dimensional aggregates whose major driving force is considered to be π-π stacking interactions. Presence of a chromophoric part in the sugar-based gels also offers an opportunity to follow the structural transformation associated with the gel-to-sol transition by UV-Vis and circular dichroism (CD) spectroscopy. Shinkai reported a series of classic examples of organogelators (**33a-e**), each comprising a porphyrin connected to four sugar moieties through amide linkages (Fig. 20a).[113,114] The synergistic effect of the π-π stacking interactions among the porphyrin moieties and the hydrogen-bonding interactions among the sugar moieties led to the formation of stable one-dimensional aggregates indispensable for the gel formation. Porphyrin derivatives **33a-c** were found to immobilize efficiently DMF/poor solvent (*e.g.*, methanol, ethanol, 2-propanol, 1-butanol and benzyl alcohol) 1:3 (v/v) mixed solvent. However, **33d** appeared as a weak gelator, whereas **33e** was completely soluble in most of the solvent systems tested.

UV-Vis spectrum of **33a** (2.3 μM) in DMF showed the Soret band at 422 nm, and the Q bands at 517, 553, 593, and 647 nm (Fig. 20b). In contrast, the Q bands experienced bathochromic shifts, whereas the Soret band shifted to a shorter wavelength along with the appearance of a shoulder around 430 nm in DMF/benzyl alcohol gel elucidating an H-type aggregation mode in the 1D-porphyrin stacks. Similar trend was followed in case of **33b** (3.9 μM) and **33c** (3.9 μM) as well. The CD spectrum of the gel of **33a** exhibited a positive exciton splitting indicating helically twisted porphyrin column by the chiral peripheral saccharide groups. Notably the CD-spectrum of the homogeneous solution of **33a** did not show any peak (Fig. 20c). Compound **33b**, which differed from **33a** by the stereochemistry of the anomeric position of the sugar skeleton, gave rise to exactly the same CD signature with

opposite sign. Completely different pattern of the CD signal of **33c** was attributed to the changes in the aggregation mode of **33c** compared to that of **33a** and **33b**.
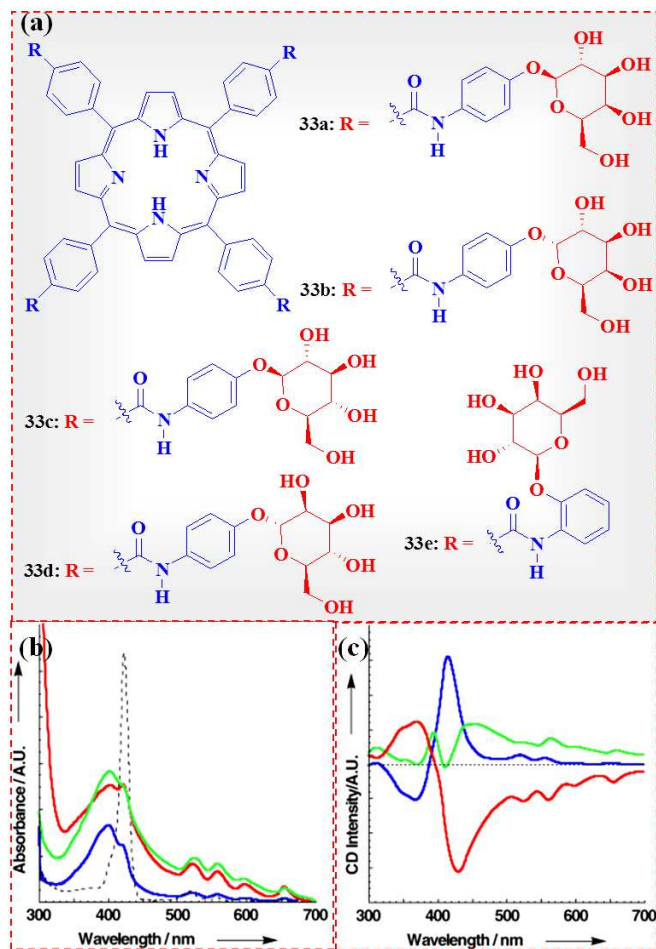

Fig. 20 (a) Molecular structures of **33a-e**. (b) UV-Vis and (c) CD-spectra of the gels: blue; **33a**, red; **33b**, and green; **33c** (DMF/benzyl alcohol 1:3 (v/v)), [**33a-c**] = 7 g/cm³ (25 °C), and dotted line; homogeneous solution of **33a** (DMF/benzyl alcohol 1:2 (v/v), [**33a**] = 2.3 μM (25 °C). Reprinted with permission from ref. 114. Copyright 2004, Wiley-VCH Verlag GmbH & Co. KGaA.

2.6. CH-π interactions

Ulijn and co-workers examined supramolecular hydrogelation mediated by self-assembly of fluorenyl methoxycarbonyl (Fmoc) integrated carbohydrate amphiphiles (Fig. 21).[142] Compounds **34a** and **34b** afforded translucent hydrogels upon cooling their hot solutions in water or PBS (pH 7.4, 0.01 M phosphate buffer, 0.0027 M KCl and 0.137 M NaCl). In contrast, compounds **34c-f** failed to form hydrogels. This was the first instance where the self-assembly of the hydrogelators (**34a** and **34b**) was promoted by a combination of CH-π and T-stacking interactions of fluorenyl groups, instead of conventional face-to-face π-π stacking and H-bonding interactions as observed with Fmoc-peptide based systems.
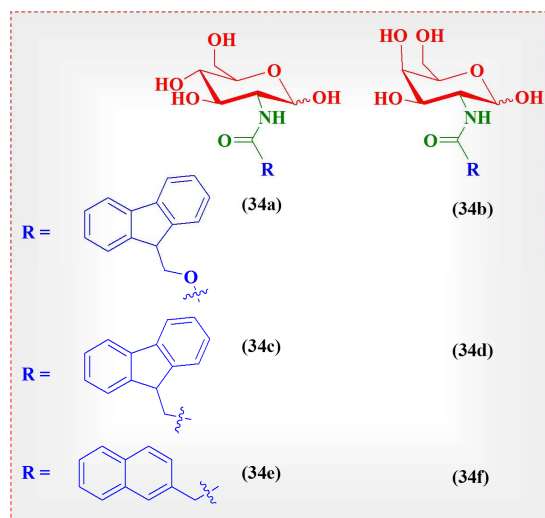

Fig. 21 Chemical structures of **34a-f**.

2.7. Metal-ligand coordination

Utilization of metal-ligand coordination as a driving force in order to induce gelation in organic solvents or aqueous medium offers another approach to get access to intriguing properties such as fluorescence, phosphorescence, catalytic and redox properties *etc*. These depend upon the metal centers, coordination geometry and coordinating ligands, which may not be easily attainable by simple gelation of small molecules.[57-61] In one of the earlier reports, Nolte described gelation properties of Pd(II) and Pt(II) complexes of the pyridine-functionalized gluconamides (Fig. 22).[143] Complex *trans*-[Pt(**35a**)₂Cl₂] exhibited efficient gelation in tetrahydrofuran (THF), toluene and MeOH. Interestingly, the analogous *trans*-palladium(II) complex of **35a** was also capable of immobilizing THF. However, *trans*-[Pd(**35b**)₂Cl₂] failed to induce gelation, presumably because of the conformational constraints of the molecule which is not favourable for rod-like geometry of the assemblies.
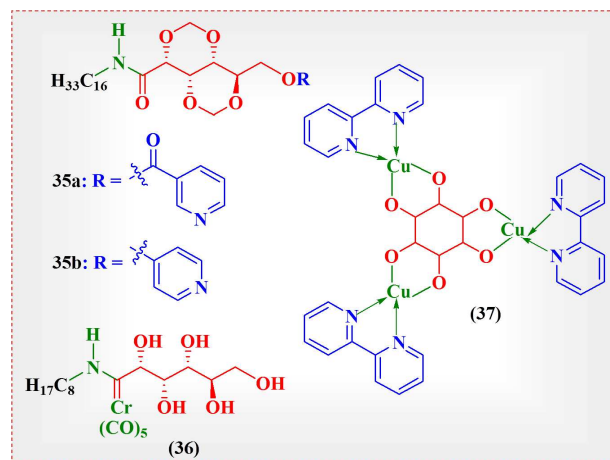

Fig. 22 Chemical structures of **35-37**.

Dötz and co-workers reported thermoreversible organogelation in chlorinated and aromatic solvents and in their mixtures by an aminocarbene-chromium complex synthesized from pentacarbonyl chromate and pentaacetylated gluconic acid chloride (**36**) (Fig. 22).[144] Substitution of the carbonyl oxygen atom by apolar pentacarbonylchromium fragment had a strong influence in the modulation of solubility of the amphiphile. Aggregation mode of this metal-carbene complex was found to depend on both the solvents (mixture) and on the cooling rate. Significant enhancement of CD signal was observed in chloroform gel compared to that of the solution at 50 °C. Furthermore, UV bands at 350 nm (metal-to-ligand charge transfer), 320 nm (ligand-field transition) and 270-260 nm (ligand-to-metal charge transfer) associated with the organometallic chromophore were observed in the absorption spectra. Though significant change was not observed in the temperature-dependent UV spectra, inversion of the CD signal around 270-260 nm (not the other ones) occurred after the third heating-cooling cycle, suggesting presence of kinetic and thermodynamic states in the aminocarbene chromium complex gel. Though the self-assembly process was driven by hydrogen bonding of the hydroxyl and amino group, reduction of the local C_{4v} symmetry on the pentacarbonyl chromium associated with the molecular packing effects on fiber formation was confirmed by FT-IR analysis.

Compound **37** is a trinuclear copper(II) complex with inositol and 2,2'-bipyridine capable of hydrogel formation at pH 12.4, promoted by H-bonding and inter- and intra-molecular π-stacking between the bipyridyls (Fig. 22).[145]

Gelation by this complex did not occur at neutral pH. The absorption maximum at 675 nm associated with the ligand field transition of $[Cu (bipy)]^{2+}$, shifted to 657 nm in the sol state of inositol-Cu-bipy (1:3:3) at natural pH due to the increase in the ligand field. However, at pH 12.4, gelation occurred and the absorption maximum appeared at 665 nm elucidating coordination of inositol and importance of the hydroxyl in the gelation process.

2.8. Dendritic sugar-derived gelators

Dendrons and dendrimers are precisely defined highly branched macromolecules with unique shapes and multiple functionalities.[146] Over the past decade, a large numbers of reports of self-assembly of dendritic organogelators and hydrogelators based on poly(amino acid), poly(amide), and poly(aryl ether) dendrons, or together with multiple alkyl chains on the periphery have appeared in literature.[147,148] However, only a few instances of sugar-derived dendrons have been reported.

Prasad and co-workers synthesized a new family of linear sugar-based poly(aryl ether) dendrons that self-assembled into gels most likely through the extensive hydrogen bonding and π-π interactions among the gelator molecules (Fig. 23).[149] Compound **38a** formed gel at a mgc value of 0.1% (w/v) in DMSO-water systems (1:9), while compound **38b** did not show gelation in the above mixture of solvents. Rather, compound **38b** immobilized alcoholic solvents to result in translucent organogels.
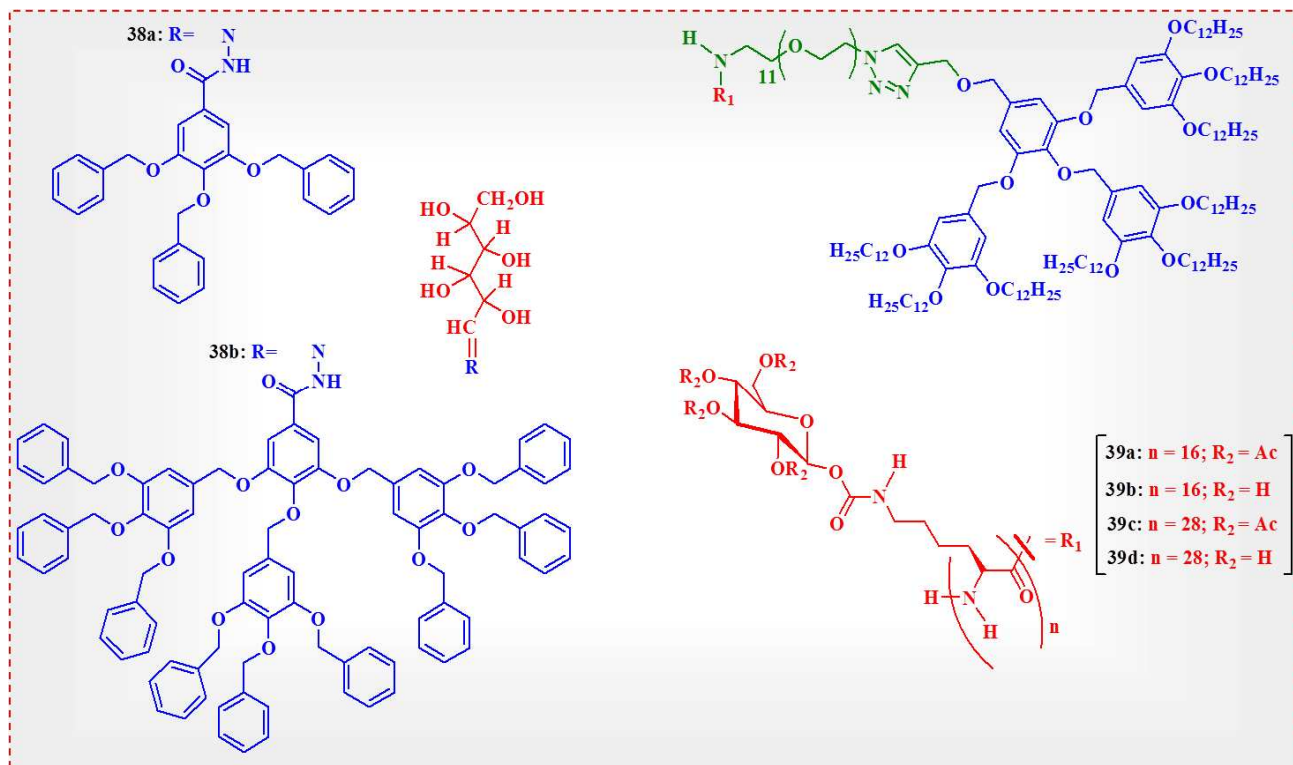

Fig. 23 Chemical structures of **38** and **39**.

Furthermore, a change in pH from neutral to basic condition (pH = 10, by addition of KOH) led to the conversion of the gel-to-sol transition accompanied by a morphological transition from nanofibers-to-spherical aggregates.

Pati *et al.* reported a series of amphiphilic glycopolypeptide (GP)-dendron conjugates (**39a-d**) based on a wedge-like dendron attached to stiff GP chains by a coil-like oligo(ethylene glycol) which self-assembled to result in organogels (Fig. 23).[150] Compound **39a** afforded organogel upon cooling a 0.7 wt-% clear solution in acetonitrile. However, **39c** did not form gel indicating that increased hydrophilicity in the amphiphilic glycopolypeptide was not conducive for gelation. Interestingly, both the glycopolypeptides (**39b** and **39d**) containing unprotected sugar moieties also formed organogels in DMSO.

2.9. Gluconamide type gelators

Amphiphilic molecules containing an aliphatic long chain attached to a carbohydrate headgroup through amide functionality form fibrous aggregates in water.[151,152] Welte and co-workers reported the first instance of gluconamide-derived gels (Fig. 24).[153] *N*-Alkyl gluconamides (**40a-c**) formed hydrogels, which generated right-handed helical fibers as revealed under electron microscope. Interestingly, the sol-to-gel transition temperature (T_g) decreased with decreasing hydrocarbon chain length. While, unstable gels formed in case of gluconamide derivatives having longer hydrocarbon chains (**40d** and **40e**) and transformed to crystalline needles. Methylation of the amide -NH of the *N*-alkylgluconamides resulted in a loss of gelation ability (**41a-e**). Compounds with two amide bonds (**42a** and **42b**) showed gelation at lower concentration similar to the monoamides. These however, showed high propensity of crystallization. Methylation of one of the amide bonds of the previous series led to another family of gluconamide derivatives (**43a-d**). Among them, only **43d** could form gel at room temperature. It also showed rope like fibrous structure with right handed helical signature similar to the *N*-alkylgluconamides. Later, Fuhrhop *et al.* demonstrated a quadruple helix formation with a magic-angle (54.7°) inclination from *N*-octyl-D-gluconamide **40c**.[115]

Maruyama and co-workers developed a series of novel LMWGs (**44a-c**) consisting of a long hydrocarbon chain and a gluconic acid moiety intervened by various amino acids (Fig. 24).[154] Interestingly, these LMWGs acted as efficient hydrogelators in a wide range of pH as well as organogelators in organic solvents, edible oil, biodiesel and ionogelator in ionic liquids at significantly low gelator concentrations (0.1-2 wt-%). This represents the first example where versatile gelation through the formation of nanofibrous networks could be achieved in aqueous media as well as in organic solvents, and ionic liquids from the same gelator system.

Fang *et al.* investigated the gelation behaviour of a family of gelators (Fig. 24), containing naphthalene unit as core attached to gluconamide functionality by linkers such as hydrazine, ethylenediamine, 1,3-propanediamine, 1,4-butanediamine, and 1,6-hexanediamine, respectively (**45a-e**).[155] In gelation

experiment, gelator **45a** acted as hydrogelator. Whereas, **45b** was capable of forming gel in both organic solvents and water, thus it acted as an "ambidextrous gelator". However, compounds **45c-e** behaved as organogelators only. Hence, a perfect transition from low-molecular mass hydrogelators (LMHGs) to ambidextrous gelator and then to low-molecular mass organogelators (LMOGs) could be achieved by a fine-tuning of the length of the spacers. Furthermore, results obtained from the UV-Vis, fluorescence spectroscopy confirmed the presence of a J-type aggregation mode of the naphthalene moieties, and an aggregation induced enhanced emission (AIEE) in the gel phase.
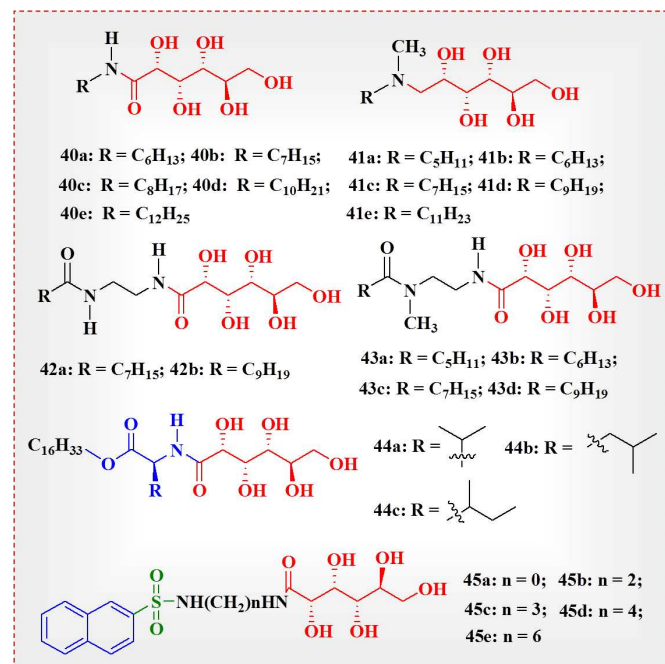

Fig. 24 Chemical structures of **40-45**.

3. Stimuli-responsiveness of sugar-based gels

Incorporation of a receptor or a stimuli-responsive functionality at the molecular level offers promising prospects for the design and construction of novel materials.[156-158] Apart from thermal responsiveness, various LMWGs also respond to other stimuli including sonication, host-guest interaction, external additives, light irradiation, pH, redox, cation, anion, enzyme, redox reactions, and solvent *etc* (Fig. 25a).[32,159] Thus, external perturbation can modulate the gel-to-sol transitions because of either reinforcement or weakening of weak non-covalent interactions involved in the assembly of molecular building blocks. These examples mimic natural phenomena like the seismonastic movement of mimosa leaves or tight curling up of millipedes upon touching and bursting of a water-filled balloon by poking a needle *etc* (Fig. 25b-d). This section will highlight some examples of this kind of stimuli-responsive gels, based on sugar-derived LMWGs endowed with various responsive groups to demonstrate the impact of molecular design principle

and future outlook for these fascinating gel-to-sol transition phenomena (Table 2).

Table 2. Stimuli-responsive properties of various sugar-derived LMWGs discussed in the present review.

Compound	Sugar Motif	Additional Functionality	Stimulus	Transition	Reversibility	Ref.
46	D-Glucoside	Terphenyl	Rate of cooling	Morphology	-	161[a]
47c	N-Acetylgalactosamine	Amide	Heat	Volume	Yes	162[b]
48a-c	D-Glucamine, N-Methyl-D-glucamine	Urea	Ultrasound	Sol-to-gel	-	164[b]
20a	D-Glucopyranoside	p-Nitrobenzylidene	Methyl-β-CD	Gel-to-sol	-	165[b]
49	β-CD	Cinnamoyl-trinitrophenyl	1-Adamantane carboxylic acid or urea	Gel-to-sol	-	166[b]
50a-b	β-CD	Acrylamide	Bisphenol A	Volume		167, 168[b]
51b-c	α-CD	C_6H_3-3,5-$(OMe)_2$	N-alkyl pyridinium	Sol-to-gel	-	169[b]
52a	D-Glucofuranose	Azo-benzene	Salt	Morphology	-	170[b]
54a-b	D-Lactose, D-Maltose	Azo-benzene	Light	Gel-to-sol	Yes	172[b]
55	N-Acetylgalactosamine	Fumaric amide	Light	Gel-to-sol	Yes	173, 174[b]
56	Gluconamide	Anthracene	Light	Gel-to-sol	No	175[b]
57	Trehalose	Acrylate	Light	Gel-to-sol	No	176[c]
58	γ-CD	Coumarin	Light	Sol-to-gel	Yes	177[b]
31a	D-Glucopyranoside	Diacetylene	Light	Colour	No	139[b]
59-62	D-Glucopyranoside	Diacetylene	Light	Colour	No	180-182[c]
63	N-Acetylgalactosamine	Amide	pH	Volume	Yes	183[b]
65a-c	D-Glucopyranoside	Amide	pH	Sol-to-gel	-	184[b]
66	Salen	D-Sorbitol	Cu^{2+}	Gel-to-sol	Yes	190, 191[a]
63	N-Acetylgalactosamine	Amide	Phosphate	Emission, FRET	-	192, 193[b]
69a	D-glucopyranoside	Aldehydephenylidene	Cysteine	Gel-to-sol	No	194[b]
70	Gluconamide	Pyrene	Insulin	Emission	No	195[b]
-	2-Glucosyloxyethyl methacrylate	Concanavalin A	Glucose	Volume	-	196[b]
71	D-glucopyranoside	Urea	Concanavalin A	Gel-to-sol	-	197[b]
72	D-glucopyranoside	Urea	Ionic Surfactants	Sol-to-gel	-	198[b]
73	Amygdalin	Fatty acid ester	Lipolase 100L, type EX	Gel-to-sol	No	94[b]
74a-77a	D-Glucosamine	Thymine, phenylalanine, phosphorylated tyrosine	Phosphatase enzyme	Sol-to-gel	No	200[b]
78a	D-Glucosamine	Fluorenylmethoxycarbonyl	Phosphatase enzyme	Sol-to-gel	No	201[b]
79a	D-Galactose	2-Naphthylacetic acid-Phe-Phe-Lys	β-Galactosidase enzyme	Sol-to-gel	No	202[b]

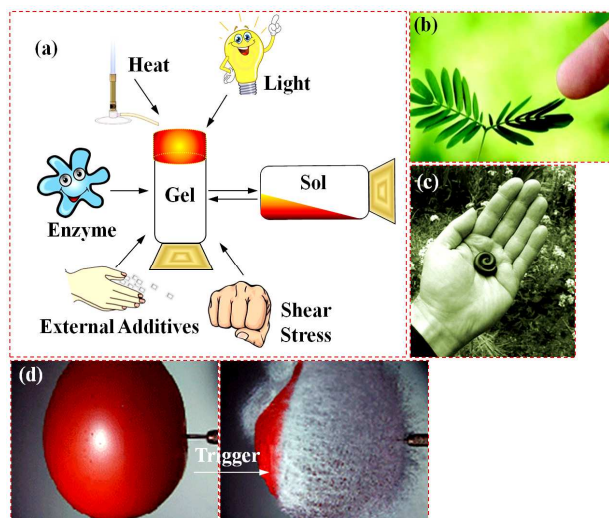[a] Aq./organic gel; [b] Hydrogel; [c] Organogel.

Fig. 25 (a) A schematic illustration of stimuli-responsive gel-to-sol transition process. Examples of stimuli-responsive natural phenomena and daily life happening; (b) seismonastic movement of mimosa leaves, (c) tight curling up of millipedes upon touching and (d) bursting of water-filled balloon by poking a needle.[160]

3.1. Temperature

3.1.1. Tuning of helicity

Supramolecular gels are often thermo-reversible and hence these are thermo-responsive in most of the cases. Compound **46**, 4"-butoxy-4-hydroxy-*p*-terphenyl-β-D-glucoside (Fig. 26a) is a LMWG which forms a thermo-reversible gel in 2:3 (v/v) H$_2$O/1,4-dioxane mixture.[161] However, it exhibits interesting features in the morphology associated with the molecular packing which is strongly influenced by the rate of cooling of the hot solution: the slow-cooling led to the formation of left-handed helical ribbons (Fig. 26b), while the right-handed counterparts are resulted in the fast-cooling process (Fig. 26c). This remarkable phenomenon could be explained by two kinds of packing modes of the gelator molecules (**46**) either in a clockwise or in an anticlockwise orientation. Hence, kinetically evolved right-handed helical ribbons gradually transform into the thermodynamically more stable left-handed helical form with further decreasing temperature. During fast cooling of the hot solution, the nuclei do not get enough time to grow thermodynamically stable state from the metastable state. Hence, the ribbons generated from them exhibited right-handedness.

3.1.2. Volume shrinkage

Kiyonaka *et al.* also reported a series of hydrogels derived from *N*-acetylgalactosamine appended amino acids (**47a-c**) which exhibited thermo-reversible swelling and shrinkage behaviour (Fig. 27a).[162] On heating, the volume of the gels remarkably shrank and expelled water instead of showing conventional gel-to-sol transition process (Fig. 27b). Furthermore, temperature induced release of DNA from these gels was examined by following the UV-Vis absorbance of the solution at 254 nm. The release of DNA enhanced significantly near the phase transition temperature of the gel (Fig. 27c). Additionally, removal of bisphenol A, a hydrophobic water pollutant, was achieved by entrapping it from an aqueous solution (840 μM) into the hydrophobic cavity of this gel **47c** (Fig. 27d).

This type of thermo-responsive soft gel matrix was further employed to regulate the rotary motion of an enzyme, F$_1$-ATPase at the single-molecule level in an on/off manner.[163]
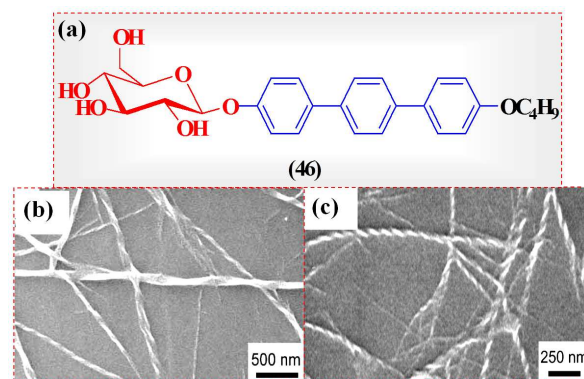

Fig. 26 (a) Molecular structure of 4"-butoxy-4-hydroxy-*p*-terphenyl-β-D-glucoside, **46**. SEM images of the gels of **46** obtained from (b) slow-cooling process, and (c) fast-cooling process in H$_2$O/1, 4-dioxane (40/60 v/v). Reprinted with permission from ref. 161. Copyright 2009, American Chemical Society.

3.2. Ultrasound

Though conventional gelation is generally achieved by heating-cooling process, application of ultrasound may induce gelation in some cases. The kinetics of gelation triggered by sonication is generally much faster compared to that of the heating-cooling process.[69] Cintas and co-workers reported a series of amphiphiles and bolaamphiphiles (**48a-c**) in which the linear hydrophilic carbohydrate group (D-glucamine or *N*-methyl-D-glucamine) and hydrocarbon backbone are linked *via* ureido or bis(ureido) functionality based spacer (Fig. 28).[164] They behaved as self-organizing nonionic surfactants which were capable of exhibiting highly efficient hydrogelation, induced by ultrasound (35 kHz). The monourea derivatives (**48a-b**) formed stable gels at room temperature induced by sonication. Whereas, the bis (ureido) derivative (**48c**) also resulted gel by sonication at room temperature, but, lowered down the mgc (1 wt-%) compared to that of the thermally induced gelation process (2 wt-%). The gelation capability of these gelators was attributed to a combined effect of hydrogen bonding between the urea groups and van der Waals interactions between the long alkyl chains.
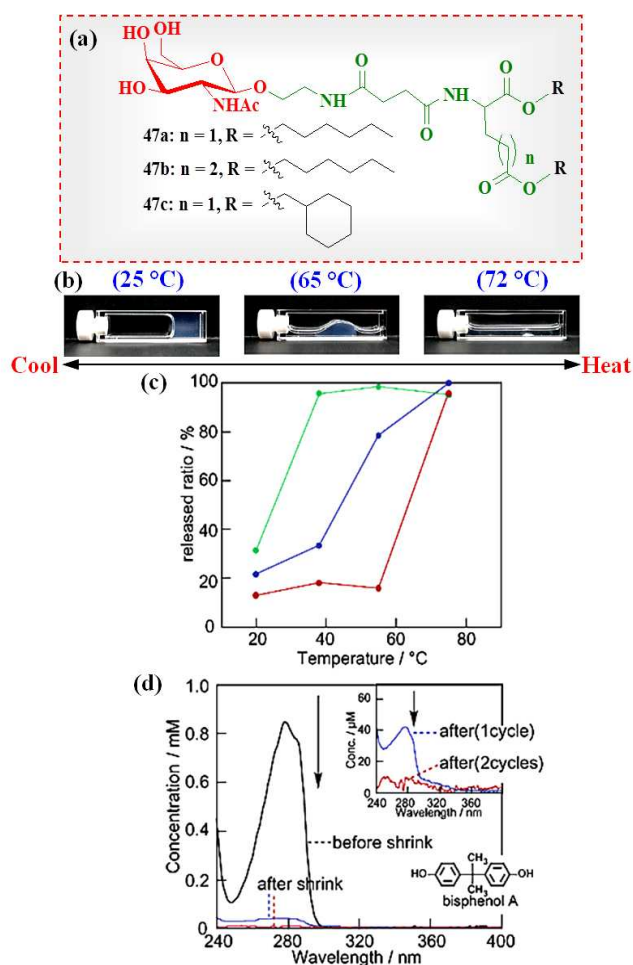
Fig. 27 (a) Molecular structures of hydrogelators (**47a-c**) derived from *N*-acetylgalactosamine appended amino acids. (b) Thermo-responsive reversible shrinkage and swelling of the hydrogel of **47c**. (c) Plots of released ratio of DNA versus temperature for the corresponding hydrogels [**47a** (blue), **47b** (green) and **47c** (red)]. (d) UV-visible spectra of the water polluted with bisphenol A before and after gel shrinkage. Reprinted with permission from ref. 162. Copyright 2002, American Chemical Society.

3.3. Host-guest interaction

Sakurai's group employed a carbohydrate derived hydrogel as a matrix for the inclusion and controlled release of DNA.[165] Mixing of DNA with 4, 6-*O*-(*p*-nitrobenzylidene)-α-D-glucopyranoside, **20a** (Fig. 14a), in stoichiometric or excess amount (w/v %) in water led to the formation of an opaque gel. DNA could be incorporated in the hydrogel because of the hydrogen bonding interactions involving the phosphodiester of DNA with the surface of the gel fibers covered with sugar hydroxyl groups. This was further supported by less green fluorescent protein (GFP) expression ability of plasmid DNA included in the hydrogel of **20a** in comparison to free DNA upon addition to E. coli T7 S30 extract solution (Fig. 29a). However, the original expression rate of the complexed DNA was regained again upon gradual addition of methyl-β-
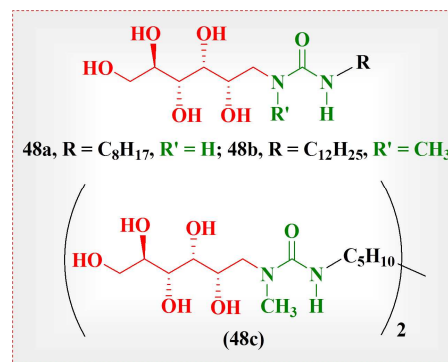

Fig. 28 Chemical structures of sugar-derived amphiphile and bolaamphiphile type gelators **48a-c**.

cyclodextrin because of the gel-to-sol transition associated with the complexation of methyl-β-cyclodextrin with the gelator (Fig. 29b). Thus, inclusion and controlled release of DNA from a hydrogel was achieved by modulating gel-to-sol transition using host-guest interaction between methyl-β-cyclodextrin and the gelator molecule (Fig. 29c).
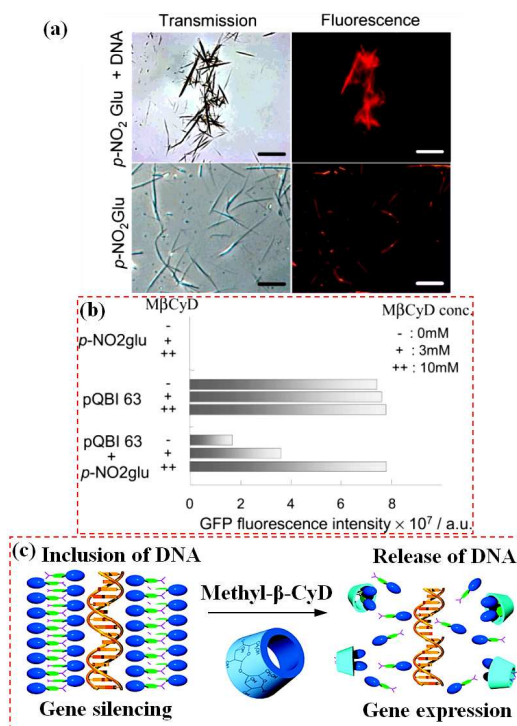

Fig. 29 (a) Comparison of the fluorescence microscopic images between 1 wt-% **20a** gel and 1 wt-% **20a** + 1 wt-% DNA gel (scale bar shows 1 μm). The right images show the location of ethidium bromide (EtBr) observed at 535 nm (λ_{ex} = 473 nm). (b) In vitro cell-free transcription/translation assay for **20a** + pQBI 63 vector gels in *E. coli* T7 S30 extract solutions and DNA release test by adding methyl-β-cyclodextrin (MβCyD). (c) A schematic illustration of inclusion and controlled release of DNA from hydrogel matrix of **20a**. Reprinted with permission from ref. 165. Copyright 2005, American Chemical Society.

Harada and co-workers demonstrated the first instance of supramolecular hydrogelation by a β-cyclodextrin (β-CD) containing a cinnamoyl-trinitrophenyl tail (**49**) without the aid of any polymer (Fig. 30a).[166] Alternate inclusion of the aromatic segment of **49** in the CD-cavity of another molecule assisted the propagation supramolecular polymer to form fibrils. While the hydrogen bonding interactions among the CD-scaffolds cross-link these fibrils eventually to form a hydrogel. Interestingly, the gel-to-sol transition could be triggered by addition of a competitive guest such as 1-adamantanecarboxylic acid (AdCA) or a denaturing agent capable of rupturing the hydrogen bonds such as urea (Fig. 30b).
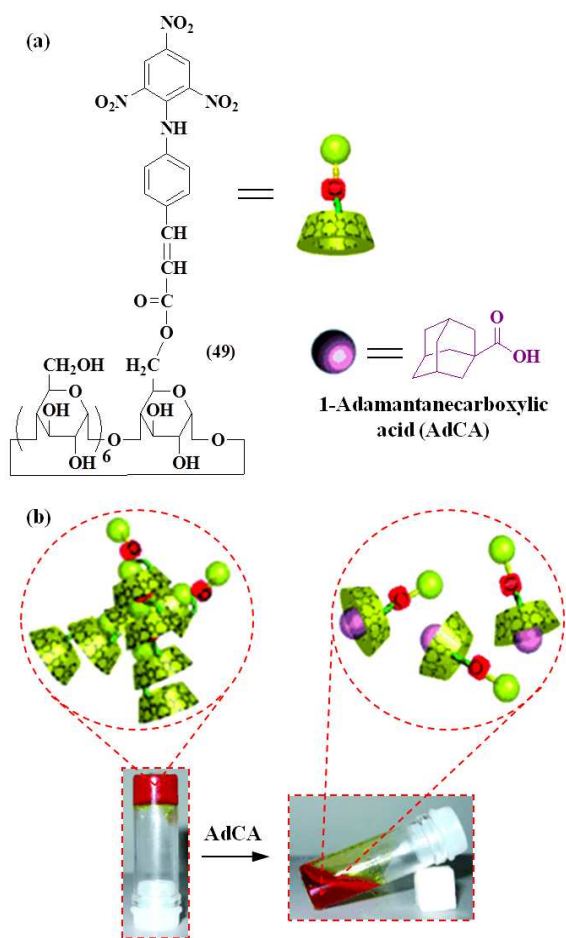

Fig. 30 (a) Molecular structures and cartoon representations of β-cyclodextrin derivative (**49**) and 1-adamantanecarboxylic acid (AdCA). (b) Photographs and schematic representation of AdCA induced gel-to-sol transition of **49**. Reprinted with permission from ref. 166. Copyright 2007, Wiley-VCH Verlag GmbH & Co. KGaA.

Bisphenol A (BPA) forms an inclusion complex with β-CD at 1:2 ratio. Miyata and co-workers used this fact to synthesize a BPA-responsive hydrogel with CDs as ligands *via* molecular imprinting.[167] As shown in Fig. 31a, the CD-BPA-CD complexes with acryloyl groups were copolymerized with acrylamide (AAm) and *N*, *N'*-methylenebisacrylamide (MBAA) during BPA-imprinted hydrogel (**50a**) preparation. In parallel a non-imprinted hydrogel (**50b**) was also synthesized in a similar manner without the BPA template (Fig. 31b). The BPA-imprinted and non-imprinted hydrogels with CD ligands were capable of exhibiting remarkable shrinkage in response to BPA. This occurred probably due to higher cross-linking density attributed to the formation of CD-BPA-CD complexes. However, the extent of shrinkage appeared to be more pronounced in case of the BPA-imprinted hydrogel compared to that of the non-imprinted hydrogel (Fig. 31c and 31d). This could be due to an appropriate arrangement of the CD ligands within the imprinted network indispensable for the formation of the 2:1 CD-BPA complexes in contrast to the randomly organized CD ligands in the non-imprinted hydrogel.

Recently, Miyata has further employed the BPA-responsive hydrogel as self-regulated micro-valves to control flow in a micro-channel.[168] Since a micro-hydrogel undergoes rapid volume-shrinkage in the presence of this target molecule (BPA), the flow rate in the micro-channel could be modulated by varying the concentration of a target molecule (BPA). Hence, this BPA-responsive micro-hydrogel may find potential utility as smart micro-valves for autonomous micro-channel flow regulation.
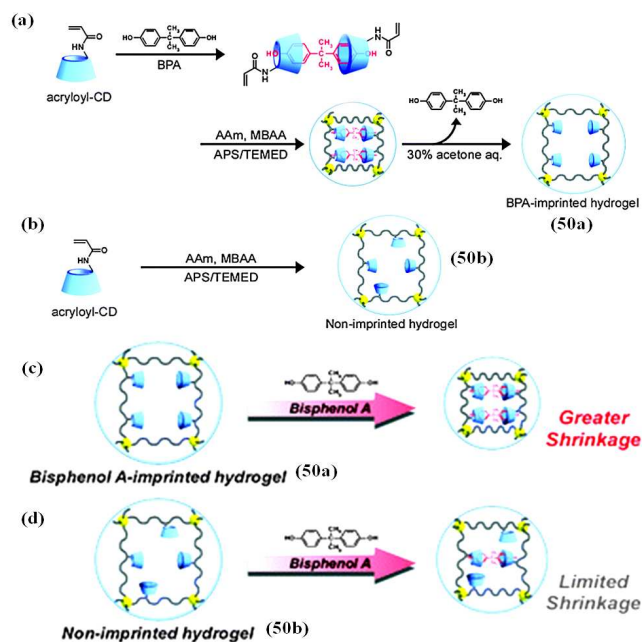

Fig. 31 Synthesis of (a) BPA-imprinted and (b) non-imprinted hydrogel. A schematic illustration of the swelling behaviour of (c) BPA-imprinted and (d) non-imprinted hydrogel. Reprinted with permission from ref. 167. Copyright 2014, The Royal Society of Chemistry.

N-alkyl pyridinium compounds [Py-*N*-(CH_2)_nOC_6H_3-3,5-(OMe)_2]$^+$(X$^-$) (**51a**: n = 8, X = Cl$^-$; **51b**: n = 10, X = Cl$^-$; **51c**: n = 12, X = Br$^-$) form micelles in water (Fig. 32a).[169] However, they are not capable of forming hydrogels even at significantly higher concentrations. Interestingly, addition of α-CD (100

mM) as an external guest to the aqueous solutions (50 mM) of **51b** or **51c** led to the formation of opaque and thermo-reversible hydrogels at 2:1 (host:guest) stoichiometric ratio (Fig. 32b, d, e). However, compound **51a** having shorter polymethylene chain failed to form gel under same conditions (Fig. 32c). Importantly, β-CD and γ-CD do not gelate aq. solution of **51b**. Furthermore, gel-to-sol transition could be triggered by addition of 200 mM of urea or phloroglucinol or $[Py-N-nBu]^+(Cl^-)$. Urea or phloroglucinol cut off the cross-linking hydrogen bonding interactions among CDs, while cationic $[Py-N-nBu]^+(Cl^-)$ stacks with the $C_6H_3-3,5-(OMe)_2$ group of the rotaxanes leading to degradation of the supramolecular polymers of the pseudorotaxane.
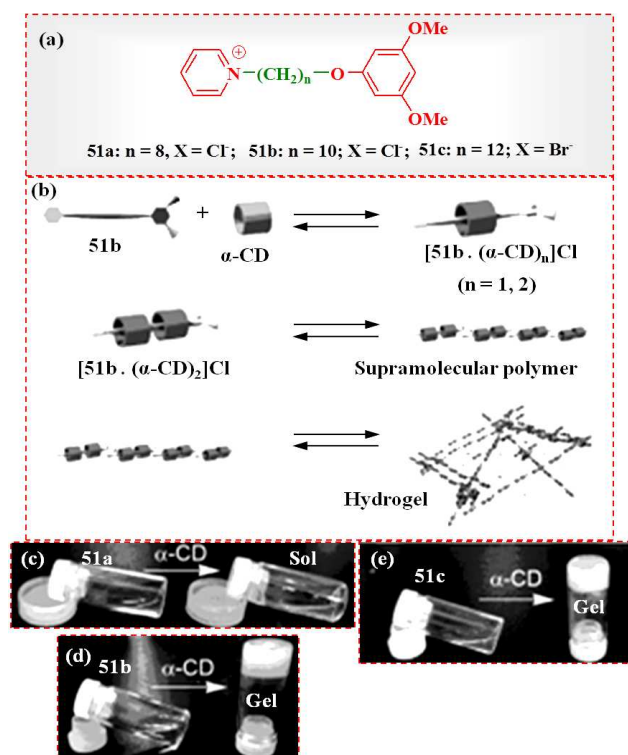

Fig. 32 (a) Molecular structures *N*-alkyl pyridinium compounds (**51a-c**). (b) A proposed mechanism of formation of the supramolecular hydrogel by **51b**. (c-e) Photographs showing α-CD induced sol and gel formation from aqueous solutions of **51a** and **51b-c** respectively. Reprinted with permission from ref. 169. Copyright 2010, Wiley-VCH Verlag GmbH & Co. KGaA.

3.4. Salt-effect

Bhattacharya described a pronounced hydrogelation at micromolar concentration by a tetrameric sugar derivative containing an azobenzene core (**52a**) in the presence of a small amount DMSO as a co-solvent (Fig. 33a).[170] As many as ~55500 water molecules could be immobilized by a single gelator molecule (gelation capacity = 1 wt-%), indicating high efficiency of hydrogelation. Inspired by this result, four similar azobenzene based tetrameric sugar derivatives, **52b-e**, were also synthesized (Fig. 33a). Furthermore, changing the

azobenzene core to the bis-amide derivative of terephthalic acid led to another series of tetrameric sugar molecules (**53a-c**). However, none of these additional sugar derivatives responded to gelation. Interestingly, the resultant hydrogel from **52a** exhibited remarkable tolerance to the pH variation of the aqueous media and hydrogelation retained in the pH range of 4-10. Investigation by UV-Vis, CD and FT-IR spectroscopy revealed that a combination of hydrogen bonding and hydrophobic force such as π-π stacking of the azobenzene groups were responsible for the growth of self-assembly which in turn led to the hydrogel formation.
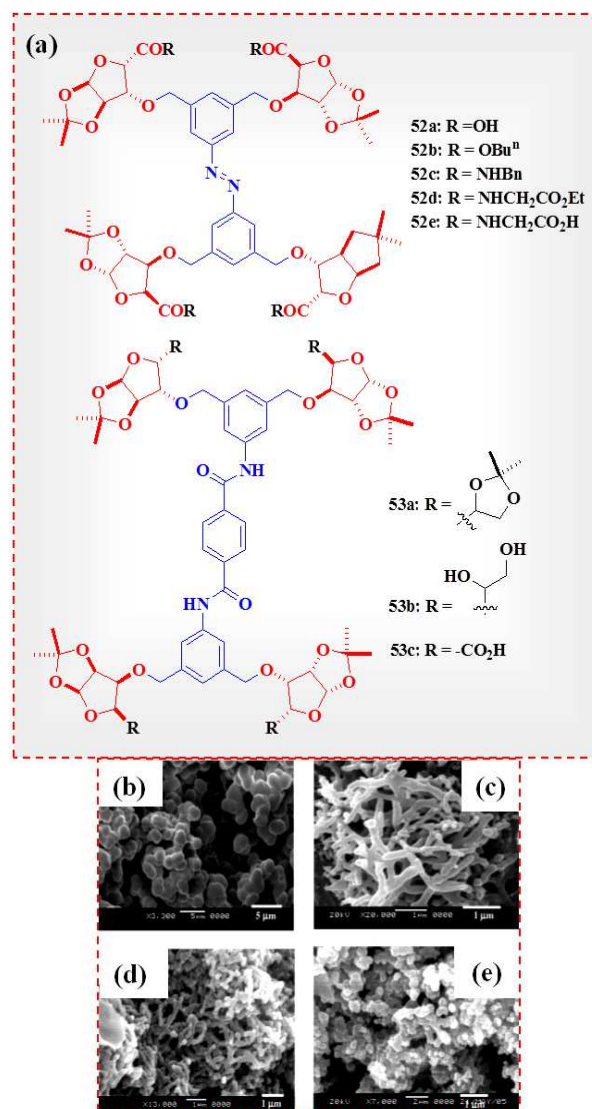

Fig. 33 (a) Chemical structures of sugar derivatives **52** and **53**. SEM images of xerogels of **52a** in (b) water, (c) 1 mM CaCl$_2$, (d) 1 mM MgCl$_2$ and (e) 1 mM NaCl. Reprinted with permission from ref. 170. Copyright 2005, American Chemical Society.

In addition, the presence of salts such as, NaCl (1 mM), KCl (1 mM), CaCl$_2$ (1 mM), and MgCl$_2$ (1 mM) had profound influence on the kinetics of gelation as well as on the

morphology of the gel aggregates (Fig. 33b-e). Gelation process was found to be delayed by addition of salts to the aqueous media. On the other hand a spongy globular morphology of the sole hydrogel of **52a** transformed to "rod-like" fibers, "fibrillar globules" and "aggregated spheres" in the presence of $CaCl_2$ (1 mM), $MgCl_2$ (1 mM) and NaCl (1 mM) respectively.

3.5. Light

3.5.1. *Cis-trans* isomerization

Azobenzene has been extensively used as an optical trigger in order to develop a diverse range of photo-responsive systems and photomodulation of interesting biological properties of peptides, proteins, lipids, and DNA owing to its remarkable property of reversible alterations in geometry and polarity associated with the light-induced *cis-trans* isomerization.[171] Azobenzene as a photo-responsive unit was integrated into LMWGs to produce photo-responsive gels. A large number of organogelators containing azobenzene moieties are reported in literature.[32] Bhattacharya's group investigated the effect of UV irradiation on a tetrameric sugar derivative containing azobenzene core (**52a**) in both solution and gel state (Fig. 33a).[170] UV light (350 nm) irradiation of a solution of **52a** in DMSO (0.1 mg/ml) resulted in gradual hypochromism of the UV-Vis band at around 325 nm indicating *trans-to-cis* isomerization of the azobenzene chromophore. Interestingly, the colour of the gel remained unchanged even upon prolonged UV irradiation (20 min) indicating inhibition of photoisomerization of the azobenzene groups due to tight intermolecular packing inside the gel phase.
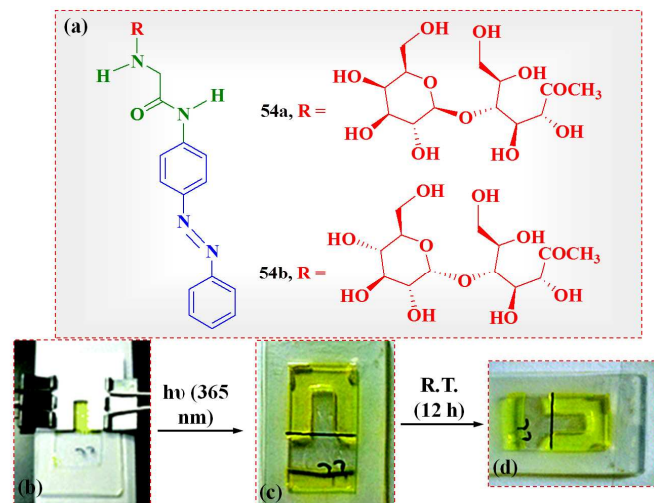

Fig. 34 Molecular structures of azobenzene group containing sugar derivatives (**54a-b**). UV-light induced gel-sol patterning of **54a** hydrogel (0.3% w/v); photographs of hydrogel with a photomask containing a rectangular window (b) before UV irradiation, (c) after UV light irradiation, and (d) after leaving at room temperature for 12 h. Reprinted with permission from ref. 172. Copyright 2012, American Chemical Society.

On the other hand, Kitaoka and co-workers demonstrated photo-stimulated *trans-to-cis* isomerization of hydrogels of **54a** or **54b** under UV light irradiation, which resulted in gel-to-sol transition (Fig. 34a).[172] As shown in Fig. 34b and 34c, the uncovered region of gel obtained from **54a**, gradually melted and moved to the bottom of the sample cell because of the *trans-to-cis* isomerization of the azobenzene groups upon irradiation with UV light. Re-aggregation of azo-gelator molecules in the *trans*-form could be achieved by thermally or by visible light exposure for 12 h (Fig. 34d). Similar observation was also found for **54b**.

3.5.1.1. Inter-conversion between fibres and vesicles

Hamachi and co-workers reported a glycolipid based hydrogelator (**55**) containing fumaric acid amide as a *trans-cis* photo-active moiety, which exhibited photo-induced reversible gel-to-sol transition (Fig. 35a and 35b).[173]
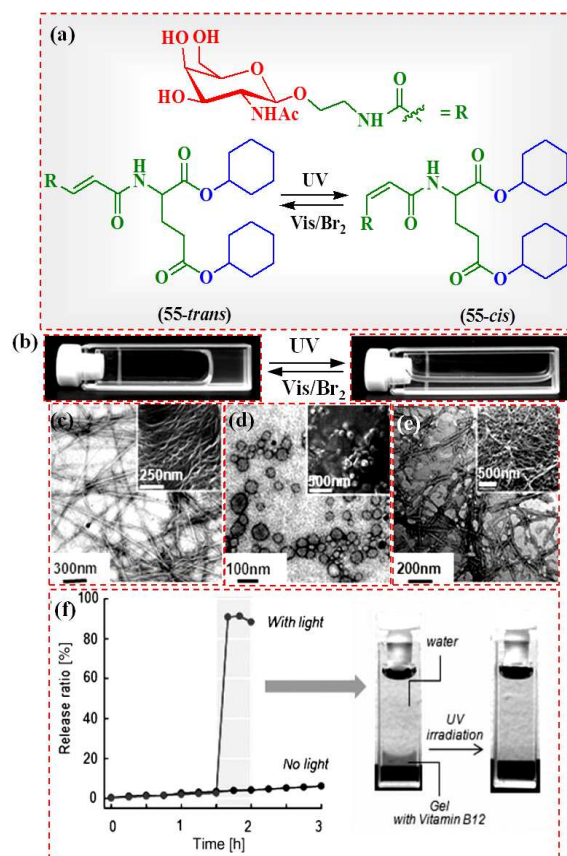

Fig. 35 (a) Schematic illustration and (b) photographs of light-induced reversible gel-sol transition of **55**. TEM and SEM (inset) images of (c) gel **55** before UV irradiation, (d) sol state after UV irradiation, and (e) reconstructed gel after Vis (Br_2) irradiation of the sol. (f) Time courses of release ratio [%] of vitamin B_{12} from hydrogel **55** to bulk solution without or with UV irradiation. Reprinted with permission from ref. 173. Copyright 2008, Wiley-VCH Verlag GmbH & Co. KGaA.

Morphological investigation of the hydrogel by microscopy revealed the presence of entangled fibrous structures having

length >10 mm and width <20 nm, while vesicle type aggregates were found in the sol state (Fig. 35c and 35d). Furthermore, the morphology of the reconstructed hydrogel was indistinguishable from the original one (Fig. 35e). This was accomplished by exposure of the sol under visible-light in the presence of traces of Br_2.

Using the advantage of photo-responsive characteristic of the hydrogel, photo-controlled release of various substrates (water-soluble vitamin B_{12}, glucose binding protein Con A) from the hydrogel was achieved. For example, a rapid release of encapsulated water-soluble vitamin B_{12} (B_{12}) from the hydrogel of **55** into the bulk aqueous solution occurred in case of UV-induced gel-to-sol transition (almost 100% of the embedded B_{12} was released in ~10 min) in comparison to the normal condition (only 7.8% of the embedded B_{12} was released in 3 h in absence of UV-light, Fig. 35f).

Hamachi also demonstrated a light-induced mass transport between gel droplets with nano- or pico-L volume derived from **55** in *n*-hexadecane.[174] The mass transport between two gel droplets was studied by introducing fluorescent probes such as water-soluble fluorescein (Fl) and Cy-5. As shown in Fig. 36, a fusion between the two gel droplets followed by diffusion of Fl only occurred after UV irradiation (*ca.* 2-3 min, low-pressure mercury vapour lamp). In addition to the simple diffusion, enzymatic reactions of alkaline phosphatase (AP) and glucosidase in the gel droplet could be triggered by light in a similar manner. Such system may find potential application in stimuli-responsive delivery of nano-micro substrates such as nanoparticles or cells as a nano- or pico-L volume container.
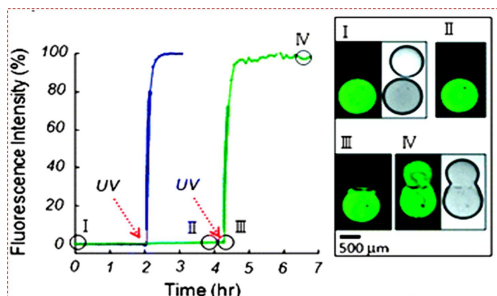

Fig. 36 Time courses of the diffusion (fluorescence intensity) (%) of Cy-5 (blue) and fluorescein (green) from the dye containing gel droplet to the blank one. Inset shows corresponding fluorescence and DIC images of the gel droplets at I, II, III and IV stages in the panel a. Reprinted with permission from ref. 174. Copyright 2008, The Royal Society of Chemistry.

3.5.2. Photo-dimerization

Sako and Takaguchi demonstrated a regioselective photo-dimerization of the anthracene scaffold of a dendritic hydrogelator (**56**) which was employed as a switch to induce gel-to-sol transition.[175] Investigation of structure of the photo-adduct by ^{1}H and ^{13}C NMR spectroscopy confirmed formation of a head-to-tail (H-T) photodimer attributed to the *anti-*

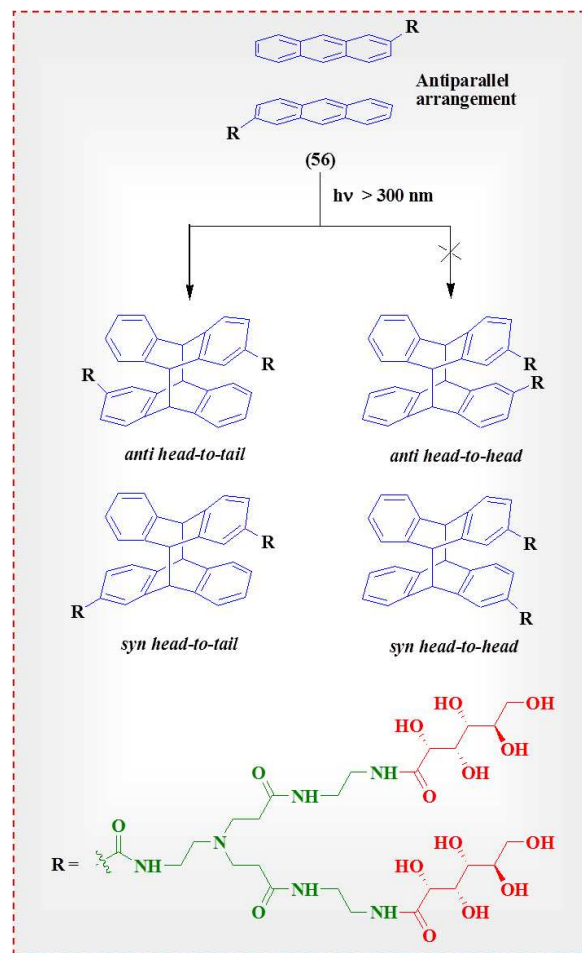parallel orientation of the anthracene moieties in the gel phase (Fig. 37).

Fig. 37 Schematic illustration of regioselective dimerization of dendron **56** upon photoirradiation of its hydrogel.

3.5.3. Photo-polymerization

Hydrogelation by trehalose is an excellent survival strategy for the preservation water in the cell walls of organisms and plants. This allows inhibition of cell disruption under the extreme desiccant conditions of nature. In order to mimic this phenomenon, John *et al.* demonstrated photo-polymerization of ethyl acetate gel of a diacrylate derivative of trehalose (**57**) upon exposure to UV light in presence of 2, 2-dimethoxy-2-phenylacetophenone (5 mol%) as a photoinitiator to generate an excellent self-supporting transparent film (Fig. 38a).[176] After lyophilization of the resulting polymerized organogel, a porous material devoid of any shrinkage was obtained (Fig. 38b). Extent of porosity of the polymerized hydrogel was much larger compared to that of the initial organogel which was not cross-linked. After drying, the cross-linked self-supporting material was immersed in water in order to generate a modest hydrogel (Fig. 38c). This was the first instance where the nanostructures were developed from self-assembled

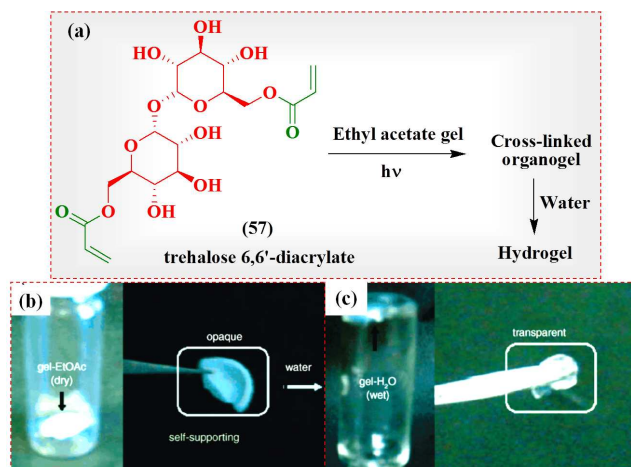precursors in organic solvents with capability of hydrogel formation.

Fig. 38 (a) A schematic illustration of photo-polymerization mediated hydrogelation by trehalose 6, 6'-diacrylate (**57**). Photographs of self-supporting (b) organo and (c) hydrogels obtained from trehalose 6, 6'-diacrylate (**57**) after polymerization. Reprinted with permission from ref. 176. Copyright 2006, Wiley-VCH Verlag GmbH & Co. KGaA.

Coumarin forms host-guest complex with γ-cyclodextrin (γ-CD) at a 2:1 ratio. Using this fact Tian and co-workers demonstrated light induced reversible gel-to-sol transition in a self-assembly of an inclusion complex derived from a tribranched coumarin derivative (**58**) and γ-CD (Fig. 39a).[177] Host-guest complexation in water resulted in a net-like supramolecular non-covalent polymeric backbone (**58-NNP**). This could be further converted to a reticulate polycatenane-like covalent polymeric structure (**58-CNP**) upon UV-light irradiation at 365 nm to furnish a robust hydrogel (Fig. 39b). This is owing to the cyclodimerization of coumarin moieties to produce a stable cyclobutane-based dimer in the cavity of γ-CD. Importantly, solution of **58** did not result in hydrogel in absence of γ-CD under the same condition. Upon exposure of 254 nm UV-light the parent net-like non-covalent polymer associated with the sol state could be regenerated indicating reversibility of this transformation (Fig. 39b).

3.5.3.1. Diacetylenic glycolipids

Gelator molecules containing polymerizable functionality may be employed for a post-gelation process by cross-linking the gel network. Gels derived from diacetylenic compounds have achieved attention as advanced sensing materials because of their capability to exhibit remarkable optical and electronic properties after photo-polymerization (Fig. 40).[178,179]

Shimizu also showed polymerization of **31a** in the corresponding hydrogel (Fig. 18) by 254 nm UV light, which resulted in red colouration accompanied by development of a new band at 540 nm in the UV-Vis spectra associated with the polymerization of **31a**. The intensity of this band monotonically increased with time and was maximized upon

32 min irradiation.[139] In addition, the CD signal of **31a** decreased significantly after polymerization indicating transformation of a well-ordered chiral packing of the hydrogel to a disordered molecular arrangement. In order to support this result, AFM experiment was performed. Morphological investigation of hydrogel **31a** under AFM revealed helical ribbons of diameter of 20-150 nm and length of several hundred μm, while typical fibrous structures with a diameter of 20 nm, were observed after polymerization. This observation led to the same conclusion that the macroscopic helicity of hydrogel of **31a** was destroyed upon polymerization.
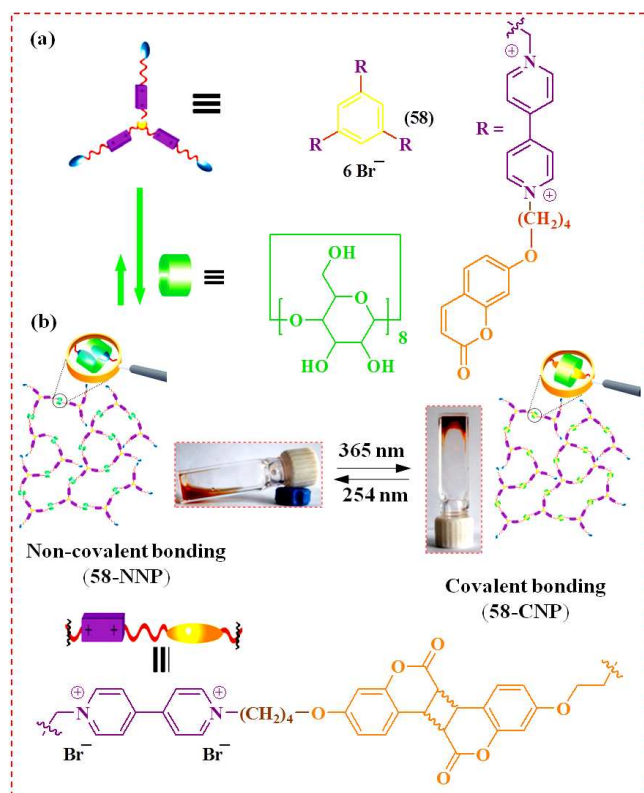

Fig. 39 (a) Molecular structure of a tribranched coumarin derivative (**58**) and a schematic illustration of the host-guest interaction mediated supramolecular non-covalent net-like polymer (**58-NNP**) formation. (b) Photographs and schematic representation of photo-responsive supramolecular inter-conversion between **58-NNP**-sol and **58-CNP**-gel. Reprinted with permission from ref. 177. Copyright 2013, The Royal Society of Chemistry.

Wang and coworkers investigated the effect of polymerization on the morphologies of organogels obtained from various diacetylenic derivatives of methyl 4, 6-*O*-benzylidene-α-D-glucopyranoside, **59-62** (Fig. 41a).[180,181] The hexane and ethanol gels obtained from these compounds transformed into blue after UV-light exposure within less than one minute (Fig. 41c, e and f). These further turned red upon heating (Fig. 41d and 41g). This process was reversible if the heating temperature was kept below 70 °C. Interestingly, polymerization was much more facile in case of **60** compared

to that of **59a**. This result suggests a favourable alignment of the two diacetylene chains in **60**, which might not be possible in case of **59a** owing to the presence of the methoxy group at the anomeric position. Dramatic changes in the birefringences of the gel matrices were observed after polymerization. As shown in Fig 41h and 41k, a belt-like structure of ethanol gel of **59b** remained unaltered upon UV-irradiation. However, their colour changed to red after this. On the other hand, hexane gel of **61b** showed blue coloured straight fibrous networks and they turned pink after UV-treatment (Fig 41j and 41m). In a recent report, Wang has also shown polymerization of remarkable helical structures of ethanol gel of a diacetylene amide, **62** (Fig 41i and 41l).[182]
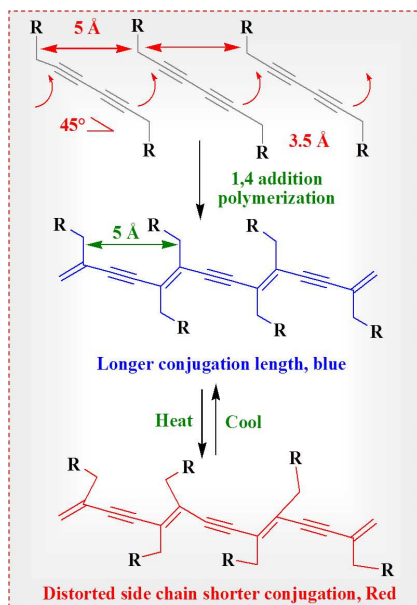

Fig. 40 A schematic representation of topochemical polymerization of diacetylene and the colour transition mechanism.

3.6. Role of pH

Investigation of self-assembly of pH-responsive gels helps in mimicking various biological phenomena. Zhou and co-workers reported an interesting supramolecular hydrogelation based on *N*-acetylgalactosamine appended glutamate ester **63** (Fig. 42a), which exhibited gel-to-sol transitions upon pH variation unlike other pH-responsive supramolecular hydrogels.[183] The pH-responsive volume change (shrinkage or swelling) function was achieved by simply mixing it with an appropriate amount of an amphiphilic carboxylic acid derivative **64a** or **64b**. The pH sensitivity of the hydrogel of **63** was not observed in absence of **64a** or **64b**. When the hydrogel was exposed to an acidic vapour, remarkable shrinkage of its volume followed by expelling of ~50% water from the original hydrogel occurred (Fig. 42b). Furthermore, the transparent hydrogel became opaque and stiffer than the original gel. This type of volume-shrinkage of gel was only observed in case of hydrogels obtained from almost equimolar mixture of **63** and

64, which did not occur in the single component of **63** or in mixtures with small amounts of **64** indicating the importance of the presence of both components in an optimal ratio. Water-soluble vitamins, such as vitamins B_1, B_6, and B_{12}, could be encapsulated in the mixed hydrogel (**63**/**64b** = 1:1) and subsequently released upon gradual acidification.
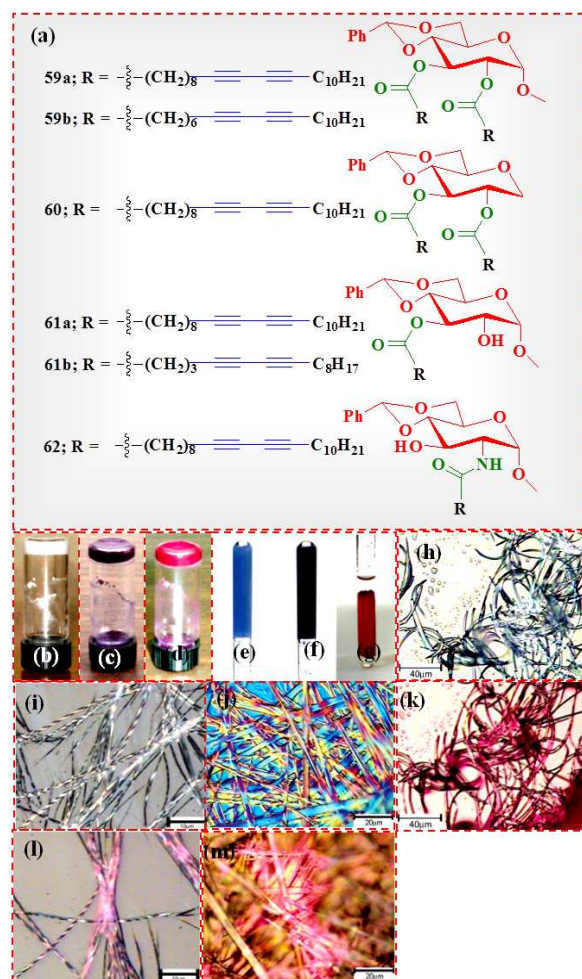

Fig. 41 (a) Chemical structures of amphiphilic and bolaamphiphilic diacetylenic glycolipids **59-62**. Photographs showing (b) a gel of **61a** in *n*-hexane, (c) which turned deep blue-purple after UV-light exposure, (d) and turned red upon further heating; similarly, blue coloured ethanol gel of **60** obtained after (e) 1 min, (f) 3 min UV-light exposure and (g) turned red upon further heating. Optical micrographs of gels obtained from **59b**, **62** and **61b** in ethanol and *n*-hexane respectively (h-j) before and (k-m) after polymerization respectively. Reprinted with permission from ref. 180 and 182. Copyright 2006 and 2014, American Chemical Society.

Kameta *et al.* employed pH-responsive hydrogels of asymmetric amphiphilic monomers as artificial chaperones to transform denatured proteins [green fluorescent protein (GFP), carbonic anhydrase, and citrate synthase] to refolded state at room temperature by encapsulating them inside the nanotube hydrogel (Fig. 43a).[184] Entrapment of GFP inside the nanotubes consisting of a monolayer membrane is attributed to

the electrostatic interaction between GFP and the inner surface of the one-dimensional channel mainly covered with amino groups.
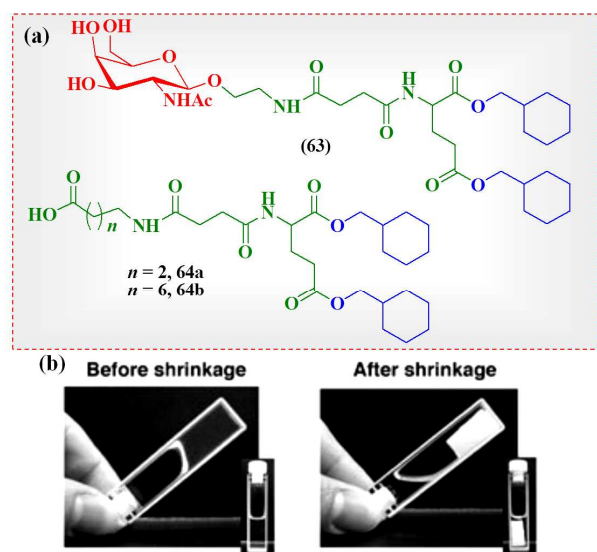

Fig. 42 (a) Molecular structures of glutamate esters (**63** and **64**). (b) Photographs of pH-responsive volume phase transition of the mixed hydrogel (**63/64b** = 1:1) before and after shrinkage. Reprinted with permission from ref. 183. Copyright 2005, Wiley-VCH Verlag GmbH & Co. KGaA.

The refolded GFP could be released into bulk solution without any specific external additives through reduction of the electrostatic interaction by increasing the pH (7.0 to 7.8) of the medium (Fig. 43b). Absence of any additives in the recovery process improved the purity of the obtainable refolded proteins to a significant extent. Affinity of the inner surface of the nanotube channels towards the GFP could be enhanced by introducing hydrophobic functionalities such as a benzyloxycarbonyl group (**65b**) and a tert-butoxycarbonyl group (**65c**) which increased the encapsulation efficiency (Fig. 43a). Furthermore, partially refolded proteins in the nanotube channel transformed into the refolded state after their release into the recovery solution.

3.7. Cation

Metal-ion coordination responsive gels are smart candidates for advanced functional materials because of the important role of metal ions in many enzymes, catalysts, molecular electronic devices *etc.*[57-61] Such alterations open easier window to examine and study various interesting properties of physical gels. Influence of external additives such as metal cations, small inorganic anions, and ion pairs as in metal salts is now of increasing current interest to tune gel properties, particularly the rheological behaviour associated with the strength and stiffness of gels.[57-61,185]

Salicylideneaniline derived LMWGs have attracted recent attention because of their unusual properties, such as photochromism,[186] thermochromism,[117,187]

solvatochromism,[188] and liquid crystalinity.[189] Fan *et al.* synthesized a new gelator (**66**) containing salen and sorbitol moieties which exhibited an efficient 'naked eye' response to Cu^{2+} selectively through a reversible gel-to-sol transition (Fig. 44).[190,191] Addition of 0.5 equiv. of Cu^{2+} to the DMSO/H$_2$O (1:1) gel of **66** resulted in a dramatic colour change from yellow to colourless accompanied by gel-to-sol transition. This phenomenon occurred due to the chelation between **66** and Cu^{2+} *via* an intra-molecular charge transfer (ICT) between naphthol O-H and N=CH groups. Gelation could be re-established through the addition of EDTA owing to the higher affinity of EDTA to Cu^{2+} (Fig. 44). Furthermore, aggregation-induced fluoresence emission (AIE) was observed after gelation (20 °C) relative to the hot sol at 80 °C. It is important to note that this gel also responded to other stimuli such as, light, pH etc. Hence, this gelator may be used in the design of a molecular logic circuit in its gel state.
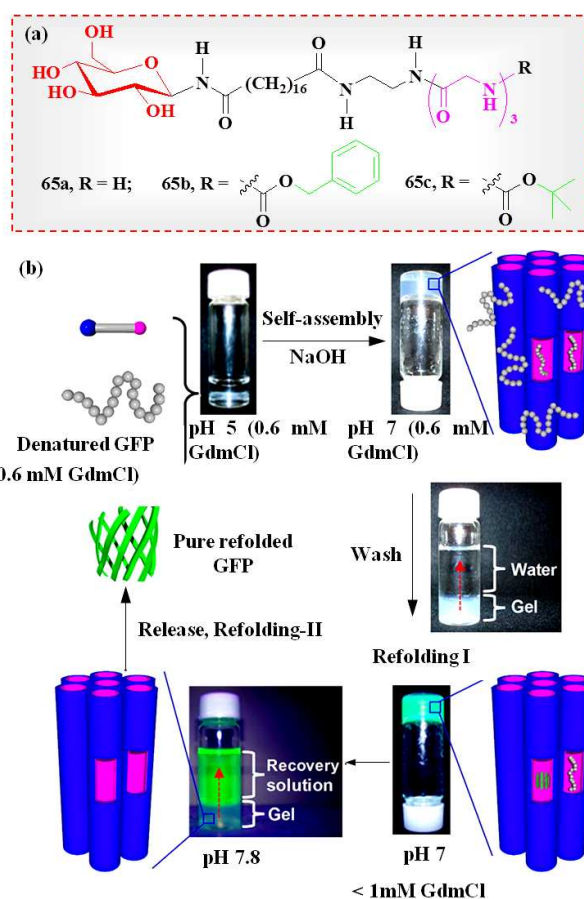

Fig. 43 (a) Molecular structures of amphiphilic artificial chaperones (**65a-c**). (b) Refolding procedure of denatured GFP in the nanotube hydrogel of **65a**. Reprinted with permission from ref. 184. Copyright 2012, American Chemical Society.

3.8. Anion

Yoshimura *et al.* demonstrated a novel semi-wet molecular recognition chip constructed by the dynamic redistribution of

the receptor molecule in the hydrogel matrix of glycosylated amino acetate type of hydrogelator **63**. This was achieved upon guest-binding between the aqueous micro-cavity and the hydrophobic nanofibers, without sacrificing the molecular recognition capability displayed in solution (Fig. 45a).[192,193] A photo-induced electron transfer (PET) type receptor bis-Zn/Dpa-anthracene **67a** incorporated in the transparent hydrogel showed 2.6-fold enhancement of emission of fluorescence at 435 nm only upon the addition of phosphate derivatives, in contrast to the other anions, such as sulfate, nitrate, acetate, azide, halide *etc*. Another phosphate receptor **67b** containing two Zn/Dpa sites like the chemosensor **67a** and decorated with environmentally sensitive dansyl fluorophore was immobilized in the supramolecular hydrogel in order to distinguish among various types of phosphates (phosphate, phospho-tyrosine, phenyl phosphate and ATP).
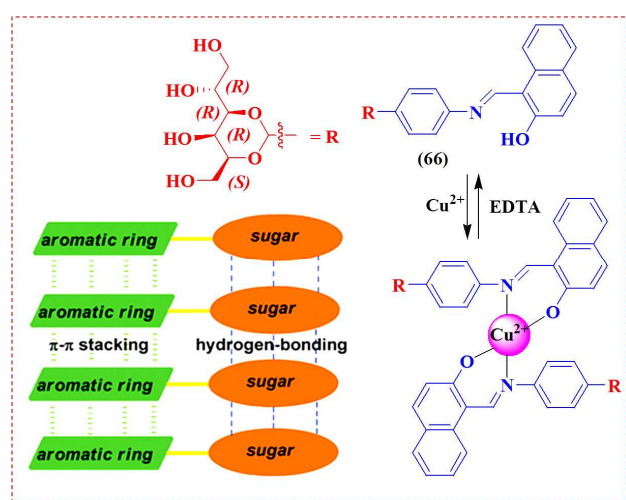

Fig. 44 Chemical structure and schematic illustration of Cu^{2+}-responsive reversible gel-to-sol transition of sorbitol-based salen-linked gelator (**66**). Reprinted with permission from ref. 191. Copyright 2013, The Royal Society of Chemistry.

For instance, an enhancement in the emission intensity of **67b** (at 512 nm) accompanied by a blue-shift was observed for the hydrophobic phenyl phosphate, while an addition of hydrophilic ATP caused a red shift in the emission of **67b** with decrease in the intensity (Fig. 45b). Hence, discrimination among the phosphate anion species could be performed by simple detection of both the intensity change and the wavelength shift. Interestingly, no significant change in the fluoresence intensity was observed either in the aqueous solution or in the case of agarose gel and a polymer-based hydrogel having no hydrophobic domains indicating the importance of the hydrophobic domain for the guest-induced fluorescence change.

Redistribution tendency of the artificial receptor depending upon the nature of the guest was further extrapolated to a fluorescence resonance energy transfer (FRET) type pair (a coumarin-appended receptor, **67c** as a FRET donor and a hydrophobic styryl dye, **68** as a FRET acceptor) in the semi-

wet supramolecular hydrogel. In absence of phosphates, the coumarin-appended receptor **67c** would prefer to stay in the bulk aq. space and the styryl dye **68** would localize in the hydrophobic domains of nanofibers. The receptor preferred to move to comparatively more hydrophobic domain attributed to the enhanced hydrophobicity upon complexation with phosphate derivatives. This resulted in close proximity between these two fluorophores and hence the FRET was facilitated (Fig. 45c).
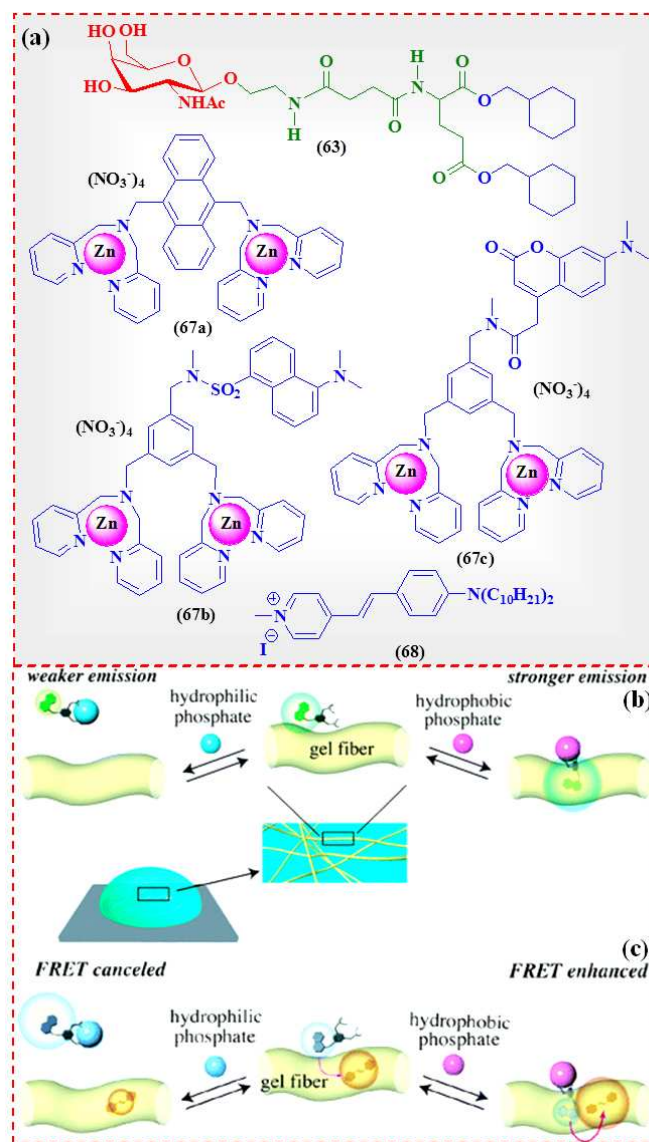
Fig. 45 (a) Molecular structures of glycosylated amino acetate type of hydrogelator (**63**), phosphate receptors (**67a-c**) and hydrophobic styryl dye (**68**). (b) A schematic illustration of redistribution of the chemosensor between the hydrophobic hydrogel nanofiber and the hydrophilic cavity upon binding to a hydrophobic or hydrophilic phosphate derivative. (c) A schematic representation of the guest-dependent FRET system using **67c** and **68** by the addition of PhP or ATP in the hydrogel matrix. Reprinted with permission from ref. 193. Copyright 2005, American Chemical Society.

FRET was suppressed upon complexation with hydrophilic phosphate derivative such as ATP, attributed to the increased distance between the two fluorophores. Furthermore, coumarin emission (485 nm) practically remained unaffected in presence of PhP or ATP without the styryl dye.

3.9. Cysteine

Compound **69a** is a chemoresponsive carbohydrate-derived hydrogelator [methyl-4, 6-*O*-(4'-aldehydephenylidene)-α-D-glucopyranoside] which exhibits selective responsiveness to cysteine (Fig. 46a).[194] Such selectivity of the hydrogel toward cysteine might be attributed to the specific thiazolidine adduct (**69b**) formation by reaction of the aldehyde with cysteine, which led to degradation of hydrogel followed by formation of a clear solution. Other amino acids (aspartic acid, lysine, alanine, serine, histidine, arginine, proline, and phenylalanine) including the acidic and the basic ones could not however, react with the aldehyde group under the same conditions. Careful addition of aqueous solution cysteine on the surface of the hydrogel followed by incubation for 4 h at 37 °C transformed the hydrogel to solution completely (Fig. 46b).
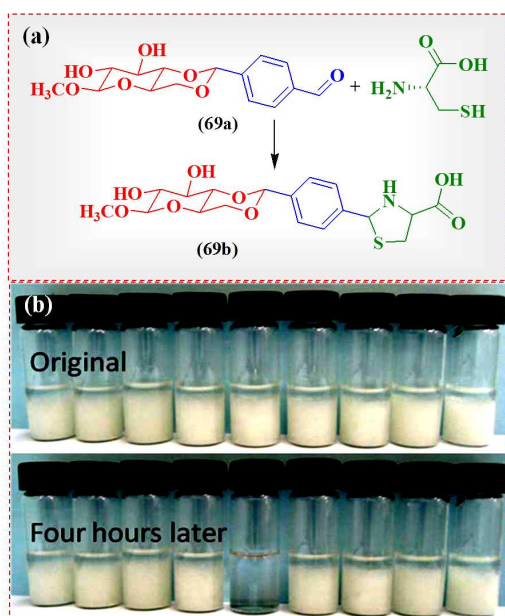

Fig. 46 (a) Schematic illustration and (b) demonstration of selective response to cysteine by the hydrogel of **69a**; the sequence of solution of amino acids added to the hydrogels from left to right is as follows: aspartic acid (13.5 mM), lysine (0.2 M), alanine (0.2 M), serine (0.2 M), cysteine (0.2 M), histidine (0.2 M), arginine (0.2 M), proline (0.2 M), phenylalanine (25 mM). Reprinted with permission from ref. 194. Copyright 2009, American Chemical Society.

3.10. Insulin

Insulin is a peptide hormone, produced by beta cells of the pancreas. It has a vital role to maintain blood glucose (blood sugar) in a very narrow range. Kim's group first reported a monosaccharide-based fluorescent hydrogelator (**70**)

comprising a D-gluconolactone headgroup linked to a nonpolar pyrene moiety through an amino acid base spacer capable of sensing insulin (Fig. 47).[195] It was observed that fluorescence intensity at 393 nm gradually quenched with increasing insulin concentration.
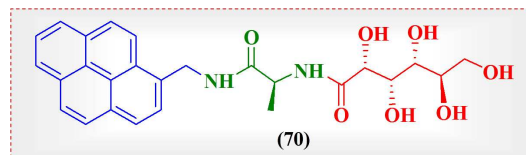

Fig. 47 Chemical structure of gluconamide type insulin sensor **70**.

3.11. Glucose

Miyata and co-workers demonstrated the glucose-responsiveness of bioconjugated gel particles (~750 nm) derived from (lectin: concanavalin A) ConA-GEMA (2-glucosyloxyethyl methacrylate) complexes as cross-linkers.[196] These were prepared by the surfactant-free emulsion copolymerization of relatively hydrophobic *N*, *N*-diethylaminoethyl methacrylate (DEAEMA), poly(ethylene glycol) dimethacrylate (PEGDMA), hydrophilic GEMA, and modified-ConA with polymerizable groups. Though, the GEMA-ConA gel particles remained colloidally stable in a phosphate buffer solution (PBS), they exhibited remarkable swelling in the presence of glucose in PBS (Fig. 48). The swelling ratio of these gel particles was found to strongly depend on the glucose concentration. It increased with an increase in the glucose concentration. In contrast, the swelling ratio remained unaffected in the presence of galactose indicating a selective response of these gel particles to glucose only. Glucose-induced swelling of these gel particles was attributed to the dissociation of GEMA-ConA complexes acting as cross-links, which caused a decrease in the cross-linking density of their shell layer. Hence, this type of gel particles may find potential applications as glucose-responsive insulin release systems to treat diabetes.
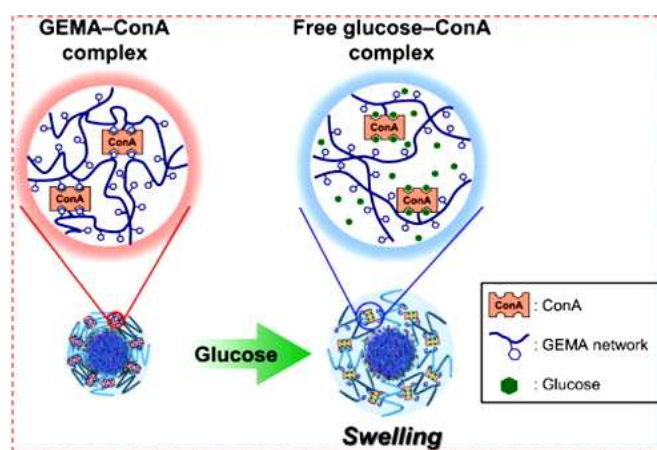

Fig. 48 Schematic of glucose-responsive behaviour of GEMA-ConA gel particles. Reprinted with permission from ref. 196. Copyright 2011, Elsevier B.V.

3.12. Concanavalin A

Yamanaka *et al*. reported a carbohydrate-based amphiphile, **71** which self-assembled into fibrous structures in water to result in a pale-yellow transparent hydrogel (Fig. 49a).[197] Since the surface of these fibers was enriched with dense packing of glucosides, the hydrogel was responsive to lectin (carbohydrate binding protein) such as, concanavalin A (ConA). Addition of ConA (3.9 ~7.8 nmol) to the hydrogel of **71** (0.43 μmol in 100 μL H$_2$O) led to a significant decrease in the CGC value and an enhancement in the thermal stability (T_{gel}) by cross-linking the fibrous aggregates. However, presence of excess ConA disrupted the gelation process and afforded cloudy sol owing to the cohesion of the fibers (Fig. 49b). Interestingly, the cloudy sol could be further transformed to an opaque gel by addition of a suitable saccharide such as, α-methyl-D-mannoside (Me-α-Man). This may be due to the relatively higher binding affinity of Me-α-Man to ConA incontrast to **71**, which prevents the interaction of **71** with ConA (Fig. 49b). On the other hand, a large excess of α-methyl-D-glucoside (Me-α-Glc, 3 equiv for ConA)/D-mannose (Man, 4 equiv for ConA)/isomaltose (Isomal, 4 equiv for ConA)/ D-glucose (Glc, 4 equiv for ConA) was necessary to induce gelation because of their lower binding affinity towards ConA. However, gelation was not observed even after addition of 260 equiv. of D-galactose (Gal) or L-glucose (L-Glc) to the cloudy sol **71** and ConA. It may be noted that the hydrogel of **71** was also responsive to various mono and divalent anions such as F⁻, Cl⁻, Br⁻, CH$_3$CO$_2$⁻, SO$_4$²⁻ etc (except I⁻ and ClO$_4$⁻). Hence, these may be useful in the detection of hardness of mineral waters.
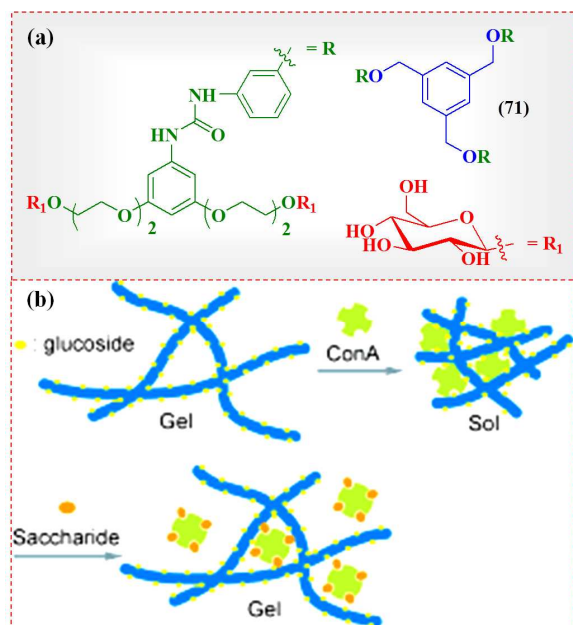

Fig. 49 (a) Chemical structure of the carbohydrate-based amphiphile, **71**. (b) Schematic representation of the gel-to-sol transition of **71** triggered by ConA and saccharide. Reprinted with permission from ref. 197. Copyright 2011, Wiley-VCH Verlag GmbH & Co. KGaA.

3.13. Ionic Surfactants

The amphiphile **72** forms an insoluble suspension in water because of the bundling of the associated one-dimensional self-assembly *via* hydrophobic interactions and intermolecular hydrogen bonding (Fig. 50a).[198] However, hydrogelation could be triggered by addition of various ionic surfactants such as, sodium alkyl sulfates (*n* = 8, 10, 12 and 14) and alkyltrimethylammonium bromides (*n* = 12 and 16). Surfactant induced gelation property; transparency and thermal stability of the resulting gels were found to depend on the gelator and surfactant ratio. Hence, the degree of bundling of amphiphile **72** could be modulated by reinforcing ionic surfactant molecules in the corresponding self-assembly. Dispersion of the hydrophilic headgroups of the surfactants on the surface of the assemblies enhances the electrostatic repulsion between the ionic headgroups which finally decreases the degree of bundling (Fig. 50b). However, gelation was not observed in case of sodium sulfates with short alkyl chains (*n* = 2 and 6), or simple ammonium salts including tetramethyl and tetrabutylammonium bromides or nonionic surfactants *n*-octyl-β-D-glucopyranoside and tetraethyleneglycol monododecyl ether.
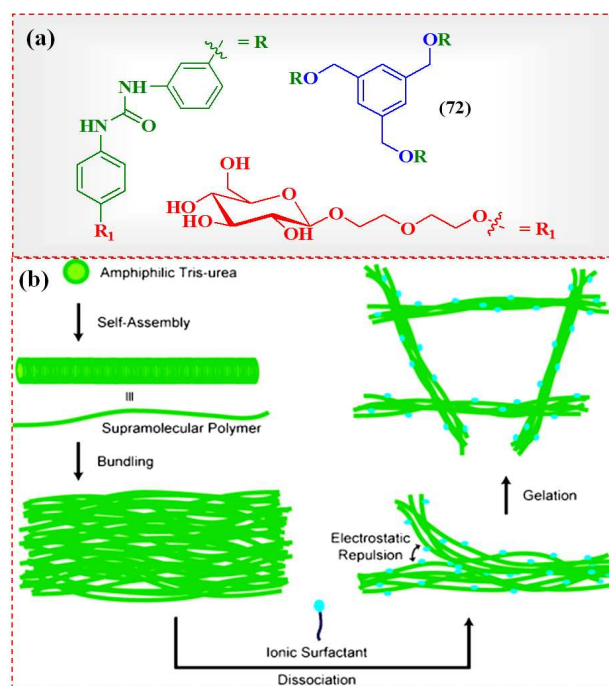
Fig. 50 (a) Molecular structure of the sugar-derived amphiphile, **72**. (b) Schematic illustration of presumed mechanism of ionic surfactant-induced hydrogelation. Reprinted with permission from ref. 198. Copyright 2012, Wiley-VCH Verlag GmbH & Co. KGaA.

3.14. Enzyme

Enzyme triggered tuning of gel-to-sol transition of small molecules has become an excellent strategy in order to develop new functional soft biomaterials and new applications of gels.

Creation of self-assembling motif with enzyme responsive moiety offers possibilities of tuning gel-to-sol transition, which may find potential applications in detecting the activity of enzymes, screening enzyme inhibitors, typing bacteria, and drug delivery *etc*.[19,20,51,56,199]

3.14.1. Lipase

John *et al.* developed an excellent strategy for encapsulating a hydrophobic chemotherapeutic drug molecule (curcumin) in the hydrophobic pockets of a hydrogel of an amphiphilic D-amygdalin-fatty acid conjugate, **73** (Fig. 51).[19,94] Furthermore, encapsulated curcumin could be released by degrading the gel using a hydrolase (Lipolase 100L, type EX). Gel degradation occurred because of the enzymatic cleavage of the ester bond in the gelator by the hydrolase (Fig. 51). Drug release was studied by monitoring the absorption spectra and characterizing the gel degradation products. Furthermore, the rate of drug release could be modulated by tuning the enzyme concentration, temperature, or both.
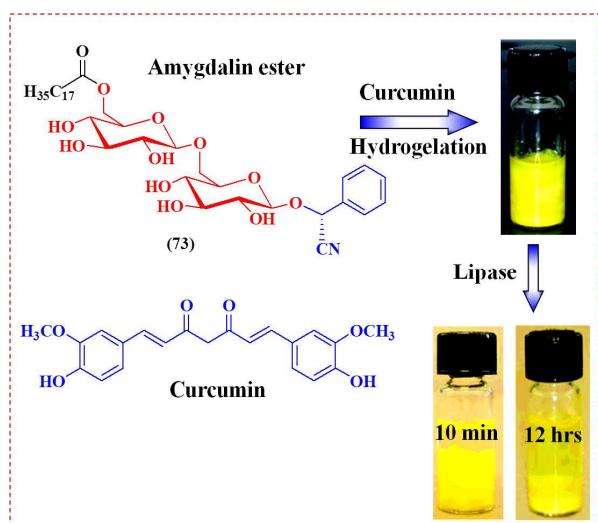

Fig. 51 Molecular structure of amygdalin ester (**73**) with real-time images of the corresponding gel samples in contact with the lipase enzyme at different time intervals. Reprinted with permission from ref. 19. Copyright 2010, American Chemical Society.

3.14.2. Phosphatase

Xu and co-workers studied enzyme triggered hydrogelation in the self-assembly of a series of conjugates (**74a-77a**) consisting of a thymine (as the nucleobase), phenylalanine(s) (as the amino acids), phosphorylated tyrosine (as the enzymatic trigger and an amino acid), and D-glucosamine (as the saccharide) (Fig. 52).[200] Phosphatase enzyme (12.5 U per mL) transformed the precursors (**74a-77a**) into hydrogelator in alkaline condition (**74b-77b**) by cleaving the phosphate that are more hydrophobic than their precursors (Fig. 52). Significant differences were found in the kinetics of hydrogelation of these peptides owing to their structural

differences. Compounds **74b** and **77b** were capable of forming stable hydrogels in ~5 minutes. In contrast, **76b** (0.5 wt-%) took ~2 h to result in a stable hydrogel, while, **75b** formed hydrogel only upon prolonged aging (~8 days).
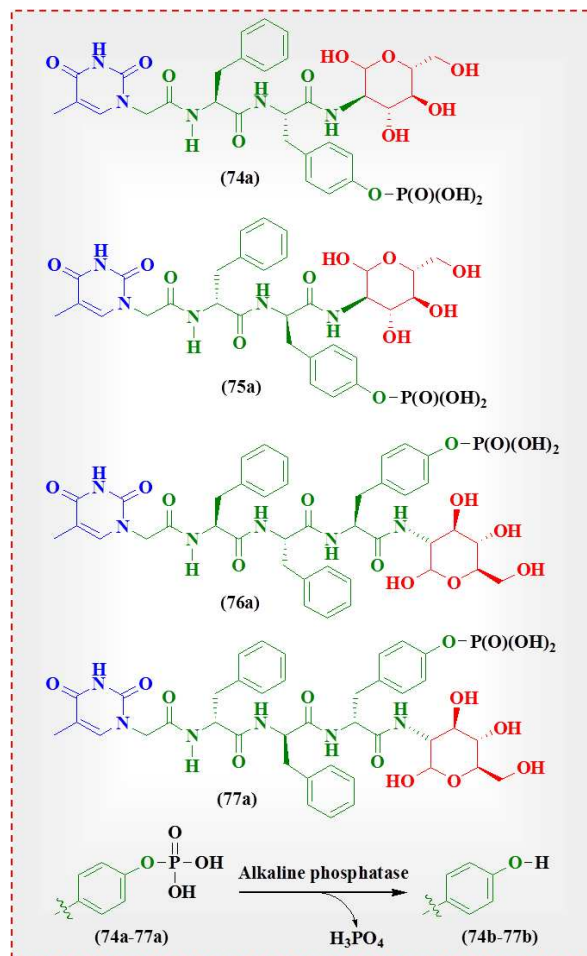

Fig. 52 Molecular structures of peptide based precursors (**74a-77a**) and schematic illustration of phosphatase triggered hydrogelation.

Recently, Pires and Ulijn have intelligently employed enzymatic dephosphorylation as an anti-osteosarcoma strategy with limited impact on the surrounding healthy cells/tissues.[201] The effect of enzyme promoted self-assembly of an aromatic carbohydrate amphiphile, *N*-(fluorenylmethoxycarbonyl)-glucosamine-6-phosphate (**78a**) was investigated *in situ*, in the presence of osteosarcoma cell line (SaOs2) known to overexpress alkaline phosphatase (ALP) (Fig. 53a). Bio-catalytic transformation of **78a** to **78b** by the membrane bound ALP results in a cytotoxic nanonet/hydrogel "cage" surrounding the cells around SaOs2 cells. This drastically inhibits metabolic activity and ultimately leads to cell apoptosis of SaOs2 cells (Fig. 53b). In contrast, the metabolic activity of the chondrogenic cell line ATDC5 with lower membrane-bound ALP expression profiles remained unaltered signifying the cell specificity of this process (Fig. 53b).
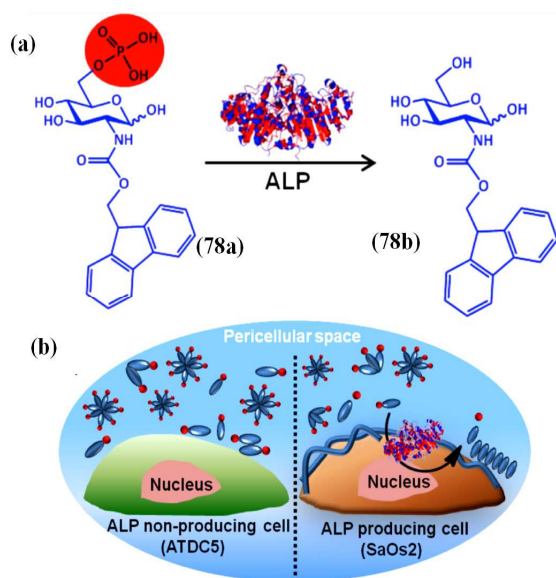
Fig. 53 A schematic illustration of bio-catalytic transformation of **78a** to **78b** upon enzymatic activity of phosphatases (*e.g.* ALP); (a) Molecular structures and (b) *in situ* bio-catalytic self-assembly. Reprinted with permission from ref. 201. Copyright 2014, American Chemical Society.

3.14.3. Glycosidase

Among glycosidases, β-galactosidase (βGal-ase) has been investigated most extensively as a model for enzymology. Xu also explored βGal-ase catalyzed hydrogelation by hydrolysis of a precursor (**79a**) containing a galactose, as the relatively hydrophilic segment, and 2-naphthylacetic acid-Phe-Phe-Lys, as the basic self-assembly platform (Fig. 54).[202] Precursor **79a** undergoes hydrolysis upon addition of 2.0 U βGal-ase (8 μL, 0.25 U μL^{-1}) to result in **79b** which self-assembles to form a transparent hydrogel (300 μL, 1.0 mg mL^{-1}) (Fig. 54). Instant hydrogelation could be achieved by addition of βGal-ase to the freshly prepared or aged solution of **79a** at higher concentration (8.0 mg mL^{-1}) at pH 7.5.
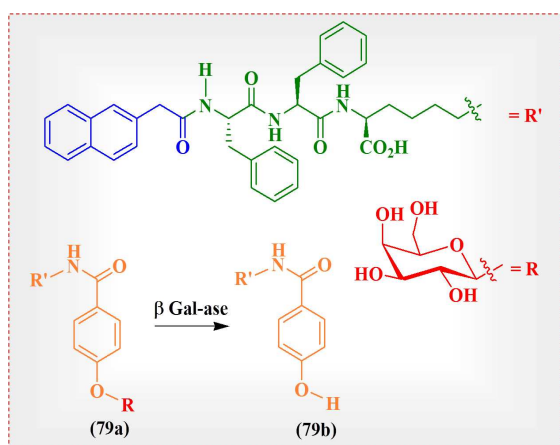

Fig. 54 Chemical structure of peptide based precursor **79a** and an illustration of β-galactosidase triggered hydrogelation.

Hamachi and co-workers reported a series of supramolecular hydrogels derived from bola-amphiphilic glycolipids, **80a-d** (Fig. 55a).[203] These hydrogels exhibited colourimetric response and gel-to-sol transition in presence of corresponding glycosidases (Fig. 55b). For instance, β-glucosidase (βGlc-ase) selectively cleaves the β-glucosidic bond of the βGlc-C11 hydrogel. Hence, addition of βGlc-ase to the hydrogel of βGlc-C11 resulted in a colour change from yellow to orange in addition to gel-to-sol transition (Fig. 55b). On the other hand, glycosidases such as α-glucosidase (αGlc-ase) or β-galactosidase (βGal-ase) remained silent. In a similar manner, the hydrogels obtained from other glycolipids (αGlc-C11, βGal-C11, and αMan-C11) showed selective yellow-to-orange colour change and gel-to-sol transitions only in the presence of the corresponding glycosidases (αGlc-ase, βGal-ase) and α-mannosidase (αMan-ase), respectively (Fig. 55b). Motivated by these results, these authors employed these hydrogels to construct a colorimetric sensing array chip for sensing glycosidases with the naked eye. It was observed that the response time of micro-size gel spots (20 min) are much less compared to that of the bulk gels (4 h).
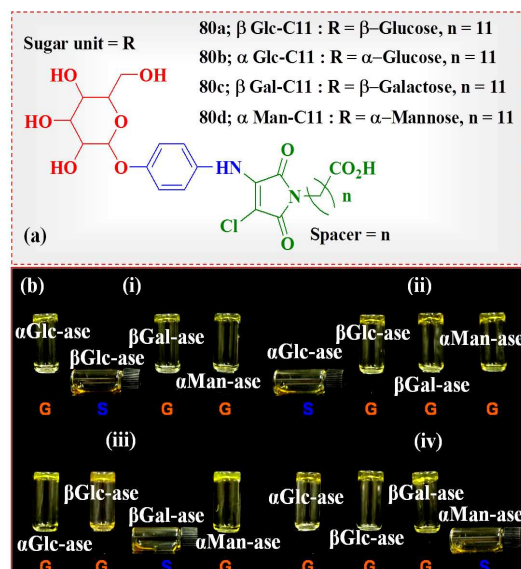
Fig. 55 (a) Chemical structures of glycolipids, **80a-d**. (b) Photographs of hydrogels of (i) βGlc-C11, (ii) αGlc-C11, (iii) βGal-C11, and (iv) αMan-C11 in 200 mM HEPES (pH 7.2) after the addition of glycosidases. Reprinted with permission from ref. 203. Copyright 2013, The Royal Society of Chemistry.

4. Gelators that co-assemble

Formation of co-assembly of two co-gelators with structurally similar or identical binding motifs is a nice strategy to get access to a wide range of gel properties not attainable with the use of only one of the two gelators. There are several literature examples of co-gelation of two or more gelators, where the gels are comprised of peptides,[204] dendrimers,[205] urethanes[206] and ureas.[55] All of them utilize hydrogen bonding between

molecules with similar binding motifs to control the interactions between the gelators.

Using the concept of co-assembled gelators, Krishnan *et al.* demonstrated a topochemical reaction at 55 °C, between two 4, 6-*O*-benzylidene-D-galactopyranoside co-organogelators (1:1). These two co-organogelators contain β-azide (**81a**) and α-propargyloxy (**81b**) functionalities at the anomeric position with complementary reacting motifs, *viz.* azides and alkynes. Two possible products (**82a** and **82b**) formed in 1:1 stoichiometry within one week (Fig. 56a and 56b).[207] The reaction kinetics was followed by time-dependent changes in the NMR spectra. Formation of the two reaction products (**82a** and **82b**) was attributed to the zigzag arrangement of **81a** and **81b** in the co-assembly to form a 1D-hydrogen bonded assembly (Fig. 56a and 56b). In contrast, reaction did not occur in a simple mixture obtained from individually prepared xerogels of **81a** and **81b**. This result clearly elucidates the importance of topochemical control by the co-assembly of the reactants in the xerogel.

Oriol's group found interesting observations in the co-gels (**I** and **II**) of maltose-based azo-amphiphiles.[208] Co-hydrogel **I** was prepared from a mixture of **83a** with **83b** at 1:10 molar ratio at 1 wt-% of **83b** in water. In this mixture, the azo-amphiphile **83a** is able to gelate (Fig. 57). Similarly, Gel **II** was formed by mixing **83c** and **83b**, in the same ratio (1:10 molar ratio), at 1 wt-% of the **83b** in water (Fig. 57). *Trans*-to-*cis* isomerization of the co-gel **I** by irradiation by 365 nm UV light was confirmed by decrease in the intensity of absorption at 365 nm band and enhancement of the UV-Vis band at 450 nm. In the CD spectra, the negative cotton effect associated with the azobenzene group abolished, while the negative peak corresponding to the triazole only decreased. The photostationary state was attained after irradiation for 2 min. Furthermore, initial UV-Vis and CD spectra were totally recovered by incubating the sample for 24 h in the dark. However, Gel **II** did not exhibit any evidence of *trans-cis* isomerization even after irradiation for 150 min. Hence, Gel **I** acted as a photoactive mixture, while Gel **II** remained unaffected after light irradiation presumably because of the location of the azobenzene moiety in the middle of the hydrocarbon chain, in comparison to the azobenzene derivative in Gel **II**, in which the azobenzene functionality is directly attached to the carbohydrate headgroup.

5. Miscellaneous applications

5.1. Phase selective gelation

Though, petroleum covers a major part of energy source of human civilization, accidental discharge of crude oil especially in marines imparts harsh effects to the ecosystem. This damaging phenomenon is called oil-spill. Oil-spill disaster in the Gulf of Mexico in 2010 is an unforgettable experience of this type of environmental calamity.
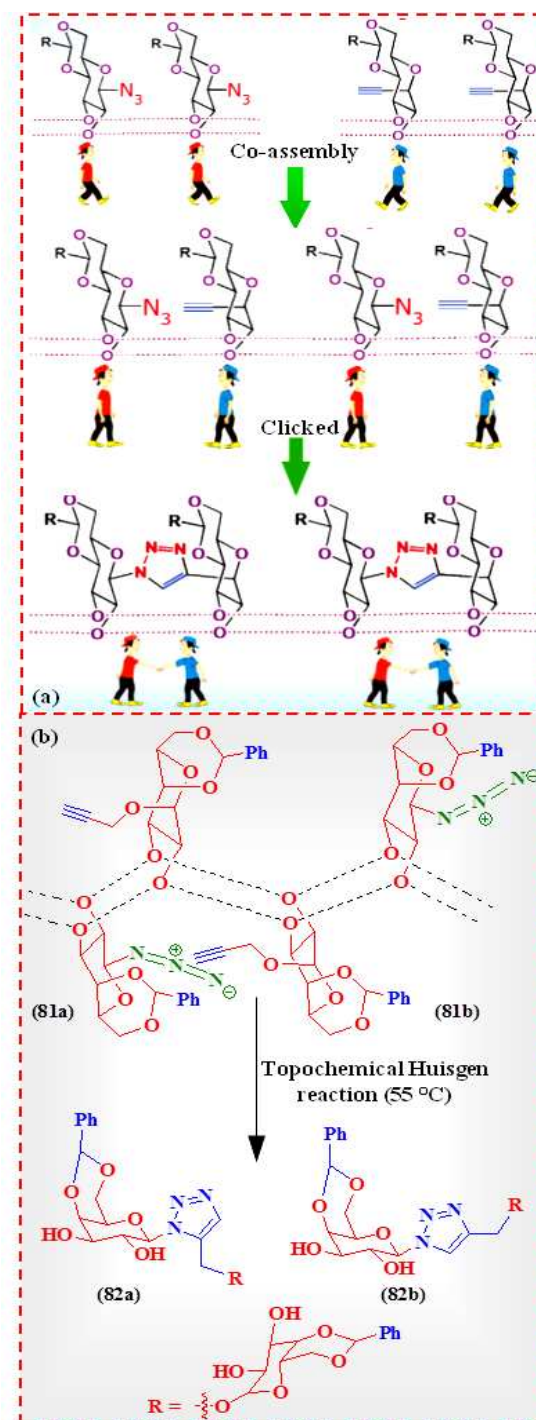
Fig. 56 (a) Cartoon representation and (b) schematic illustration of possible packing arrangement of **81a** and **81b** in the co-assembled state and their topochemical reaction in the xerogel state. Reprinted with permission from ref. 207. Copyright 2013, The Royal Society of Chemistry.

In this context, phase selective gelators (PSGs) have achieved marked attention recently because of their capability of selectively gelling oil in a water-oil mixture. Phase selective gelators (PSGs) are defined as the LMWGs, which are capable of immobilizing a particular solvent preferentially over the

others in a given solvent mixture (*e.g.,* petrol and water). The first report of phase-selective gelation was introduced by Bhattacharya *et al.* with *N*-lauroyl-L-alanine in 2001.[209] Herein we will discuss about sugar-derived phase-selective gelators.

Fig. 57 Chemical structures of maltose-based amphiphiles (**83a-c**).

5.1.1. External solvent as carrier

An effective phase-selective-gelation by sugar derivatives was demonstrated by John and co-workers (Fig. 58a).[210] PSGs base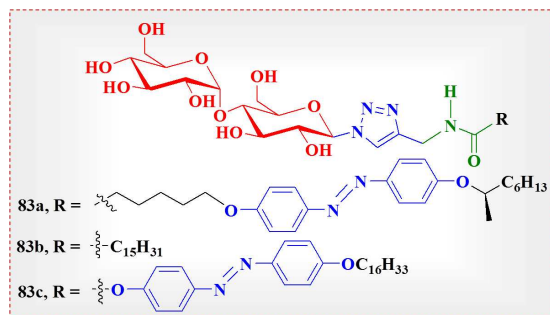d on sugar alcohols mannitol (**84a** and **84b**) and sorbitol (**85a** and **85b**) formed gels in a diverse range of organic liquids including diesel and mineral and silicone oils *etc.* with high efficiency (mgc = 1.5 to 5% w/v). Furthermore, the mgc values of these gelators were found to be influenced significantly upon variation of length of the hydrocarbon chain. Dioctanoate derivatives **84b** and **85b** having comparatively longer hydrocarbon tails attached to carbohydrate functionality were undertaken for phase-selective-gelation experiment because of their much lower mgc values compared to that of the dibutanoates (**84a** and **85a**).

In a typical oil-simulation experiment, compound **84b** predissolved in ethanol (carrier solvent) was introduced a biphasic mixture of diesel (20 mL) and water (40 mL). The final concentration of **84b** in diesel was 5% wt/v. Instant selective gelation of the diesel layer occurred and the immobilized diesel layer could hold its weight including the water layer after 1 h (Fig. 58b-e). In order to mimic the real oil-spill situation, they even experimented the phase-selective-gelation test on a thin layer (<1 mm) of diesel floating on a large pool of water (in a Petri dish). After separation of the water layer using a syringe, the diesel was recovered by melting the gel at 125 °C ($T_{gel-sol}$) followed by distillation (Fig. 58f and 58g).

In a recent report, Fang's group has reported the fastest phase selective gelation (< 45 s) of oil (either commercial fuels or pure organic liquids) from an oil-water mixture at room temperature by two sugar-derived PSGs, **86a-b** (Fig. 59).[211]

5.1.2. Removal of toxic dye

Discharge of industrial toxic wastes originated from dye, textile, lather, rubber, cosmetics, paper, printing, plastic and drug industries pollutes water in large extent. They are extremely hazardous, carcinogenic and difficult to biodegrade.[212-214] The self-assembly present in the gel phase contains various hydrophobic or hydrophilic domains depending upon the features of the gelator molecule. Hence, it is possible to entrap various cationic and anionic dye molecules in those cavities. Recently, Mukherjee's group showed removal of crystal violet efficiently (~97%) from water to toluene *via* phase-selective-gelation of a galactoside amphiphile, **87** (Fig. 59).[215] The dye was adsorbed in the toluene gel and purified water could be collected by simple filtration. The efficiency (97.6%) of dye removal was studied by UV/Vis spectroscopy (λ_{max} = 583 nm).
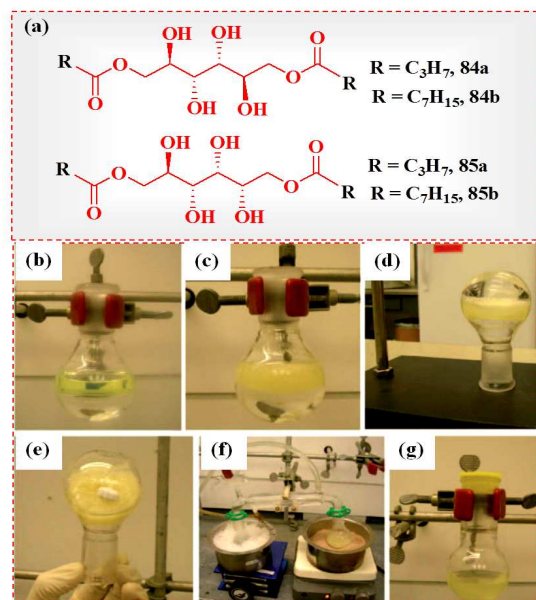

Fig. 58 (a) Chemical structures of phase selective gelators based on sugar alcohols mannitol (**84a** and **84b**) and sorbitol (**85a** and **85b**); (b-e) Demonstration of phase selective gelation of bulk diesel by **84b** in presence of water, and (f and g) recovery of diesel through vacuum distillation. Reprinted with permission from ref. 210. Copyright 2010, Wiley-VCH Verlag GmbH & Co. KGaA.

5.1.3. Co-solvent as carrier

It is not practically viable to use a water-miscible external solvent (*ca.* methanol, ethanol *etc.*) for practical applications. Prathap *et al.* first overcame this problem by introducing a mannitol based PSG (**88**) in the oil-water biphasic mixture pre-dissolved in the same oil as a carrier without using any other persisting chemicals/solvents (Fig. 59).[216] In order to mimic the real situation of oil-spill, phase-selective-gelation was performed in a mixture of diesel and seawater taken in a large flat glass vessel kept on a mechanical shaker. Addition of a warm concentrated solution of gelator **88** in a small volume of diesel to the biphasic mixture resulted in immobilization of the oil layer selectively at a final concentration of 0.75%. Oil could be recovered from the congealed diesel layer by simply

scooping out using a sieve spatula followed by distillation (Recovery efficiency ~92% by volume).
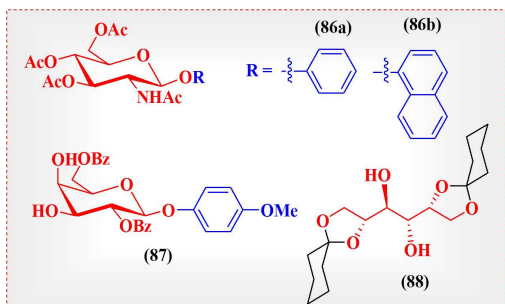

Fig. 59 Chemical structures of some sugar-derived phase selective gelators **86-88**.

5.2. Self-healing

Self-healing and self-repairing properties have attracted remarkable interest because of their capability to offer shatter-free materials with higher longevity.[217-220] These properties are however more important in polymer chemistry owing to inability of conventional polymers to self-heal.[221] In the context of non-covalent approach, host-guest interaction is beneficial due to its reversibility and stimuli-responsiveness nature.[222,223]

5.2.1. Preorganized hydrogel

Harada's group employed preorganization of the host and guest monomers to accomplish self-healing materials with improved (~ 99%) healing efficiencies.[223] Herein, *N*-adamantane-1-yl-acrylamide (Ad) and acrylamide-β-CD were used as guest and host monomers, respectively (Fig. 60a). Host-guest interaction mediated inclusion complex with acrylamide-β-CD rendered the Ad-monomer water soluble. The resulting complex could be copolymerized with acrylamide using ammonium peroxodisulfate (APS) as an initiator and *N*, *N*, *N'*, *N'*-tetramethylethane-1, 2-diamine (TEMED) as a co-catalyst to furnish a self-healable hydrogel. In order to demonstrate the self-healing property, a cube-shaped slice of the gel was cut into two separate pieces (Fig. 60b and 60c). They could be adhered again to reconstruct the single gel (Fig. 60b and 60c). Interestingly, the adhesive strength associated with the joint surface improved over time and the initial gel strength was almost fully restored after 24 h.

5.2.2. Flexible optical devices

Sureshan and co-workers developed a convenient method to make shatter-free, soft optical devices from amphiphilic supergelator, **88** (Fig. 61a) based on diketal derivative of mannitol (mgc in alkane solvents = 0.2 wt-%).[224] The resulting organogels exhibited remarkable rheological properties such as high strength, stiffness and self-healing properties originated from the restricted conformational freedom and high extent of inter-molecular interaction because of close proximity in self-

assembly. These unique combinations of such properties of the gels allowed them to gain various self-supporting shapes (Fig. 61a-i). These transparent hydrocarbon gels showed high transmittance (Fig. 61f) in the visible region with glass-like refractive indices ($n \approx 1.5$) which may find potential application for selective UV filtering (*e.g.*, UV protective goggles, skin cream). Furthermore, soft optical devices such as flexible planoconvex lens, a double convex lens made of these gels showed excellent capability to magnify objects (Fig. 61d-e). Prisms prepared in the similar way refracted white light into its components (Fig. 61b and c).
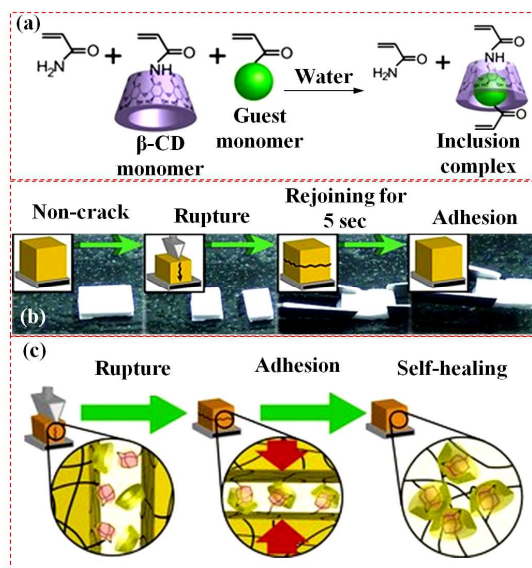

Fig. 60 Schematic illustration of (a) formation of pre-organized inclusion complex by host acrylamide modified β-CD monomer and guest *N*-adamantane-1-yl-acrylamide; (b) Photographs and (c) schematic illustration of self-healing property of the hydrogel derived from the pre-organized complex after copolymerization. Reprinted with permission from ref. 223. Copyright 2013, Wiley-VCH Verlag GmbH & Co. KGaA.

5.3. Controlled release devices for pheromones

Pheromones are naturally occurring volatile biopesticides.[225] They disrupt sexual communication of pests.[226] They are highly specific towards a given species which further enables pest control without weakening the beneficial organisms.[227] Numerous reservoir-type controlled release devices (CRDs) have been developed for effective pest control because pheromones are volatile and unstable owing to their propensity towards photo-oxidation, auto-oxidation, isomerization *etc*.[228] Recently, Bhattacharya and co-workers have reported a simple and straightforward method to prepare pheromone nanogels that exhibit high residual activity, excellent efficacy in open orchard even during adverse seasons.[229] Jadhav *et al*. employed a molecular gelator, mannitol dioctanoate (**84b**) (Fig. 58a) as an efficient alternative material in order to develop reservoir-type release devices for controlled release of pheromones with high pheromone-loading capacity.[230] 2-Heptanone is a volatile

pheromone produced and used by honey bees to dissolve plantwaxes as well as beeswax. These authors developed suitable CRDs to control its evaporation rate. It contains a reservoir of 2-heptanone gel (7% wt/v) covered by a semi-permeable membrane. Activation of this device by creating a small hole on the membrane allowed slow release of 2-heptanone. It is important to note that evaporation rate of 2-heptanone from the gel-based CRD was similar to the CRD made from 1:1 blends of beeswax and 2-heptanone. However, the gel-based CRD exhibited higher loading efficiency (~ 92% wt/wt) compared to that of the beeswax containing device (~ 50% wt/wt).
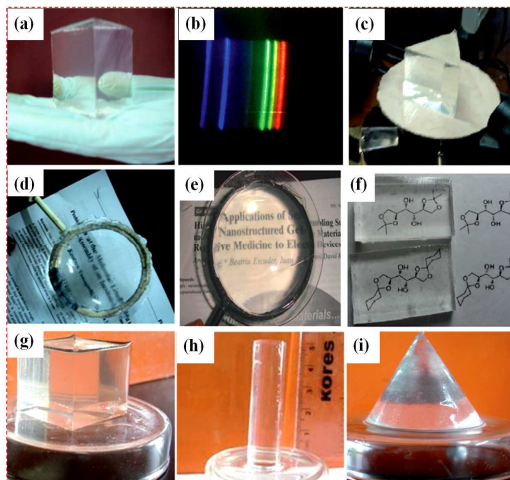

Fig. 61 (a) A self-supporting gel prism made from pump oil gel of **88**. (b) The diffraction pattern observed using the gel prism. (c) The gel prism mounted on a spectrometer table. Photographs of (d) a double convex and (e) a planoconvex lens made from the pump oil gel of **88**. (f) Demonstration of transparency of paraffin oil gel of **88**. Photographs of self-supporting (g) gel cube, (h) gel cylinder and (i) gel cone. Reprinted with permission from ref. 224. Copyright 2011, Wiley-VCH Verlag GmbH & Co. KGaA.

5.4. Biological applications

Another important advantage of using sugar derivatives as a platform of gelation lies in their biocompatibility, biodegradability, non-toxicity and eco-friendly behaviour. Because of these features, they may be applicable in biomedical applications.[231]

5.4.1. Wound healing

Xu's group used biocompatible D-glucosamine-based hydrogelators (**89a** and **89b**) for rapid wound healing of mice (Fig. 62).[232] Aminosaccharide derivatives, **89a** and **89b** are capable of forming stable hydrogels at pH 7. Biocompatibility of these hydrogels was confirmed by cytotoxicity assay of 3-(4, 5-dimethylthiazol-2-yl)-2, 5-diphenyl-tetrazolium bromide (MTT). It was observed that 73.8% and 79.0% of HeLa cells survived in 100 μM of **89a** and **89b** at 24 h, respectively. Furthermore, the hydrogel of **89b** was implemented for wound

healing on a mouse model. Interestingly, much faster wound healing process and smaller scars were found at 6th day for the mice group treated with the hydrogel **89b** compared to those without the treatment.
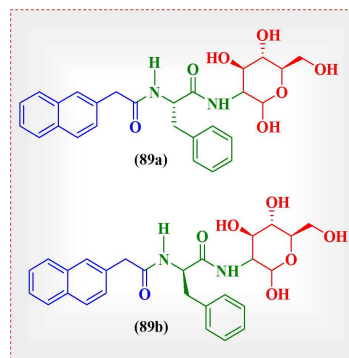

Fig. 62 Chemical structures D-glucosamine-based hydrogelators (**89a** and **89b**).

5.4.2. Gene delivery

These authors also developed a series of biocompatible, biostable molecules (Fig. 63a) consisting of nucleobases, amino acids, and glycosides (**90a-d** and **91a-d**).[233,234] Among these molecules, only **90b** was not capable of hydrogelation. All the other members in this series exhibited nanofibrous structures in their corresponding hydrogel phases. The biocompatibility of these hydrogelators was confirmed by MTT assay. The cell viability was maintained at 90% upon incubation for 72 h with 500 μM of the hydrogelator (**90a**, **90d**, **91a**, **91b**, **91c** or **91d**). However, the cell viability was found to be slightly lowered after being incubated with 500 μM **90b** or **90c** for 72 h, though IC50 value still remained >500 μM. Furthermore, the biostability of the hydrogelators (**91a**, **91b**, **91c** and **91d**) was examined by incubating them with Proteinase K, a powerful protease that catalyzes the hydrolysis of a wide range of peptidic substrates. After 24 h of the incubation with Proteinase K, more than 85% of **91a** and **91d** and 95% of **91b** and **91c** remained intact.

Furthermore, addition of a single stranded oligomeric deoxyadenosine (A$_{10}$) to a 2.1 wt-% viscous solution of **90a** at pH 7 transformed it to a stable gel followed by 2.2 times enhancement in the mechanical strength (storage modulus = G'). This result clearly indicates that the presence of inter-base pairing and phosphate-sugar interactions drive the supramolecular assembly process of **90a** and A$_{10}$. This was further supported by distinguishable change in the CD spectra after addition of A$_{10}$ to the hydrogel of **90a**. Incubation of HeLa cells with **90a** and a fluorescein-labeled single strand oligonucleotide (FAM-A$_{10}$) for 24 h resulted in the green fluorescence in both the cytosols and the nuclei of the HeLa cells (Fig. 63b). In contrast, green fluorescence was absent from the cytosols and nuclei of the HeLa cells in the control experiment (*i.e.*, in absence of **90a**), indicating the deliver the oligonucleotide FAM-A$_{10}$ into live cells.
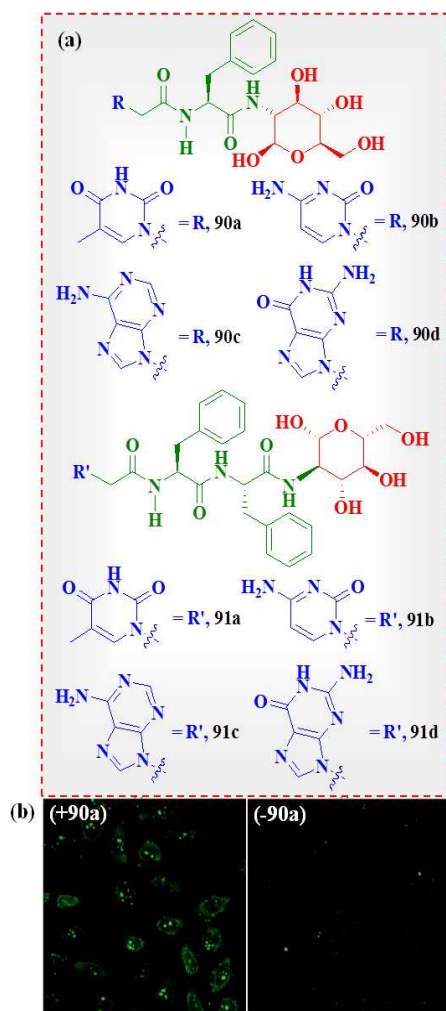
Fig. 63 (a) Chemical structures nucleobases, amino acids, and glycosides derived hydrogelators, **90a-d** and **91a-d**. (b) Fluorescence microscopy images of (left) 500 µM **90a** and 1 µM FAM-A$_{10}$ and (right) 1 µM FAM-A$_{10}$ incubated with HeLa cells for 24 h. Reprinted with permission from ref. 233. Copyright 2011, American Chemical Society.

5.5. Separation of proteins

Yamanaka utilized a tris-glycine-SDS solution gel derived from an amphiphilic low-molecular-weight hydrogelator (**72**) for electrophoresis to separate various combinations of proteins [β-galactosidase (116 kDa) and ovalbumin (45 kDa); ovalbumin and lysozyme (14.4 kDa); ovalbumin and aprotinin (6.5 kDa); lysozyme and aprotinin] (Fig. 50a).[235] Proteins could be recovered efficiently from the above mixture using the hydrogel by centrifugation. Interestingly, the smaller proteins (< 45 kDa) exhibited remarkably poorer mobility in contrast to the larger ones, *i.e.*, the smaller proteins were retained closer to the cathode side. This unique separation observed in the supramolecular gel electrophoresis (SUGE) approach was attributed to the properties of the pseudopolymer of **72** itself.

In a recent report, these authors also demonstrated an electrophoretic separation of native acidic proteins using supramolecular hydrogel matrix of an amphiphilic tris-urea derivative (**92**) in tris (hydroxymethyl) aminomethane-glycine buffer (Fig. 64).[236] The basic principle of this method of separation of acidic proteins depends on their isoelectric points rather than their molecular weights. After electrophoresis in the supramolecular hydrogel matrix of **92**, proteins could be recovered using a simple procedure and importantly their activities remained unaltered after this treatment.
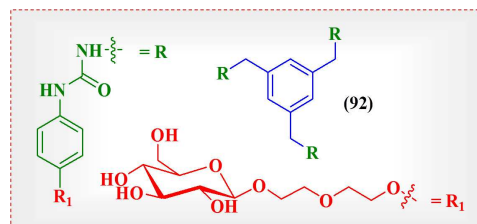

Fig. 64 Chemical structure of the carbohydrate-derived amphiphilic hydrogelator, **92**.

5.6. Gel-nanocomposites

5.6.1. Gel-nanoparticle composites

Gel nano-composites have acheived marked attention because of their potential applications in optics, electronics, ionics, mechanics, biology, fuel and solar cells, catalyst, sensors, *etc*.[24,36] The two or three dimensional structure of gel matrix has been widely used for stabilization of various nanoparticles (NPs) such as AgNP, AuNP, CdS, Fe$_2$O$_3$, FePt, TiO$_2$, ZnO *etc*. and has been shown to improve the thermal, mechanical and electrical properties of the gel network depending on the extent of interactions among them.[24] Importantly, the added NPs have strong propensity to arrange themselves along the direction of growth of the gel fibers.[31]

John and co-workers used amphiphilic ascorbic acid derivatives (**93a-c**) for *in situ* synthesis of AuNPs (Fig. 65a).[95] All of these amphiphilic molecules exhibited excellent gelation abilities and significant thermal stability in a diverse range of solvents at reasonably low concentrations. Since the ascorbic acid moiety present in the molecule has inherent redox ability, HAuCl$_4$ could be reduced to AuNP and subsequently stabilized within the self-assembled fibrillar network of the gel. Formation of AuNPs was confirmed by detecting the surface plasmon band at ~555 nm (Fig. 65b). Furthermore, TEM analysis revealed the presence of well-dispersed spherical shaped AuNPs of 11-18 nm distributed throughout the gel matrix (Fig. 65c).

5.6.2. Gel-nanocarbon composites

Carbon allotropes such as zero-dimensional fullerene, one-dimensional carbon nanotubes (CNTs) and two-dimensional graphene have been incorporated inside gel networks by means of π-stacking or van der Waals interactions between the π-surface of the carbon allotropes and the gelator molecules.[24,25]

Both covalent and non-covalent modifications of these carbon allotropes have been employed to improve their solubility in aqueous or organic solvents which results in composite materials of various interesting properties. Furthermore, the composites often show high mechanical strength, remarkable conductivity and good optoelectronic property *etc*.[24,25]
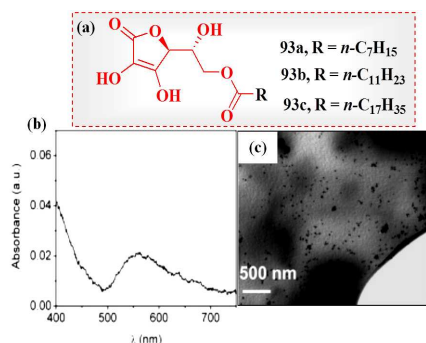

Fig. 65 (a) Chemical structures of ascorbic acid-derived amphiphilic hydrogelators, **93a-c**. (b) Absorption spectrum and (c) TEM image of AuNPs-containing **93c**-hydrogel. Reprinted with permission from ref. 95. Copyright 2007, American Chemical Society.

Harada and co-workers explored the first report of reversible hydrogelation by single-walled carbon nanotubes (SWNTs) cross-linked to poly(acrylic acid) (M_w = 250 000) containing 2 mol % of dodecyl groups (PAA2) through host-guest interactions.[237] SWNTs could be solubilized in water in presence of pyrene functionalized β-CD (Py-β-CD) by sonication. This occurred due to the strong affinity pyrenyl moiety to π-surface of SWNTs. Since, cavity of the CDs was available to host hydrophobic dodecyl groups, PAA2 was mixed with Py-β-CD/SWNT hybrid in aq. solution to result in a hydrogel (Fig. 66a). Furthermore, gel-to-sol transition could be achieved by addition of sodium adamantane carboxylate (AdCNa, 100 equiv to dodecyl moieties of PAA2) as a competitive guest (Fig. 66b). Similarly, addition of α-CD, a competitive host for the dodecyl chains led to the same result (Fig. 66c).

Zhang and Han showed preparation GO-hydrogels and organogels through supramolecular assembly of amphiphilic molecules (**94a** and **94b**), which have a polar carbohydrate headgroup joined to a nonpolar pyrene moiety (Fig. 67).[238] Organogel or hydrogel formation was achieved by adding a solution of the gelator (10 mg/ml) in organic solvent or water respectively to a GO (4 mg/ml) dispersion in organic solvent or water respectively followed by heating, stirring and sonication. However, neither organogelation nor hydrogelation was observed in absence of GO. The evidence of π-π stacking interaction between pyrene groups of the gelator and GO surface was confirmed by gradual decrease of fluorescence emission of the gelator. Furthermore, hydrogen-bonding interactions among −OH and −CO−NH− groups of the gelator and −OH and −COOH groups on GO surface involved in the gelation process was probed by IR-spectroscopy. Interestingly,

mechanical strength of the hydrogels and the organogels with **94a** were found to be improved significantly compared to that of the GO-suspension. While, addition of **94b** did not show any significant influence in the mechanical strength of the organogel and the hydrogel systems. The difference in their mechanical behaviours might be attributed to the difference in the configuration of the -OH groups in the headgroup.
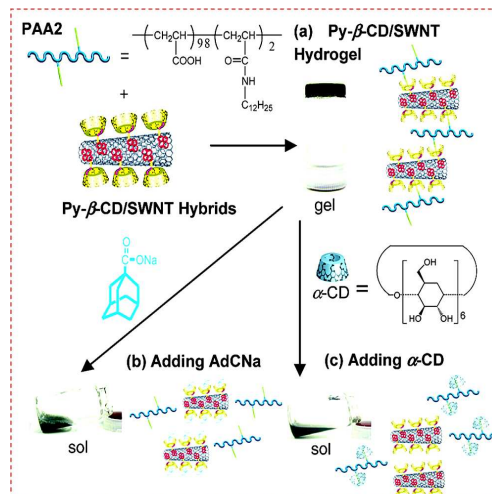

Fig. 66 Schematic illustration of hydrogel formation by host-guest interaction of Py-β-CD/SWNT with PAA2; gel-to-sol transitions upon addition of (b) competitive guest AdCNa and (c) competitive host α-CD. Reprinted with permission from ref. 237. Copyright 2007, American Chemical Society.

5.7. Gel matrix templated synthesis of silica nano-structures

Gelation of this class of LMWGs involves anisotropic 3D-growth of molecules in the self-assembly which ultimately generates various supramolecular architectures of diverse shapes and sizes such as ribbons, platelets, tubular structures or cylinders *etc*. Replication of these structural features offers opportunities for the development of interesting and textured inorganic materials.[37,72,239] In this section, we explore various strategies to prepare a variety of silica nano-structures through sol-gel reaction of sugar-based gels.
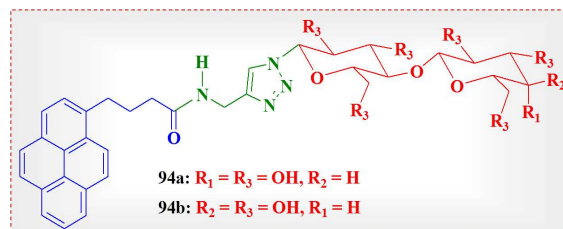

Fig. 67 Chemical structures of pyrene and sugar-derived gelators, **94a-b**.

5.7.1. Nanotubes

In one of the earlier report, ethanol gels of D-glucose-based (Fig. 68a), **95b** (α) and **96** (β) were used for fabrication of lotus

shaped silica nanotubes because of strong resemblance to the lotus root (Fig. 68b-e).[239,240] While, the nitro derivative **95a** generated conventional granular silica structures under the same polycondensation conditions indicating the vital role of the hydrogen bonding interaction between the $-NH_2$ group and the silica precursor, tetraethyl orthosilicate (TEOS).
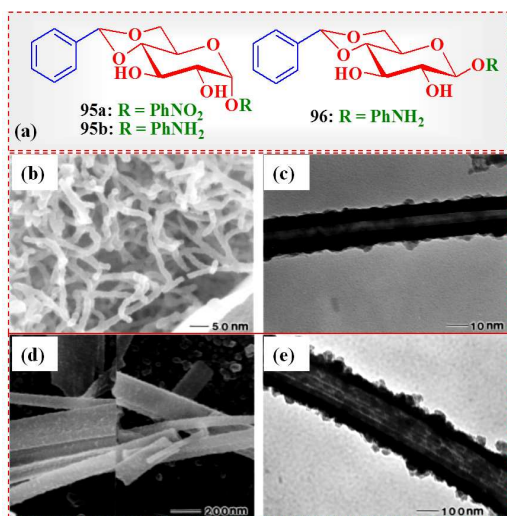

Fig. 68 (a) Molecular structures of D-glucose derivatives **95a-b** and **96**. (b and d) SEM and (c and e) TEM images of the silica nanotubes obtained from the ethanol organogels **95b** or **96**. Reprinted with permission from ref. 239. Copyright 2001, The Royal Society of Chemistry.

Compound **97a** equilibrates between 'azo' and hydrazone forms (Fig. 69). The amino group present in the hydrazone form interacts with negatively charged silica particles through hydrogen bonding interaction. In sol-gel polymerization of TEOS, transcription of superstructures of 3 wt-% of an aqueous gel of **97a**, into their silica structures results in silica nanotubes with 1000 nm outer diameter.[241] However, compound **97b** being locked in the 'azo' form produced granular structures after transcription of the corresponding aqueous gel.
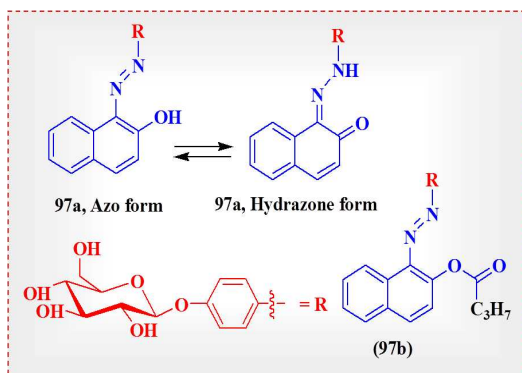

Fig. 69 Chemical structures of azo benzene functionalized sugar derivatives (**97a** and **97b**) and schematic illustration of equilibrium between 'azo' and hydrazone forms of **97a**.

5.7.2. Helices

Huang and co-workers presented a sugar-based amphiphile (**98**) which self-assembled to form one-dimensional double helix (Fig. 70a).[242] This double helical organic superstructure was used as soft template for fabrication of inorganic silica double helices through sol-gel reaction of TEOS. Sol-gel polycondensation of TEOS in **98** solution resulted in helical SiO_2 (Fig. 70b). Furthermore, these double helices transformed into non-helical fibers in presence of conventional ionic surfactant (*e.g.*, CTAB and SDS) attributed to the electrostatic repulsion inside double helix which is unfavourable for close chiral packing of amphiphiles. These non-helical fibers of co-assembly of **98** and cationic surfactant produced single helices of SiO_2 (Fig. 70c).
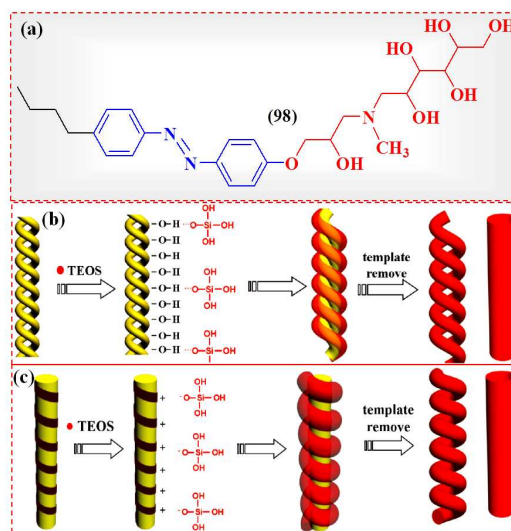
Fig. 70 (a) Chemical structure of sugar-based amphiphile **98**; Schematic representation of sol-gel reaction of TEOS in (b) **98** to form double helical SiO_2 and (c) **98**/CTAB to form helical SiO_2 nanomaterials. Reprinted with permission from ref. 242. Copyright 2010, American Chemical Society.

6. Conclusions and future perspectives

In this review, we have made a journey across various areas of sugar-derived LMWGs urbanized in the last two decades or so uncovering the mechanism of gelation, tailorable properties and other beneficial applications ranging from sensing to their uses as biomaterials. The most important advantages of using sugar derivatives as platform of gelation are their easy commercial availability, biodegradability, non-toxic nature and eco-friendly behaviour. We have also systematically explored how one may utilize various non-covalent forces that endow the sugar-based LMWGs system with desired properties. The inherent chirality of the sugar derivatives further allows extracting of chiral information directly translated from the molecular level to the microscopic level, which is generally expressed as supramolecular helicity in most of the cases.

Furthermore, various stimuli-responsive moieties are incorporated in the sugar-derived gelators to develop

fascinating stimuli-responsive soft-materials and unveil the secrets of various biological phenomena such as signaling machinery of extracellular matrices. Gelation ability of sugar-based LMWGs at reasonably low concentration and their significantly high mechanical strength have proven them as promising candidates for phase selective gelation. In this context, phase-selective-gelation has been explored in biphasic solvent mixtures. However, it would be exciting to extend this idea to multiple solvent systems. In combination with remarkable rheological properties such as high strength, stiffness and self-healing properties sugar-derived gels allowed them to gain various self-supporting shapes such as flexible planoconvex lenses, double convex lenses and prisms *etc*. Furthermore, they often lead to the formation of transparent gels with high transmittance in the visible region with glass-like refractive indices. Hence, they have promising potential to become a substitute of glass as well.

Supramolecular gel matrix has been extensively utilized as template for synthesis and stabilization of the different kind of nanomaterials in order to develop novel nanocomposites with interesting properties. Incorporation of nanoparticles or nanocarbons (SWNTs and graphene *etc*.) synergistically enhances the mechanical strength of the hybrid gels. Despite of large number of reports of gel nanocomposites, it is not adequately explored with sugar-derived gels. However, various architectural domains of sugar-derived supramolecular gel networks have indeed acted as excellent templates for the fabrication of inorganic silica nano-structures with efficient transcription of gel superstructures. High biocompatibility and biodegradability of building blocks of these gels offer potential applications in the area of drug delivery, screening of enzyme inhibitors and tissue engineering *etc*. Still, lots of hurdles have to be surpassed for application in large scale and vast daily life uses and imitating challenging complex environment encountered in human cells. We believe that this review will become a very useful source for such future design and innovation.

Acknowledgements

Notes and references

1 J. M. Lehn, *Comprehensive Supramolecular Chemistry*, ed. Pergamon Press, Oxford, UK, 1996.

2 J. M. Lehn, *Supramolecular Chemistry: Concepts and Perspectives*, VCH, Weinheim, 1995.

3 M.-Q. Zhao, Q. Zhang, G.-L. Tian and F. Wei, *Nanoscale*, 2014, **6**, 9339.

4 S. Datta, S. K. Samanta and S. Bhattacharya, *Chem. Eur. J.*, 2013, **19**, 11364.

5 S. Bhattacharjee, S. Datta and S. Bhattacharya, *Chem. Eur. J.*, 2013, **19**, 16672.

6 S. K. Samanta and S. Bhattacharya, *Chem. Commun.*, 2013, **49**, 1425.

7 D. Kiriya, M. Ikeda, H. Onoe, M. Takinoue, H. Komatsu, Y. Shimoyama, I. Hamachi and S. Takeuchi, *Angew. Chem., Int. Ed.*, 2012, **51**, 1553.

8 L. A. Estroff and A. D. Hamilton, *Chem. Rev.*, 2004, **104**, 1201.

9 L. E. Buerklea and S. J. Rowan, *Chem. Soc. Rev.*, 2012, **41**, 6089.

10 A. Noro, M. Hayashi and Y. Matsushita, *Soft Matter*, 2012, **8**, 6416.

11 E. A. Appel, J. del Barrio, X. J. Loh and O. A. Scherman, *Chem. Soc. Rev.*, 2012, **41**, 6195.

12 M. Suzuki and K. Hanabusa, *Chem. Soc. Rev.*, 2010, **39**, 455.

13 J. Raeburn, A. Z. Cardoso and D. J. Adams, *Chem. Soc. Rev.*, 2013, **42**, 5143.

14 N. M. Sangeetha and U. Maitra, *Chem. Soc. Rev.*, 2005, **34**, 821.

15 M. O. M. Piepenbrock, G. O. Lloyd, N. Clarke and J. W. Steed, *Chem. Rev.*, 2010, **110**, 1960.

16 J. Boekhoven and S. I. Stupp, *Adv. Mater.*, 2014, **26**, 1642.

17 P. K. Vemula, N. Wiradharma, J. A. Ankrum, O. R. Miranda, G. John and J. M. Karp, *Curr. Opin. Biotechnol.*, 2013, **24**, 1174.

18 J. B. Matson and S. I. Stupp, *Chem. Commun.*, 2012, **48**, 26.

19 G. John, B. V. Shankar, S. R. Jadhav and P. K. Vemula, *Langmuir*, 2010, **26**, 17843.

20 F. Zhao, M. L. Ma and B. Xu, *Chem. Soc. Rev.*, 2009, **38**, 883.

21 A. R. Hirst, B. Escuder, J. F. Miravet and D. K. Smith, *Angew. Chem., Int. Ed.*, 2008, **47**, 8002.

22 J. Nanda, A. Biswas, B. Adhikari and A. Banerjee, *Angew. Chem., Int. Ed.*, 2013, **52**, 1.

23 V. S. Balachandran, S. R. Jadhav, P. K. Vemula and G. John, *Chem. Soc. Rev.*, 2013, **42**, 427.

24 D. Das, T. Kar and P. K. Das, *Soft Matter*, 2012, **8**, 2348.

25 S. K Samanta, K. S. Subrahmanyam, S. Bhattacharya and C. N. R. Rao, *Chem. Eur. J.*, 2012, **18**, 2890.

26 S. Samanta, A. Pal, S. Bhattacharya and C. N. R. Rao, *J. Mater. Chem.*, 2010, **20**, 6881.

27 S. K. Samanta, A. Gomathi, S. Bhattacharya and C. N. R. Rao, *Langmuir*, 2010, **26**, 12230.

28 A. Pal, B. S. Chhikara, A. Govindaraj, S. Bhattacharya and C. N. R. Rao, *J. Mater. Chem.*, 2008, **18**, 2593.

29 H. Basit, A. Pal, S. Sen and S. Bhattacharya, *Chem. Eur. J.*, 2008, **14**, 6534.

30 G. John and P. K. Vemula, *Soft Matter*, 2006, **2**, 909.

31 S. Bhattacharya, A. Srivastava and A. Pal, *Angew. Chem., Int. Ed.*, 2006, **45**, 2934.

32 X. Yang, G. Zhang and D. Zhang, *J. Mater. Chem.*, 2012, **22**, 38.

33 P. K. Vemula, J. E. Kohler, A. Blass, M. Williams, C. Xu, L. Chen, S. R. Jadhav, G. John, D. I. Soybel and J. M. Karp, *Sci. Rep.*, 2014, **4**, 4466.

34 N. Dey, S. K. Samanta and S. Bhattacharya, *ACS Appl. Mater. Interfaces*, 2013, **5**, 8394.

35 M. Ikeda, T. Yoshii, T. Matsui, T. Tanida, H. Komatsu and I. Hamachi, *J. Am. Chem. Soc.*, 2011, **133**, 1670.

36 S. Banerjee, R. K. Das and U. Maitra, *J. Mater. Chem.*, 2009, **19**, 6649.

37 K. J. C. van Bommel, A. Friggeri and S. Shinkai, *Angew. Chem.*, *Int. Ed.*, 2003, **42**, 980.

38 S. K. Samanta and S. Bhattacharya, *Chem. Eur. J.*, 2012, **18**, 16632.

39 S. K. Samanta and S. Bhattacharya, *J. Mater. Chem.*, 2012, **22**, 25277.

40 S. K. Samanta and S. Bhattacharya, *Chem. Eur. J.*, 2012, **18**, 15875.

41 S. Bhattacharya and S. K. Samanta, *Langmuir*, 2009, **25**, 8378.

42 D. D. Díaz, D. Kühbecka and R. J. Koopmans, *Chem. Soc. Rev.*, 2011, **40**, 427.

43 J. W. Steed, *Chem. Commun.*, 2011, **47**, 1379.

44 S. Datta and S. Bhattacharya, *Soft Matter*, 2015, **11**, 1945.

45 H. Svobodová, V. Noponen, E. Kolehmainen and E. Sievänen, *RSC Adv.*, 2012, **2**, 4985.

46 M. George and R. G. Weiss, *Acc. Chem. Res.*, 2006, **39**, 489.

47 D. J. Abdallah and R. G. Weiss, *Adv. Mater.*, 2000, **12**, 1237.

48 P. Terech and R. G. Weiss, *Chem. Rev.*, 1997, **97**, 3133.

49 A. Dasgupta, J. H. Mondal and D. Das, *RSC Adv.*, 2013, **3**, 9117.

50 C. Tomasini and N. Castellucci, *Chem. Soc. Rev.*, 2013, **42**, 156.

51 Y. Gao, F. Zhao, Q. Wang, Y. Zhang and B. Xu, *Chem. Soc. Rev.*, 2010, **39**, 3425.

52 M. Suzuki and K. Hanabusa, *Chem. Soc. Rev.*, 2009, **38**, 967.

53 S. Bhattacharya and A. Pal, *J. Phys. Chem. B*, 2008, **112**, 4918.

54 A. Pal, Y. K. Ghosh and S. Bhattacharya, *Tetrahedron*, 2007, **63**, 7334.

55 J. W. Steed, *Chem. Soc. Rev.*, 2010, **39**, 3686.

56 P. K. Vemula and G. John, *Acc. Chem. Res.*, 2008, **41**, 769.

57 A. Y.-Y. Tam and V. W.-W. Yam, *Chem. Soc. Rev.*, 2013, **42**, 1540.

58 J. H. Jung, J. H. Lee, J. R. Silverman and G. John, *Chem. Soc. Rev.*, 2013, **42**, 924.

59 Y. Kobayashi, Y. Takashima, A. Hashidzume, H. Yamaguchi and A. Harada, *Sci. Rep.*, 2013, **3**, 1243.

60 N. Lanigan and X. Wang, *Chem. Commun.*, 2013, **49**, 8133.

61 N. N. Adarsh and P. Dastidar, *Chem. Soc. Rev.*, 2012, **41**, 3039.

62 M. Kumar, K. V. Rao and S. J. George, *Phys. Chem. Chem. Phys.*, 2014, **16**, 1300.

63 A. Das and S. Ghosh, *Angew. Chem., Int. Ed.*, 2014, **53**, 2038.

64 Z. Qi and C. A. Schalley, *Acc. Chem. Res.*, 2014, **47**, 2222.

65 J. A. Foster and J. W. Steed, *Angew. Chem., Int. Ed.*, 2010, **49**, 6718.

66 P. Dastidar, *Chem. Soc. Rev.*, 2008, **37**, 2699.

67 A. Pal, H. Basit, S. Sen, V. K. Aswal and S. Bhattacharya, *J. Mater. Chem.*, 2009, **19**, 4325.

68 D. K. Kumar and J. W. Steed, *Chem. Soc. Rev.*, 2014, **43**, 2080.

69 X. Yu, L. Chen, M. Zhang and T. Yi, *Chem. Soc. Rev.*, 2014, **43**, 5346.

70 G. Yu, X. Yan, C. Han and F. Huang, *Chem. Soc. Rev.*, 2013, **42**, 6697.

71 B. Zheng, F. Wang, S. Dong and F. Huang, *Chem. Soc. Rev.*, 2012, **41**, 1621.

72 J. H. Jung, M. Park and S. Shinkai, *Chem. Soc. Rev.*, 2010, **39**, 4286.

73 G. Cravotto and P. Cintas, *Chem. Soc. Rev.*, 2009, **38**, 2684.

74 D. K. Smith, *Chem. Soc. Rev.*, 2009, **38**, 684.

75 Z. Yang, G. Liang, and B. Xu, *Acc. Chem. Res.*, 2008, **41**, 315.

76 R. G. Weiss and P. Terech, *Molecular Gels: Materials with Self-Assembled Fibrillar Networks*, ed. Springer, Dordrecht, 2006.

77 C. Boettcher, B. Schade and J. H. Fuhrhop, *Langmuir*, 2001, **17**, 873.

78 F. M. Menger and K. L. Caran, *J. Am. Chem. Soc.*, 2000, **122**, 11679.

79 R. A. Gortner and W. F. Hoffman, *J. Am. Chem. Soc.*, 1921, **43**, 2199.

80 M. Yamanaka and H. Fujii, *J. Org. Chem.*, 2009, **74**, 5390.

81 K. Hanabusa, M. Yamada, M. Kimura and H. Shirai, *Angew. Chem., Int. Ed.*, 1996, **35**, 1949.

82 L. A. Estroff and A. D. Hamilton, *Angew. Chem., Int. Ed.*, 2000, **39**, 3447.

83 Y. Zhang, Z. M. Yang, F. Yuan, H. W. Gu, P. Gao and B. Xu, *J. Am. Chem. Soc.*, 2004, **126**, 15028.

84 B. G. Xing, C. W. Yu, K. H. Chow, P. L. Ho, D. G. Fu and B. Xu, *J. Am. Chem. Soc.*, 2002, **124**, 14846.

85 M. C. Branco and J. P. Schneider, *Acta Biomater.*, 2009, **5**, 817.

86 R. V. Ulijn, N. Bibi, V. Jayawarna, P. D. Thornton, S. J. Todd, R. J. Mart, A. M. Smith and J. E. Gough, *Mater. Today*, 2007, **10**, 40.

87 Z. Yang and B. Xu, *J. Mater. Chem.*, 2007, **17**, 2385.

88 A. P. Nowak, V. Breedveld, L. Pakstis, B. Ozbas, D. J. Pine, D. Pochan and T. J. Deming, *Nature*, 2002, **417**, 424.

89 B. T. Houseman, and M. Mrksich, *Top. Curr. Chem.*, 2002, **218**, 1.

90 N. Nagahori and S. Nishimura, *Biomacromolecules*, 2001, **2**, 22.

91 R. A. Dwek, *Chem. Rev.*, 1996, **96**, 683.

92 M. Yamanaka, N. Haraya and S. Yamamichi, *Chem. Asian J.*, 2011, **6**, 1022.

93 D. A. Jones, *Phytochemistry*, 1998, **47**, 155.

94 P. K. Vemula, J. Li and G. John, *J. Am. Chem. Soc.*, 2006, **128**, 8932.

95 P. K. Vemula, U. Aslam, V. A. Mallia and G. John, *Chem. Mater.*, 2007, **19**, 138.

96 O. Gronwald and S. Shinkai, *Chem. Eur. J.*, 2001, **7**, 4328.

97 O. Gronwald, K. Sakurai, R. Luboradzki, T. Kimura and S. Shinkai, *Carbohydr. Res.*, 2001, **331**, 307.

98 K. Yoza, N. Amanokura, Y. Ono, T. Akao, H. Shinmori, M. Takeuchi, S. Shinkai and D. N. Reinhoudt, *Chem. Eur. J.*, 1999, **5**, 2722.

99 K. Yoza, Y. Ono, K. Yoshihara, T. Akao, H. Shinmori, M. Takeuchi, S. Shinkai and D. N. Reinhoudt, *J. Chem. Soc., Chem. Commun.*, 1998, 907.

100 R. Luboradzki, O. Gronwald, M. Ikeda, S. Shinkai and D. N. Reinhoudt, *Tetrahedron*, 2000, **56**, 9595.

101 P. R. Muddasani, B. Bernet and A. Vasella, *Helv. Chim. Acta*, 1994, **77**, 334.

102 K. Sakurai, Y. Jeong, K. Koumoto, A. Friggeri, O. Gronwald, S. Sakurai, S. Okamoto, K. Inoue and S. Shinkai, *Langmuir*, 2003, **19**, 8211.

103 Images are adapted from wikipedia.org.

104 G. Wang, S. Cheuk, K. Williams, V. Sharma, L. Dakessian and Z. Thorton, *Carbohydr. Res.*, 2006, **341**, 705.

105 S. Cheuk, E. D. Stevens and G. Wang, *Carbohydr. Res.*, 2009, **344**, 417.

106 G. Wang, S. Cheuk, H. Yang, N. Goyal, P. V. N. Reddy and B. Hopkinson, *Langmuir*, 2009, **25**, 8696.

107 N. Goyal, S. Cheuk and G. Wang, *Tetrahedron*, 2010, **66**, 5962.

108 M. Mathiselvam, D. Loganathan and B. Varghese, *RSC Adv.*, 2013, **3**, 14528.

109 H. P. R. Mangunuru, H. Yang and G. Wang, *Chem. Commun.*, 2013, **49**, 4489.

110 J. H. Jung, G. John, M. Masuda, K. Yoshida, S. Shinkai and T. Shimizu, *Langmuir*, 2001, **17**, 7229.

111 S. Bhattacharya and S. N. G. Acharya, *Chem. Mater.*, 1999, **11**, 3504.

112 J. H. Jung, S. Shinkai and T. Shimizu, *Chem. Eur. J.*, 2002, **8**, 2684.

113 S.-i. Tamaru, M. Nakamura, M. Takeuchi and S. Shinkai, *Org. Lett.*, 2001, **3**, 3631.

114 S.-i. Kawano, S.-i. Tamaru, N. Fujita and S. Shinkai, *Chem. Eur. J.*, 2004, **10**, 343.

115 J. Köning, C. Boettcher, H. Winkler, E. Zeitler, Y. Talmon and J.-H. Fuhrhop, *J. Am. Chem. Soc.*, 1993, **115**, 693.

116 T. Muraoka, H. Cui and S. I. Stupp, *J. Am. Chem. Soc.*, 2008, **130**, 2946.

117 S. Datta and S. Bhattacharya, *Chem. Commun.*, 2012, **48**, 877.

118 J. Cui, Z. Shen and X. Wan, *Langmuir*, 2010, **26**, 97.

119 A. Brizard, R. Oda and I. Huc, *Topics in Current Chemistry*, Springer-Verlag: New York, 2005, **256**, 167.

120 E. Ostuni, P. Kamaras and R. G. Weiss, *Angew. Chem., Int. Ed.*, 1996, **35**, 1324.

121 Y. Yan, Y. Lin, Y. Qiao and J. Huang, *Soft Matter*, 2011, **7**, 6385.

122 J.-L. Li and X.-Y. Liu, *Adv. Funct. Mater.*, 2010, **20**, 3196.

123 S. Grassi, E. Carretti, L. Dei, C. W. Branham, B. Kahrd and R. G. Weiss, *New J. Chem.*, 2011, **35**, 445.

124 M. J. Meunier, *Ann. Chim. Phys.*, 1891, **22**, 412.

125 S. Yamamoto, *Kogyokagakuzasshi*, 1943, **46**, 779.

126 S. Yamamoto, *Kogyokagakuzasshi*, 1942, **45**, 695.

127 D. J. Mercurio and R. J. Spontak, *J. Phys. Chem. B*, 2001, **105**, 2091.

128 E. A. Wilder, C. K. Hall, S. A. Khan and R. J. Spontak, *Langmuir*, 2003, **19**, 6004.

129 S. J. Craythorne, C. L. Pollock, A. J. Blake, M. Nieuwenhuyzen, A. C. Marr and P. C. Marr, *New J. Chem.*, 2009, **33**, 479.

130 J. Zhou and H. Ritter, *Polym. Chem.*, 2010, **1**, 1552.

131 C. De Rango, P. Charpin, J. Navaza, N. Keller, I. Nicolis, F. Villain and A. W. Coleman, *J. Am. Chem. Soc.*, 1992, **114**, 5475.

132 M. F. Abreu, V. T. Salvador, L. Vitorazi, C. E. N. Gatts, D. R. dos Santos, R. Giacomini, S. L. Cardoso and P. C. M. L. Miranda, *Carbohydr. Res.*, 2012, **353**, 69.

133 U. Maitra, P. Vijay Kumar, N. Chandra, L. J. D'Souza, M. D. Prasanna and A. R. Raju, *Chem. Commun.*, 1999, 595.

134 A. Friggeri, O. Gronwald, K. J. C. van Bommel, S. Shinkai and D. N. Reinhoudt, *J. Am. Chem. Soc.*, 2002, **124**, 10754.

135 S. Nandi, H.-J. Altenbach, B. Jakob, K. Lange, R. Ihizane and M. P. Schneider, *Org. Lett.*, 2011, **13**, 1980.

136 S. Nandi, H.-J. Altenbach, B. Jakob, K. Lange, R. Ihizane, M. P. Schneider, U. Gün and A. Mayer, *Org. Lett.*, 2012, **14**, 3826.

137 N. Kameta, K. Ishikawa, M. Masuda, M. Asakawa and T. Shimizu, *Chem. Mater.*, 2012, **24**, 209.

138 G. John, J. H. Jung, M. Masuda, and T. Shimizu, *Langmuir*, 2004, **20**, 2060.

139 J. H. Jung, J. A. Rim, W. S. Han, S. J. Lee, Y. J. Lee, E. J. Cho, J. S. Kim, Q. Ji and T. Shimizu, *Org. Biomol. Chem.*, 2006, **4**, 2033.

140 M. J. Clemente, J. Fitremann, M. Mauzac, J. L. Serrano and L. Oriol, *Langmuir*, 2011, **27**, 15236.

141 M. J. Clemente, P. Romero, J. L. Serrano, J. Fitremann and L. Oriol, *Chem. Mater.*, 2012, **24**, 3847.

142 L. S. Birchall, S. Roy, V. Jayawarna, M. Hughes, E. Irvine, G. T. Okorogheye, N. Saudi, E. De Santis, T. Tuttle, A. A. Edwards and R. V. Ulijn, *Chem. Sci.*, 2011, **2**, 1349.

143 R. J. H. Hafkamp, B. P. A. Kokke, I. M. Danke, H. P. M. Geurts, A. E. Rowan, M. C. Feiters and R. J. M. Nolte, *Chem. Commun.*, **1997**, 545.

144 G. Bühler, M. C. Feiters, R. J. M. Nolte and K. H. Dötz, *Angew. Chem., Int. Ed.*, 2003, **42**, 2494.

145 S. A. Joshi and N. D. Kulkarni, *Chem. Commun.*, 2009, 2341.

146 D. Astruc, *Nat. Chem.*, 2012, **4**, 255.

147 Y. Feng, Y.-M. He and Q.-H. Fan, *Chem. Asian J.*, 2014, **9**, 1724.

148 M. McWatt and G.-J. Boons, *Eur. J. Org. Chem.*, 2001, **2001**, 2535.

149 P. Rajamalli, P. S. Sheet and E. Prasad, *Chem. Commun.*, 2013, **49**, 6758.

150 D. Pati, N. Kalva, S. Das, G. Kumaraswamy, S. S. Gupta and A. V. Ambade, *J. Am. Chem. Soc.*, 2012, **134**, 7796.

151 R. J. H. Hafkamp, M. C. Feiters and R. J. M. Nolte, *Angew. Chem., Int. Ed.*, 1994, **33**, 986.

152 J.-H. Fuhrhop and W. Helfrich, *Chem. Rev.*, 1993, **93**, 1565.

153 B. Pfannemuller and W. Welte, *Chem. Phys. Lipids*, 1985, **37**, 227.

154 N. Minakuchi, K. Hoe, D. Yamaki, S. Ten-no, K. Nakashima, M. Goto, M. Mizuhata and T. Maruyama, *Langmuir*, 2012, **28**, 9259.

155 N. Yan, G. He, H. L. Zhang, L. P. Ding and Y. Fang, *Langmuir*, 2010, **26**, 5909.

156 T. Nakamura, Y. Takashima, A. Hashidzume, H. Yamaguchi and A. Harada, *Nat. Commun.*, 2014, **5**, 4622.

157 X. Yan, F. Wang, B. Zheng and F. Huang, *Chem. Soc. Rev.*, 2012, **41**, 6042.

158 Y. Takashima, S. Hatanaka, M. Otsubo, M. Nakahata, T. Kakuta, A. Hashidzume, H. Yamaguchi and A. Harada, *Nat. Commun.*, 2012, **3**, 1270.

159 M. D. Segarra-Maset, V. J. Nebot, J. F. Miravet and B. Escuder, *Chem. Soc. Rev.*, 2013, **42**, 7086.

160 Images adapted from http://focusscience.blogspot.in/2014/02/why-touch-me-not-plant-is-sensitive.html, http://www.vianegativa.us/tag/millipedes/ and http://www.keyence.de/products/microscope/high-speed-microscope-vw-6000/features/index.jsp

161 J. Cui, A. Liu, Y. Guan, J. Zheng, Z. Shen and X. Wan, *Langmuir*, 2010, **26**, 3615.

162 S. Kiyonaka, K. Sugiyasu, S. Shinkai and I. Hamachi, *J. Am. Chem. Soc.*, 2002, **124**, 10954.

163 S. Yamaguchi, S. Matsumoto, K. Ishizuka, Y. Iko, K. V. Tabata, H. F. Arata, H. Fujita, H. Noji and I. Hamachi, *Chem. Eur. J.*, 2008, **14**, 1891.

164 M. Ávalos, R. Babiano, P. Cintas, A. G. Carretero, J. L. Jiménez, M. Lozano, A. L. Ortiz, J. C. Palacios and A. Pinazo, *Chem. Eur. J.*, 2008, **14**, 5656.

165 R. Karinaga, Y. Jeong, S. Shinkai, K. Kaneko and K. Sakurai, *Langmuir*, 2005, **21**, 9398.

166 W. Deng, H. Yamaguchi, Y. Takashima and A. Harada, *Angew. Chem., Int. Ed.*, 2007, **46**, 5144.

167 A. Kawamura, T. Kiguchi, T. Nishihata, T. Uragami and T. Miyata, *Chem. Commun.*, 2014, **50**, 11101.

168 Y. Shiraki, K. Tsuruta, J. Morimoto, C. Ohba, A. Kawamura, R. Yoshida, R. Kawano, T. Uragami and T. Miyata, *Macromol. Rapid Commun.*, 2015, **36**, 515.

169 T. Taira, Y. Suzaki and K. Osakada, *Chem. Eur. J.*, 2010, **16**, 6518.

170 A. Srivastava, S. Ghorai, A. Bhattacharjya and S. Bhattacharya, *J. Org. Chem.*, 2005, **70**, 6574.

171 O. Pieroni, A. Fissi, N. Angelini and F. Lenci, *Acc. Chem. Res.*, 2001, **34**, 9.

172 Y. Ogawa, C. Yoshiyama and T. Kitaoka, *Langmuir*, 2012, **28**, 4404.

173 S. Matsumoto, S. Yamaguchi, S. Ueno, H. Komatsu, M. Ikeda, K. Ishizuka, Y. Iko, K. V. Tabata, H. Aoki, S. Ito, H. Noji and I. Hamachi, *Chem. Eur. J.*, 2008, **14**, 3977.

174 S. Matsumoto, S. Yamaguchi, A. Wada, T. Matsui, M. Ikeda and I. Hamachi, *Chem. Commun.*, 2008, 1545.

175 Y. Sako and Y. Takaguchi, *Org. Biomol. Chem.*, 2008, **6**, 3843.

176 G. John, G. Zhu, J. Li and J. S. Dordick, *Angew. Chem. Int. Ed.*, 2006, **45**, 4772.

177 Q. Zhang, D.-H. Qu, X. Ma and H. Tian, *Chem. Commun.*, 2013, **49**, 9800.

178 K. Sada, M. Takeuchi, N. Fujita, M. Numata and S. Shinkai, *Chem. Soc. Rev.*, 2007, **36**, 415.

179 J.-H. Fuhrhop, P. Blumtritt, C. Lehmann and P. Luger, *J. Am. Chem. Soc.*, 1991, **113**, 7437.

180 X. Nie and G. Wang, *J. Org. Chem.*, 2006, **71**, 4734.

181 G. Wang, H. Yang, S. Cheuk and S. Coleman, *Beilstein J. Org. Chem.*, 2011, **7**, 234.

182 G. Wang, N. Goyal, H. P. R. Mangunuru, H. Yang, S. Cheuk, P. V. N. Reddy, *J. Org. Chem.*, 2015, **80**, 733.

183 S. L. Zhou, S. Matsumoto, H. D. Tian, H. Yamane, A. Ojida, S. Kiyonaka and I. Hamachi, *Chem. Eur. J.*, 2005, **11**, 1130.

184 N. Kameta, M. Masuda, and T. Shimizu, *ACS Nano*, 2012, **6**, 5249.

185 H. Komatsu, S. Matsumoto, S.-i. Tamaru, K. Kaneko, M. Ikeda and I. Hamachi, *J. Am. Chem. Soc.*, 2009, **131**, 5580.

186 P. Xue, R. Lu, G. Chen, Y. Zhang, H. Nomoto, M. Takafuji and H. Ihara, *Chem. Eur. J.*, 2007, **13**, 8231.

187 P. Chen, R. Lu, P. Xue, T. Xu, G. Chen and Y. Zhao, *Langmuir*, 2009, **25**, 8395.

188 A. Ohshima, A. Momotake and T. Arai, *Bull. Chem. Soc. Jpn.*, 2006, **79**, 305.

189 S. Laschat, A. Baro, N. Steinke, F. Giesselmann, C. Hägele, G. Scalia, R. Judele, E. Kapatsina, S. Sauer, A. Schreivogel and M. Tosoni, *Angew. Chem.*, *Int. Ed.*, 2007, **46**, 4832.

190 K. Fan, J. Yang, X. Wang and J. Song, *Soft Matter*, 2014, **10**, 8370.

191 K. Fan, J. Song, J. Li, X. Guan, N. Tao, C. Tong, H. Shen and L. Niu, *J. Mater. Chem. C*, 2013, **1**, 7479.

192 I. Yoshimura, Y. Miyahara, N. Kasagi, H. Yamane, A. Ojida and I. Hamachi, *J. Am. Chem. Soc.*, 2004, **126**, 12204.

193 S. Yamaguchi, I. Yoshimura, T. Kohira, S.-i. Tamaru and I. Hamachi, *J. Am. Chem. Soc.*, 2005, **127**, 11835.

194 Q. Chen, Y. Lv, D. Zhang, G. Zhang, C. Liu and D. Zhu, *Langmuir*, 2010, **26**, 3165.

195 S. Bhuniya and B. H. Kim, *Chem. Commun.*, 2006, 1842.

196 A. Kawamura, Y. Hata, T. Miyata and T. Uragami, *Colloids Surf. B*, 2012, **99**, 74.

197 M. Yamanaka, N. Haraya and S. Yamamichi, *Chem. Asian J.*, 2011, **6**, 1022.

198 Y. Jinno and M. Yamanaka, *Chem. Asian J.*, 2012, **7**, 1768.

199 M. Ikeda, T. Tanida, T. Yoshii, K. Kurotani, S. Onogi, K. Urayama and I. Hamachi, *Nat. Chem.*, 2014, **6**, 511.

200 D. Yuan, R. Zhou, J. Shi, X. Du, X. Li and B. Xu, *RSC Adv.*, 2014, **4**, 26487.

201 R. A. Pires, Y. M. Abul-Haija, D. S. Costa, R. Novoa-Carballal, R. L. Reis, R. V. Ulijn and I. Pashkuleva, *J. Am. Chem. Soc.*, 2015, **137**, 576.

202 F. Zhao, C. S. Weitzel, Y. Gao, H. M. Browdy, J. Shi, H.-C. Lin, S. T. Lovett and B. Xu, *Nanoscale*, 2011, **3**, 2859.

203 R. Ochi, K. Kurotani, M. Ikeda, S. Kiyonaka and I. Hamachi, *Chem. Commun.*, 2013, **49**, 2115.

204 M. Suzuki, H. Saito and K. Hanabusa, *Langmuir*, 2009, **25**, 8579.

205 J. G. Hardy, A. R. Hirst, D. K. Smith, C. Brennan and I. Ashworth, *Chem. Commun.*, 2005, 385.

206 R. K. Das, R. Kandanelli, J. Linnanto, K. Bose and U. Maitra, *Langmuir*, 2010, **26**, 16141.

207 B. P. Krishnan, S. Ramakrishnan and K. M. Sureshan, *Chem. Commun.*, 2013, **49**, 1494.

208 M. J. Clemente, R. M. Tejedor, P. Romero, J. Fitremann and L. Oriol, *RSC Adv.*, 2012, **2**, 11419.

209 S. Bhattacharya and Y. Krishnan-Ghosh, *Chem. Commun.*, 2001, 185.

210 S. R. Jadhav, P. K. Vemula, R. Kumar, S. R. Raghavan and G. John, *Angew. Chem., Int. Ed.*, 2010, **49**, 7695.

211 S. Mukherjee, C. Shang, X. Chen, X. Chang, K. Liu, C. Yu and Y. Fang, *Chem. Commun.*, 2014, **50**, 13940.

212 S. Dutta, D. Das, A. Dasgupta and P. K. Das, *Chem. Eur. J.*, 2010, **16**, 1493.

213 B. Adhikari, G. Palui and A. Banerjee, *Soft Matter*, 2009, **5**, 3452.

214 S. Ray, A. K. Das and A. Banerjee, *Chem. Mater.*, 2007, **19**, 1633.

215 S. Mukherjee and B. Mukhopadhyay, *RSC Adv.*, 2012, **2**, 2270.

216 A. Prathap and K. M. Sureshan, *Chem. Commun.*, 2012, **48**, 5250.

217 Z. Wei, J. H. Yang, J. Zhou, F. Xu, M. Zrınyi, P. H. Dussault, Y. Osada and Y. M. Chen, *Chem. Soc. Rev.*, 2014, **43**, 8114.

218 S. Bhattacharjee and S. Bhattacharya, *J. Mater. Chem. A*, 2014, **2**, 17889.

219 D. Higashi, M. Yoshida and M. Yamanaka, *Chem. Asian J.*, 2013, **8**, 2584.

220 M. Nakahata, Y. Takashima, H. Yamaguchi and A. Harada, *Nat. Commun.*, 2011, **2**, 511.

221 A. Harada, Y. Takashima and M. Nakahata, *Acc. Chem. Res.*, 2014, **47**, 2128.

222 M. Nakahata, Y. Takashima, H. Yamaguchi and A. Harada, *Nat. Commun.*, 2011, **2**, 511.

223 T. Kakuta, Y. Takashima, M. Nakahata, M. Otsubo, H. Yamaguchi and A. Harada, *Adv. Mater.*, 2013, **25**, 2849.

224 A. Vidyasagar, K. Handore and K. M. Sureshan, *Angew. Chem. Int. Ed.*, 2011, **50**, 8021.

225 D. R. Thomson, L. J. Gut and J. W. Jenkins, *Biopesticides: Use and Delivery*, ed. F. R. Hall and J. J. Menn, Humana Press Inc., New Jersey, 1999, 385.

226 D. G. Campion, B. R. Critchley and L. J. McVeigh, *Mating Disruption. In Insect Pheromones in Plant Protection*, Ed. A. R. Jutsum and R. F. S. Gordon, Wiley: New York, 1985, 89.

227 T. A. Evans, T. Z. Dawes, P. R. Ward and N. Lo, *Nat. Commun.*, 2011, **2**, 262.

228 A. Cork, *Pheromone Manual. Chatham Maritime*, UK: Natural Resources Institute, Chapter 4, 2004, 13.

229 D. Bhagat, S. K. Samanta and S. Bhattacharya, *Sci. Rep.*, 2013, 3: 1294.

230 S. R. Jadhav, B.-S. Chiou, D. F. Wood, G. DeGrande-Hoffman, G. M. Glenn and G. John, *Soft Matter*, 2011, **7**, 864.

231 X. Du, J. Zhou and B. Xu, *Chem. Asian J.*, 2014, **9**, 1446.

232 Z. Yang, G. Liang, M. Ma, A. S. Abbah, W. W. Luc and B. Xu, *Chem. Commun.*, 2007, 843.

233 X. Li, Y. Kuang, J. Shi, Y. Gao, H.-C. Lin and B. Xu, *J. Am. Chem. Soc.*, 2011, **133**, 17513.

234 X. Li, Y. Kuang and B. Xu, *Soft Matter*, 2012, **8**, 2801.

235 S. Yamamichi, Y. Jinno, N. Haraya, T. Oyoshi, H. Tomitori, K. Kashiwagi and M. Yamanaka, *Chem. Commun.*, 2011, **47**, 10344.

236 K. Munenobu, T. Hase, T. Oyoshi and M. Yamanaka, *Anal. Chem.*, 2014, **86**, 9924.

237 T. Ogoshi, Y. Takashima, H. Yamaguchi and A. Harada, *J. Am. Chem. Soc.*, 2007, **129**, 4878.

238 Q.-Y. Cheng, D. Zhou, Y. Gao, Q. Chen, Z. Zhang and B.-H. Han, *Langmuir*, 2012, **28**, 3005.

239 J. H. Jung, M. Amaike, K. Nakashima and S. Shinkai, *J. Chem. Soc., Perkin Trans. 2*, 2001, 1938.

240 J. H. Jung, M. Amaike and S. Shinkai, *Chem. Commun.*, 2000, 2343.

241 J. H. Jung, S. Shinkai and T. Shimizu, *Nano Lett.*, 2002, **2**, 17.

242 Y. Lin, Y. Qiao, C. Gao, P. Tang, Y. Liu, Z. Li, Y. Yan and J. Huang, *Chem. Mater.*, 2010, **22**, 6711.